ADVANCED MATERIALS TECHNOLOGIES
www.advmattechnol.de

Significance of Flexible Substrates for Wearable and Implantable Devices: Recent Advances and Perspectives

Muhammad Hassan, Ghulam Abbas, Ning Li, Annum Afzal, Zeeshan Haider, Saad Ahmed, Xiuru Xu, Caofeng Pan, and Zhengchun Peng**

In the past decade, flexible electronics have attracted significant research attention due to their distinct features and emerging applications in numerous fields such as, flexible displays, implantable sensors, and energy storage systems, among other applications. Due to the development of flexible electronics, this paper details the substrates employed to produce flexible electronic devices, given that substrates generally govern the overall device properties. The increase in research attention can be attributed to the use of films as flexible substrates, which enable the implementation of numerous design strategies and engineering methodologies, thus leading to extensive advances in the manufacturing quality and prospect of flexible electronics in various applications. This paper provides a comprehensive review of the significance of substrates in flexible wearable electronics over the past decade, such as, the substrate properties requirements, processing classification, important flexible devices, and applications, including sensing, energy storage, and other electronic devices.

1. Introduction

Flexible electronics as an emerging technological trend has demonstrated significance for viable economic growth and practical implementation in improving the human quality of life.[1] With the increasing demand for portable, lightweight, and low-cost flexible and wearable electronics, significant research attention is required to solve future challenges with respect to the construction of next-generation electronic devices, thus allowing for essential technological advancements in terms of performance characteristics and a wide range of potential applications. Moreover, the reported global revenue ratio in rigid, flexible, and stretchable electronics reveals the highest interest of researchers, scientists, industries, and market professionals for the global entry and mega opportunities in nanofabrication and flexible and stretchable electronics manufacturing (**Figure 1**a).[2] In addition to the market growth of flexible electronics, the research trend has shifted in recent years, as indicated by the continuous increase in the total number of publications on flexible and wearable electronics studies (Figure 1b). Moreover, the previously reported data revealed that the flexibility of devices underwent extensive progress from plane devices to flexible (2013) and stretchable (2018) devices with a current and future focus on foldable and deformable (2021) devices, as shown in Figure 1c.[3]

The demand for wearable and implantable devices has effectively motivated the market for flexible electronic materials. The concept of wearable electronics eliminates discomfort and the limitations on the monitoring of human movement due to bulky, rigid materials and metal components. Specifically, the most recent advancements in wearable systems provide revised and feasible specifications with respect to contact with soft human skin, thus solving skin breakdown problems. With the significant capacity of the real-time monitoring of human movements, bio-signals, environmental factors, and other physical and chemical changes; intelligent wearables are becoming increasingly pervasive. Moreover, they benefit the data economy in various application areas such as, education, fashion, healthcare, energy manufacturing, and security, with an estimated increase of 150 billion USD by 2026 for wearable shipments.[4] At present, research is focused on the construction of highly flexible, soft, non-irritating, and nontoxic characteristics, in addition to cost-effective processes.[5]

The realization of the abovementioned multi-characteristics in terms of variable flexibility, action mechanisms, and utilization modes require a significant investigation of flexible

M. Hassan, G. Abbas, N. Li, X. Xu, Z. Peng
Key Laboratory of Optoelectronic Devices and Systems of Ministry of Education and Guangdong Province
College of Physics and Optoelectronic Engineering
Shenzhen University
Shenzhen 518060, China
E-mail: xiuruxu@szu.edu.cn; zcpeng@szu.edu.cn

A. Afzal, Z. Haider
Department of Electronic Science and Technology
University of Science and Technology of China
Hefei 230027, China

S. Ahmed
College of Chemical Engineering and Materials Science
Zhejiang University of Technology
The State Key Laboratory Breeding Base of Green Chemistry-Synthesis Technology
Hangzhou 310014, China

C. Pan
Beijing Institute of Nanoenergy and Nanosystems Chinese Academy of Sciences
CAS Center for Excellence in Nanoscience National Center for Nanoscience and Technology (NCNST)
Beijing 100083, China

The ORCID identification number(s) for the author(s) of this article can be found under https://doi.org/10.1002/admt.202100773.

DOI: 10.1002/admt.202100773

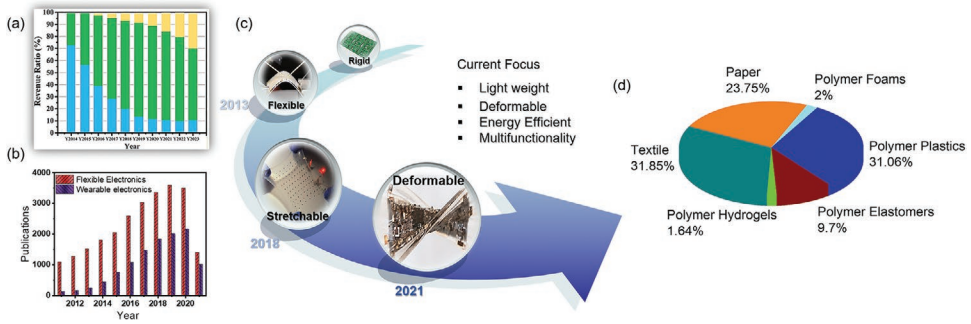

Figure 1. a) Global revenue ratio of stretchable, flexible, and rigid electronics. b) The number of publications for the last 10 years for ''wearable electronics'' and ''flexible electronics.'' c) Graphical presentation for the development in the flexibility of devices. d) Relative distribution of a number of the paper published for last 10 years for different polymer substrates including polymer plastics substrates with the keyword, (PET substrate, PI substrate, PEN substrate, and PC substrate) and polymer elastomer substrates with keywords (PDMS substrate, PU substrate, TPU substrate, SEBS substrate. Other substrates including polymer hydrogels, polymer foams, textile substrate, and paper substrates data are also indexed in the Web of Science in June 2021.

substrates. In addition, flexible substrates play a critical role in importing several characteristics to realize various properties such as user comfort, flexibility, and the capacity to be fashion-designed and miniaturized.[6] In general, the device infrastructure in a flexible and wearable system comprises three main constituents: a conductive network, a base substrate, and a functional material layer. All three components should be configured and hybridized to fulfill the on-demand requirements of flexible electronic devices. Among these components, the substrate governs the overall device properties, which are dependent on the material composition.[7] Furthermore, to achieve excellent mechanical robustness, a high electronic performance, and the critical characteristics required for flexible and wearable devices; the selection and integration of substrate technology with suitable features is necessary. These features may include mechanical flexibility, wettability, permeability, biocompatibility, bioresorbability, heat resistance stability, surface smoothness, low thickness, low cost, and optical transparency properties. Additionally, for a system to endow stretchability and mechanical flexibility, different design strategies and engineering methodologies are critical for the modification of the device structure and its arrangement.

The most recent reviews on flexible and wearable electronics were focused on functionality, the individual demonstration of materials,[8] structures and processes,[6,9] and device applications including electronic skins,[8a,10] energy systems,[11] displays,[12] and health care applications.[8b] However, these reviews were limited with respect to the scope of substrates considered for flexible and wearable systems.

This paper presents an overview of the progress of flexible and wearable systems with focus on critical flexible substrates for integrating flexibility and stability, to realize the construction and operation of flexible electronic devices. We provide a comprehensive list of selection rules in terms of the chemical, thermal, mechanical, adhesion, and biocompatible characteristics required for substrate selection in flexible electronic devices. In addition, a brief discussion is presented to highlight the general and state-of-the-art achievements in strategies for the design, assembly, fabrication, and application of flexible substrates with respect to flexible and wearable devices. This is to validate the use of flexible substrates as one of the most effective platforms for providing excellent adhesion characteristics and device stability under high compression, stretching, or twisting conditions; thus resulting in superior performances and a higher controllability in various potential applications. Finally, a discussion is presented on the future challenges and perspectives on flexible substrates, including the environment necessary to catalyze the current progress.

2. Advantages and Combined Property Requirements of Substrates for Flexible Wearable Electronic Devices

The concept of flexible electronics comprises various features, such as the technology, electronic materials, action mechanisms, variable flexibility, and utilization modes; in addition to the advantages, disadvantages, and limitations. In a flexible electronic system, the main component involves the selection of a substrate with an exceptional blend of performance characteristics, thus ensuring suitability for all applications. The flexible substrate-covered system surrounding the electronic components is bendable, thus allowing for various degrees of flexibility; including bendability, rollability, elastic stretchability, and permanent deformability.[13] Furthermore, flexible substrates exhibit a bending capacity while maintaining the other properties; and excellent adhesion during compression, stretching, or twisting. Compared with rigid substrates, flexible substrates impart various properties to flexible electronic devices, including flexibility, low mass and thickness, high mechanical strength, low cost, and the capacity for modification. In addition, the increased use of thin-film modules can drive the demand for flexible substrates during the forecast period. The extensive use and increasing demand for flexible substrates in medical and healthcare applications, in addition to consumer electronics applications, is a key opportunity for market growth. Therefore, the market size of flexible substrates is projected to reach 775.8 million USD at a compound annual growth rate (CAGR) of 14.0% from 2018–2023, thus demonstrating rapid growth due to the increasing use of flexible substrates.[14] The importance of flexible substrates was demonstrated in several studies based on

the use of these substrates over the past decade (Figure 1d), thus indicating increasing research attention on flexible substrates for flexible and wearable devices.

To establish flexible and wearable systems, it is necessary to achieve the mechanical flexibility and stretchability of the substrate. Generally, the following issues may be considered for the selection of a substrate (thin films, textiles, or fibers) to prepare flexible wearable devices. 1) Thin film-based substrates are readily obtained, and their performance is relatively stable when compared with textile- or fiber-based devices. 2) With the development of wearable electronics, long-term on-skin devices are in high demand for the marketing of future wearable devices. Traditional thin-film flexible substrates are typically limited by their inhibition of air and sweat penetration, which does not allow for long-term use and prevents an appropriate fit to the human skin. In this case, textile-based flexible sensors are ideal due to their excellent permeability of air, sweat, and skin adhesion.[15] 3) For several organic or quantum dot-based flexible wearable devices on light-emitting devices (LEDs) or transistors, the device performances are significantly related to the surface roughness of the substrates.[16] 4) In general, mechanical properties such as the flexibility and stretchability of thin films and fiber substrates are similar for the same substrate materials. However, when the substrates require higher flexibility and stretchability, the strains can be significantly improved by fabrication into textile structures.[17] 5) The reduction in the device size and increase in device density were reported to significantly improve the performance of flexible wearable devices. Thin films and fiber-based devices can be fabricated by the shadow mask-assisted chemical and physical vapor deposition method or solution process, and their film thicknesses or diameters can be decreased to the nanoscale. For example, Kottapalli et al. reported 1D flexible piezoresistive sensors from single carbon nanofibers, where the diameter of a single nanofiber was 200–600 nm. The gauge factor was a maximum of 11.4, which is higher than that of carbon black based thin-film devices by factors of 5–10; and an excellent linearity performance was demonstrated.[18]

The comprehensive list for the selection of substrates includes various physicochemical aspects, including thermal stability, chemical stability, surface smoothness, adhesion properties, water repellency, permeability, and optical clarity. However, for wearable systems intended for contact with the human body, biocompatibility, and bioresorbability allow for the substrate to be safely used over long periods of time. Furthermore, the scalability of the substrate is critical for the large-scale availability of flexible electronics. Several properties of the substrate are listed in **Table 1** and illustrated below.

2.1. Mechanical Flexibility

The term flexible refers to the tolerance of various mechanical deformation modes. For flexible electronic devices, the substrate should undergo deformation while retaining the functional characteristics and electronic performance parameters under high strain levels. However, in flexible electronic devices, the flexibility requirements vary significantly due to the wide application range. For example, high strain implementations are required for implantable sensing/communications devices that involve integration directly onto the skin or other organs; whereas other applications involve small and repeated strain cycles. Additionally, another series of applications involves the acceptance of moderate one-time strains.[19] In general, flexible substrates exhibit inherently ductile-plastic behavior that prevents mechanical fracture beyond the elastic limit. With an increase in ductility, the strain limit is increased, thus resulting in increased flexibility and elongation in the substrate. Hence, combining the mechanical requirements of the substrate such as a low Young's modulus, high strain, and high elastic limit; flexible and stretchable systems can be realized.[20] Among other requirements, the material stiffness commonly expressed in terms of the Young's modulus is defined as the ratio of the strain to stress in the linear elasticity system of uniaxial deformation. A low modulus value of the substrate results in a wide stress range, which exhibits desirable properties with no degradation of the mechanical and electrical properties. Moreover, with the downscaling of the thickness of polymer plastic substrates such as, polyethylene terephthalate (PET) and polyimide (PI), the modulus can be reduced by decreasing the film thickness, thus resulting in an inversely proportional relationship with the modulus of the strained film. The relationship can be expressed as follows:

$$E = 54.872 \times h^{0.226} \tag{1}$$

where h is the thickness of the film, which is defined both theoretically and experimentally.[21]

To clarify the association between mechanical factors and flexible and wearable devices, **Figure 2** presents various Young's modulus ranges of commonly used substrates for flexible and wearable systems.[22] In addition, during the processing of substrates as electrodes in flexible and stretchable applications, the final stress of the electrodes is directly proportional to the Young's modulus of the substrate that encapsulates the conductive material.[23] Thus, for the enhancement of the flexibility with respect to the elastic modulus, the most critical characteristics are substrate selection and optimization, material structures, and processing methods. For flexible and wearable systems, the substrate should exhibit a low modulus, thus allowing for the full deformation of electrodes above the plane, and the maintenance of significant stretchability after their largest incorporation.[24] For example, polydimethylsiloxane (PDMS) with an elastic modulus of E = 360–870 kPa exhibits an excellent mechanical compatibility under mechanical deformation conditions, thus enabling its high applicability to flexible and wearable systems.

2.2. Stretchability

Large stretchability is highly desirable to deliver an edge for failure, to ensure a high electrode performance. The stretchability of the electrode is expressed in terms of its capacity to retain its conductivity under mechanical deformation. Quantitatively, the stretchability of an electrode is related to the critical strain, which is the state wherein there is a change from the conductive to non-conductive modes. The specific term related to the wearable system can be correlated with the electrode

Table 1. Properties of different flexible substrates.

Substrate	PI	PET	PC	PEN	PDMS	PU	Cellulose paper	Cotton textile
Glass transition temp. (Tg)	155–360	70–110	145	120–155	–125	80	–	–
Melting temperature (Tm)	250–452	115–258	115–160	269	–	180	–	–
Coefficient of thermal expansion (CTE) (ppm °C^{-1})	8–20	15–33	75	20	310	153	–	–
Density (g cm+^{3})	1.36–1.43	1.39	1.20–1.22	1.36	1.03	1.18	1.4	1.55
Working temp. (°C)	Up to 400	–50 to 150	–40 to 130	–	–45 to 200	130	Room temperature (RT)	RT
Water adsorption (%)	1.3–3	0.4–0.6	0.16–0.35	0.3–0.4	>0.1	0.2	-	8.5
Solvent resistance	Good	Good	Poor	Good	Poor	Good	Poor	Poor
Transparency	Poor	Good	Good	Good	Good	Good	Poor	Poor
Dimensional stability	Fair	Good	Fair	Good	Good	Good	Poor	Poor
Ultimate elongation (%)	80	90	1–2	85	50–500	300–800	5–15	7–10
Surface roughness (nm)	30	30	74	15	–	–	50–100	–

capacity to hold strain induced by body motion or skin deformation, which demonstrates a complex structure and reversible stretchability of up to 100%. For wearable applications, soft elastomers prevent mechanical cracks before the elastic limit due to the slight intrinsically ductile–plastic behavior, thus demonstrating stretchability up to the required bonding value, and allowing for out-of-plane deformation. Due to the large strain limit and low elastic modulus, various elastomers such as PDMS, polyurethane (PU), and styrene-ethylene-butylene-styrene (SEBS) are inherently stretchable, which promotes the development of wearable devices with respect to the mechanical properties. At present, the stretchability of electrodes is at a maximum of 1300%, which is achieved by using various elastic components, including polymer elastomers such as PDMS, Ecoflex, and other co-block polymers.[7,25] Other structures such as polymer hydrogels, sponges, and fiber configurations exhibit excellent stretching properties.[26] To date, in numerous studies conducted on stretchable electronics using stretchable substrates, two approaches were identified for the fabrication of stretchable electrodes: 1) Substrate structural modification and 2) the utilization of a naturally stretchable substrate. The first approach involves various patterning structures such as serpentine,[27] fractal,[28] mesh-type,[29] merged,[30] origami and kirigami engineered,[31] and mogul pattern[32] structures. Such stretchable structures containing conductive materials on polymeric substrates demonstrate highly conductive properties under mechanical conditions. In addition to these structures, the island-interconnect structure is excessively used to realize the mechanical stability of electrodes under high strain conditions. This structure is generally fabricated by relocating a pre-lithographic mesh structure to a biaxially-stretched PDMS, following the releasing of the stretched substrate, to bend the interconnecting structure. Based on this technique, the device undergoes no deformation in the island structure by

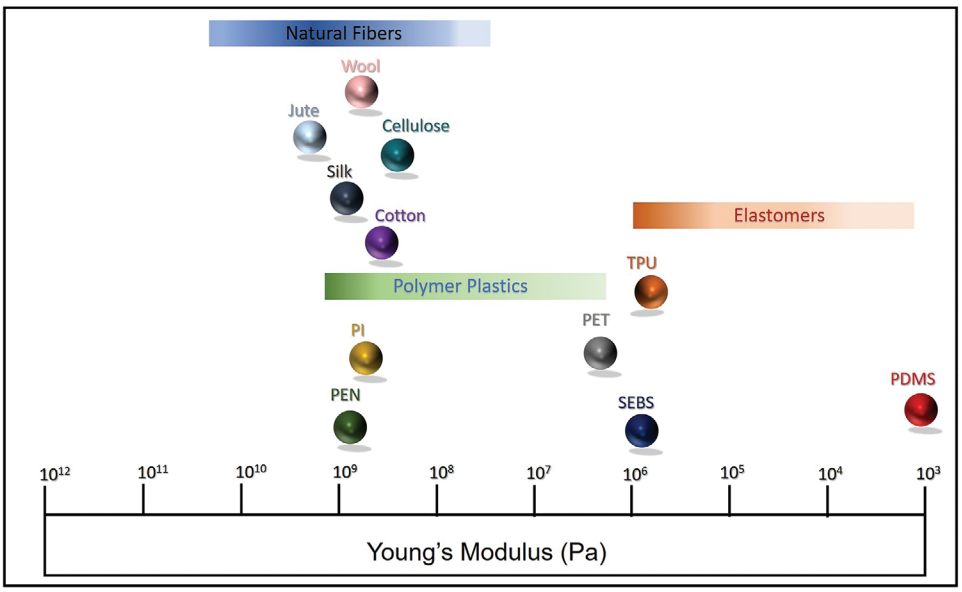

Figure 2. Young's modulus (unit: Pa) of widely used materials for flexible and wearable systems.

the application of the external force, given the capacity of the device to adjust the connecting conductor. Furthermore, the restrain value of the substrate determines the stretchability of the structure. With an increase in the interconnecting length, the stretchability and compressibility of electronic devices increases. Rogers et al. extended the application of the island structure to curve the PDMS surface. By preparing the PDMS on a curved surface, radial stretching was applied to the curved PDMS, and then a prefabricated circuit was transferred onto the strained PDMS. Releasing the strain to the normal position resulted in a curved conductor with high stretchability.[33]

An alternative approach is the fabrication of composites with desirable stretchability and functionality. Instead of fabricating layered systems on substrates, the integration of filler materials can be performed within a plastic system by random or orderly distribution. Due to the non-stretchable properties of several fillers, numerous low-dimensional nanomaterials such as, 1D[34] or hybrid forms[35] are desirable for enhancing stretchability while ensuring transparency. Furthermore, ultrathin 2D materials with excellent inherent conductivity and scalability are potential candidates for future electronics.

2.3. Adhesion Properties

Adhesion is generally measured in terms of the separation of constituent materials by an applied force or energy. Due to the various physical and chemical characteristics of the substrate and metal, poor adhesion occurs, particularly between the elastic substrate and film electrode.[36] In flexible electronic devices, excellent adhesion between the substrate and depositing film is critical due to the high external loads, which provide energy for the separation of poorly bonded materials and render the device inoperable. The governing factor for the adhesion of materials is typically the surface energy, which is provided by the polar and dispersive properties of the substrates. For improved adhesion, the substrates should exhibit a surface energy that is 7–10 dyn higher than that of the adhesive material, given that most adhesives demonstrate an average surface energy of 34–36 dyn cm^{-2}. Among other properties, the high surface contamination and low activation of the substrate are the major causes of a low activation energy. Moreover, during the strong adhesion between layers, cohesive failure (the integral materials may fail individually) occurs before adhesive failure (i.e., failure that occurs at an interface). To achieve excellent adhesion between the substrate and conductive material, two approaches are extensively used: The construction of chemical bonds between the metal and polymer, and physical interlocking. In implantable devices, most chemical bonds are unstable. In such a case, physical methods are superior, such as, the fabrication of a transition layer between the metal and substrate, for the realization of the fulfillment of the adhesion requirements and stability of the device. For example, simultaneous stretching and adhesion properties can be achieved by forming an interlocking layer based on nanoparticles (NPs). However, adhesion problems may occur for composite structures, which involves the dispersion of metal nanowires (NWs) on a gel/polymer. Hence, excellent adhesion properties are critical for the realization of a stable electrode performance. In addition, for the encapsulation of electrodes, the adhesion of the electrode and encapsulation layer is critical, and a double interfacial layer scheme is necessary for suitable electrode encapsulation.

2.4. Permeability

The constituent parts of flexible and wearable devices establish a complex environment comprising gases, liquids, and molecules that may deteriorate the device performance and sensitivity by penetration into the surfaces of flexible devices. Furthermore, stagnant water under the devices due to moisture exposure reduces the device performance and damages the epidermis, thus inducing pain, infection, and delayed healing.[37] The substrate should therefore be impermeable or selectively permeable to proteins, liquid gases, moisture, and other molecular elements that arise from the biological environment. Stretchable substrates are mostly permeable to oxygen and water due to their long chains and larger pore sizes when compared with small molecules.[27a] For example, PDMS, which has excellent flexibility and biocompatibility, exhibits permeability to small lipophilic molecules, organic solvents, and water. This shortcoming is mostly overcome by conducting a multilayer coating process using an additional layer of coating. For example, parylene demonstrates a low moisture permeability and can provide a high stability by tuning the permeability of the substrate surface. Lewis et al. deposited parylene on a PDMS polymerase chain reaction chip device using three steps: vaporization, pyrolysis, and deposition. A layer of parylene with a thickness of 4.5 μm was deposited to decrease the permeability of the device to moisture and gases.[38] Another example is PI, which demonstrates significant durability and flexibility, and is considered a potential candidate due to its lower permeability. Moreover, it can demonstrate electrical properties for a long time-period in water and saline solutions when compared with PDMS.[39] An alternative method is inorganic encapsulation, such as thermal SiO_2 with a silicon nitride bilayer, which has been used to salvage electronic devices in harsh environments and maintain the low permeability to water and ions.[40] Wang et al. fabricated materials via Ga-based liquid metal (LM) and Mg particle mixing, and used them in tumor therapy by arranging Mg–GaIn electrodes on paper substrates. The fabricated device exhibited a greater photothermal conversion effect of ≈61.5% with a low permeability. However, the development of a thin-film barrier may lead to mechanical failure due to the brittle nature of the inorganic materials. Significant research has been conducted on the construction of devices with no brittle components.[40] However, mechanically flexible inorganic films are required for several devices such as flexible organic light-emitting diodes (OLEDs). Thus, further research is required to better understand the failure limits and mechanisms, to overcome the mechanical limits of films, which is critical for the realization of future flexible and wearable devices.

The high permeability of the substrate allows for excellent breathability, which is considered as critical for wearable systems, as it allows for the long-term wearing and firm adhesion of wearable systems through perspiration. For example, the

Table 2. Properties of flexible polymer substrate-based devices.

Substrate	Processing method	*T* [°C]	Material deposited	Typical devices	Ref
PI	Screen printing	250	Ag NPs	Conductive boards	[71]
	Inkjet	150	Ag NPs	Antennas, OLEDs,	[101]
	Bar coating	150	Ag NPs	Printed electronics applications	[102]
	Inkjet	–	Cu NPs	Radio frequency identification	[103]
	Inkjet	300	GO	Electric circuits and sensors	[104]
	Spin coating	400	GO	Memory cards	[105]
	Screen printing	Laser	Cu NPs	Electrically conductive films	[79b]
	Inkjet	107–201	Au NPs	Bioelectronics	[106]
	Screen printing	240	Cu NPs	Flexible printed electronics	[12]
	Spraying	–	Ni NPs	Electronics applications	[107]
	Spin coating	–	Ni NPs	Electrochemical sensors	[8c]
	Gravure	250	rGO	Printed electronics.	[108]
	Inkjet	250	rGO	Printable ink	[109]
	Inkjet	400	rGO	Inkjet printing	[110]
	Screen printing	350	rGO	Printed flexible electronics	[111]
	Screen printing	300	rGO	High-resolution screen printing	[112]
	Screen printing	–	rGO	Printed flexible electronics	[111]
	Inkjet	–	rGO	Wearable e-textile	[113]
	Inkjet printing	RT	MnO_2	Flexible micro-supercapacitor	[86b]
	inkjet printing	100	Single-walled carbon nanotubes (SWCNTs)	Conformal Electronics	[114]
PET	Inkjet	–	rGO	Printed electronic devices	[115]
	Inkjet	RT	Ag NPs	Printed devices	[8c]
	Inkjet	–	Ag NPs	Capacitive pressure/touch sensors,	[116]
	Inkjet	120	Ag NPs	Flexible and wearable electronics.	[117]
	Lithography	RT	Ag NPs	Flexible electronic applications	[118]
	Inkjet	RT	Ag NPs	Flexible solar cells	[119]
	Inkjet	–	GO	Wide band Dipole-Antenna	[120]
	Inkjet	HBr,80	GO	Flexible electronics	[121]
	Screen printing	HI,80	GO	Circuit screen printing	[122]
	Inkjet	HI,100	GO	Carbon transistor	[123]
	Inkjet	-	GO	Sensors and electrodes	[124]
	Inkjet	HBr,80	GO	Flexible and elastic electronics	[125]
	Spray coating	–	CNTs	Field-effect transistors	[126]
	Spray coating	–	CNTs	Conducting thin films	[127]
	Spray coating	–	CNTs	Transparent conducting films	[128]
	Screen printing		rGO	Flexible Printed Electronics	[83]
	Spray coating	–		Flexible Supercapacitors	[88]
	spray coating	100	WO_3	Electrochromic Supercapacitor	[129]
	Screen printing	140	SWCNTs	Thin-Film Transistors	[130]
	bar-coating	60	Ag NWs	Force-Sensitive Touch Screens	[91]
	Inkjet printing	150	–	Stretchable Transistor	[95]
	Screen printing	120	LiF	Organic Light-Emitting	[82a]
	Inkjet printing	150	–	Stretchable Transistor	[95]
	Inkjet printing	60	Ti_3C_2Tx	Micro-supercapacitors	[89]
	spin-coating	–	PiI_2T-Si	Pressure sensitive OTFTs	[131]

Table 2. Continued.

Substrate	Processing method	T [°C]	Material deposited	Typical devices	Ref
	Spin coating	RT	Ag NWs	Strain sensor	[132]
PEN	Inkjet	150	Ag NPs	Antennas, OLEDs, organic	[101]
	Inkjet	–	Ag NPs	Photovoltaics	[133]
	Inkjet	–	Ag NPs	OLED and OPV applications.	[134]
	Drop casting	Laser	Cu NPs	Printing nano particle ink	[135]
	Air-brush	–	Cu NPs	Flexible Electronics	[136]
PDMS	Inkjet printing	RT	Ag NWs	Microfluidic Pressure Sensor	[137]
	electrospinning	RT	PVDF-HFP	Pressure sensor and nanogenerator	[138]
	Screen printing	150	CNTs	Strain sensors	[139]
	Physical interaction	–	Pt	Strain-gauge sensor	[140]
	Inkjet printing	120	Ag NPs Ink	Printed microelectrode arrays	[86a]
TPU	Dip coating	140	rGO-PU	Piezoresistive sensor	[93]
	Screen printing	90	Carbon ink	Carbon-fiber supercapacitors	[141]

high permeability of the substrate to water vapor and gases decreases the potential threats of skin inflammation by not blocking the sweat gland ducts.[41] Recent reports demonstrated that by controlling the porosity and pore size of the substrate materials, the successful modulation of the selective permeability can be realized.[42] Alternative substrates such as fabrics/textiles demonstrate porous structures and excellent permeability.[43]

2.5. Water Repellency

As mentioned previously, the stagnant water in the flexible devices due to the environmental moisture diminishes the device performance and sensitivity, and causes skin injuries in the case of wearable systems. Hence, the surface modification of the substrate by chemical or structural treatment is highly desirable, as it changes the water affinity and renders the substrate resilient to water absorption or water passage from sweating, breathing, showering, and washing.[44] Various methods for utilizing the water affinity of flexible substrates were recently developed, all of which contribute to the development of water repellency.[25] Numerous polymer substrates, including PET, PDMS, silicon rubber, and Ecoflex, are hydrophobic. Among them, PDMS is commonly used due to its hermeticity deficiency in water vapor over time. To solve this issue, significant research was conducted on the use of alternative hydrophobic elastomers such as poly(styrene-isoprene-styrene) in sweat sensors, which demonstrates excellent barrier properties when compared with PDMS.[45] In addition, the device performance and sensitivity can be enhanced by making the substrate superhydrophobic, which has a direct influence on other device-building processes. However, when hydrophilic nanomaterials are coated on the substrate, a surface treatment is carried out beforehand to increase the surface hydrophilic functional groups; which leads to the penetration of water from the external environment.[46] Thus, the hydrophobic properties of the substrate should be considered to provide sufficient repellency to water.

2.6. Softness

The softness of a substrate is generally demonstrated in terms of the Young's modulus, including the apparent and intrinsic modulus. For biomedical devices, both stretchability and softness are critical to ensure mechanical compatibility between the human tissue and the electrode. However, any mismatch between the properties results in tissue damage or infection. Therefore, the simultaneous realization of these two properties is highly desirable for biocompatible devices. Softness has not been comprehensively investigated in previous studies when compared with substrate stretchability. Moreover, to examine this feature, substantial research is necessary to study the tissue interactions with the implanted device at the cellular level. The action mechanism of the cellular reaction to the implanted device has not been determined. Polymer elastomers such as PDMS, which is a commonly used elastic substrate for stretchable electrodes, were investigated to study the match between the electrode and human tissue. In addition to the softness of the substrate for stretchable electrodes, numerous techniques and materials were used to ensure the softness of the conductive layer, which is essential for implantable devices. Finally, the switching between the softness and stiffness of the electrodes is critical, given that softness and stretchability play a minor role in surgery operations, especially for deep brain stimulation, which requires the insertion of an electrode into the brain. Therefore, removable rigid substrates and shape-memory polymers can be utilized for the insertion of stretchable electrodes. However, for minimal injury to the tissue during insertion and removal, these materials should be further optimized.

2.7. Chemical Stability

The fabrication process of flexible electronic devices requires solvents or chemicals, which damage the substrate. Hence, the substrate should be compatible with acidic, basic, and other solvents with low-boiling points. Moreover, protecting the substrate from such chemicals by fabricating a thin-film barrier is

ideal; however, it is not practical. In general, a chemical hard coating on the substrate side can provide a distinct method for protecting the substrate, with the advantage of an excellent barrier against permeation by atmospheric gases.[47]

2.8. Thermal Stability

For flexible electronic devices, the high stability of the substrate with respect to temperature is highly desirable. Specific processes require different temperatures and changes with respect to temperature. Thermal stability generates dimensional stability, which is critical for flexible substrates under high-temperature conditions, given that the reliability and quality of flexible devices are mainly dependent on the dimensional stability of flexible substrates. To optimize thermal and dimensional stability, a general rule is applied for tolerable temperature differences ($|\Delta CTE \cdot \Delta T| \leq 0.1$ 0.3%). The variations in the coefficients of thermal expansion (CTE) between the substrate and device layer and the temperature deviation during manufacturing are represented by ΔCTE and T, respectively. Moreover, the temperature difference between the device film and substrate may result in the convex bending of the substrate, thus leading to various failures in the fabrication of the devices, including cracking and delamination. Hence, to prevent thermal cracking under thermal cycling conditions, the device film should be designed to withstand thermal expansion mismatches.

2.9. Surface Smoothness

To avoid adverse effects on the device performance, control over the surface texture and morphology of the substrate is required. An ultra-smooth surface with a smoothness of (1 nm rms roughness) and no local surface abnormalities (e.g., spikes) greater than a several tens of nanometers is desirable. However, over short distances, asperities and roughness should be avoided, although they are acceptable over long distances. In general, metal substrates demonstrate short-and long-distance surface roughness characteristics, whereas plastic substrates may only demonstrate long-distance roughness characteristics.[47a]

2.10. Optical Clarity

An optically transparent substrate is critical for transmissive or bottom-emitting displays with low birefringence, especially for liquid-crystal displays (LCDs). For flexible display applications, a light transmission of >85% over 400–800 nm is required, with a haze value of less than 0.7%. For example, it is improbable for polymer plastic films such as PET and polyethylene naphthalate (PEN) to be used as base substrates, as they can change the polarization state due to their high birefringence values. However, polyester films are desirable for enhancing LCD performance, for example, brightness-enhancing films. In addition, amorphous polymer films exhibit low birefringence values, and are considered to be more appropriate as base substrates for LCDs.[48] Numerous PDMS composites with metals exhibit high transparency in the visible light region, including PDMS/(Au NWs/Ag NWs) with a transparency of 86%,[49] Ag NWs/PDMS with a transparency of 88.3%,[30] and Ag NPs/PDMS with a transparency of 86%.[50] In addition, PU demonstrates a high transparency of 77% for (NPs)/(PU).[51]

2.11. Biocompatibility

The biocompatibility of a material refers to its capacity to realize a suitable host response in a specific scenario. For wearable systems, the biocompatibility of the substrate is considered as critical, as it requires direct association with biological interfaces. Various factors such as the surface charge, chemical composition, and pH are responsible for inducing cytotoxicity and decreasing biocompatibility. Despite the numerous factors governing biocompatibility, various materials such as, PDMS, cellulose substrates, and silk-based textile substrates are biocompatible. In addition, to increase biocompatibility, various naturally occurring materials, including hard gelatin, starches, and caramelized glucose, have been demonstrated as suitable substrates for electronic devices.[52] Similarly, biomimicking nanofibril polymers such as chitin, cellulose, and silk, which generate hierarchical structures with natural bio-repetitive sequences, are suitable substrates.[53] Bacterial cellulose (BC) was recently reported as a biocompatible fiber for wearable health monitoring applications.[54] An alternative strategy to achieve biocompatibility is to encapsulate flexible devices with biocompatible substrates, and various attempts were made to encapsulate devices with PU,[55] Ecoflex,[56] and PDMS.[47c]

2.12. Bioresorbability

Bioresorbable substrates eliminate environmental, chemical, and physical damage by dissolving, disintegrating, or decomposing without environmental and toxic residues. This concept was first presented in 2009, and significant research was conducted on the integration of such bioresorbable substrates into flexible and wearable electronics.[57] Moreover, resorbable substrates were used to improve the conformability of devices. Litt et al. reported electrocorticography and cardiac electrophysiology devices on mechanically compliant substrates.[58] By using bioresorbable silk substrates, the conformability of the devices was further enhanced for deposition or implantation within or on the surface of the brain.[59] Moreover, significant research was conducted on the development of biocompatible and bioresorbable substrate-based devices, thus allowing for the integration of devices with the human body.

3. Substrate-Based Flexible Electronic Devices: Processing Technologies, Applications, and Challenges

Flexibility can signify extensive information to the manufacturers and users of flexible electronics. While considering mechanical properties, flexible devices are categorized into three categories: Rollable, bendable, stretchable, and

permanently-shaped.[60] Flexible and wearable electronic devices generally use flexible substrates such as, polymer films, paper, and textile fabrics because they have excellent mechanical properties, are readily processed, and are highly compatible;[7] thus demonstrating significant versatility in their proposed applications, including energy devices (supercapacitors, batteries, and solar cells), sensors, and other electronic devices such as photovoltaics, transistors, and display devices.

In this section, a broad overview of substrate-based flexible electronics is presented, with focus on design strategies and engineering methodologies, including their principles, operations, and specific applications with advantages and disadvantages.

3.1. Polymer Substrates Based Flexible Electronic Devices

Most flexible and wearable devices are designed to perform numerous applications during attachment to a body without support. To realize these devices for flexible and wearable applications, their components and materials should exhibit bendability or foldability. Different from conventional devices fabricated on hard 2D substrates, flexible devices should follow the contours of the human body. Hence, the construction of electronic components on flexible substrates is critical. Due to their unique features such as low cost, low thickness, low mass, and excellent mechanical deformability; flexible polymer substrates have been extensively researched to meet the flexibility requirements of flexible electronic devices.[61] Moreover, polymer substrates can endure the harsh environmental, chemical, and thermal environments required for the construction of electronic circuits while sustaining their mechanical flexibility. Plastic substrates, including thermoplastic semicrystalline polymers such as, PEN and PET; thermoplastic non-crystalline polymers including such as polyethersulfone and polycarbonate (PC); and materials with high glass transition temperatures such as, polycorbonyl, PI, and polyacrylates are the most common flexible substrates utilized in flexible electronics due to their applicability to the most advanced semiconductor processes such as low-cost printing and coating processes. Considering common polymer plastic substrates such as, PET, PEN, and PI with only bendability and no stretchability, the development of elastic substrates with excellent stretchability is necessary. Polymer elastomers such as, PDMS, thermoplastic polyurethane (TPU), Ecoflex, SEBS, and polymer hydrogels are established stretchable substrates with low elastic moduli and high stretchability.[62] Several properties of polymer substrates are presented in Table 1. In addition, flexible and wearable devices also require high compressibility and excellent mechanical elasticity. Hence, polymer sponges are considered as excellent substrate structures for providing numerous advantageous such as a large strain range, low mass, and low cost. Various well-established sponge materials such as, TPU foam, TPU/epoxy sponge, PI sponge, poly(3,4-ethylenedioxythiophene) polystyrene sulfonate (PEDOT:PSS)@Melamine sponge, metal (Cu, Ag/Cu, Au/Cu)-coated PDMS sponge, and graphene and carbon black coated PU sponge have been reported as suitable templates.[63]

In addition to their highly flexible properties, polymer substrates are subject to several limitations such as thermal and dimensional instability when compared with glass substrates, high permeability to oxygen and water, and significant shrinkage by heating and cooling cycles.[64] The glass transition temperature (T_g) should be compatible with the device process temperature for device fabrication, given that prolonged heating above the threshold temperature of polymer substrates causes irreversible deformation and the disruption of the films, thus resulting in the performance degradation of the printed devices.[12] Hence, the most suitable substrate for flexible electrode preparation can be selected depending on the application.

3.1.1. Functional Materials and Methods for Development of Conductive Polymer Electrodes

Substrate modification is mainly dependent on the type of substrate used. Numerous materials, including both inorganic and organic materials, have been reported for the fabrication of conductive polymer substrates for implementation in flexible electronic devices. Inorganic materials such as, 0D, 1D, and 2D nanomaterials of metals and metal oxides demonstrate high electrical conductivities. However, they are costly and subject to processing difficulties. Alternatively, organic materials such as conductive polymers and carbon nanomaterials are low cost and demonstrate high flexibility and solution processability. However, they demonstrate poor conductivity and long-term stability.[8b] In addition, the fundamental techniques utilized are mostly additive deposition techniques that involve various printing and coating methods. In these techniques, new materials are not produced, and mild conditions are required to process polymer substrates using the abovementioned materials for flexible electrode fabrication.

Advanced Printing Technologies for Polymer Substrate: In the printing process, the selection of the polymer substrate is highly dependent on the active material; however, the polymer substrate should demonstrate several general properties such as a relatively low mass, low cost, and suitability for the manufacturing of printed electronics. Similarly, properties such as the electrical, structural, and optical transparency of polymer substrates significantly influence the performance of printed electronic devices. For printed electronics, various polymer substrates have been utilized with major classification into three categories: i) Semi-crystalline, ii) amorphous, and iii) solution-cast amorphous.[65] Due to their excellent mechanical properties, ease of processing, and significant barrier to oxygen and water penetration, these polymeric plastic substrates are considered as excellent candidates for printed electronic devices. In addition, elastomers such as PU, PDMS, and the multiblock co-polymer SEBS have been previously used for stretchable and wearable printed devices. In addition, polymeric materials with low melting points[66] or photopolymerizable inks that produce rubbery polymers after ultraviolet (UV) irradiation are commonly used for printing flexible 3D electronic devices.[67] However, the low thermal stability of the polymer substrate limits its utilization for printed electronics in high-temperature sintering because of the low glass transition temperature (T_g) of less than 150 °C; for example, 120–125 °C for PEN, 60–80 °C for PET, and 140–150 °C for PC, with the exception of PI with T_g of 310–365 °C.[68] Hence, the heating of these polymer substrates above

their T_g temperatures for a long time-period causes irreversible deformation, thus resulting in the degradation of the printed device performance.[69] To achieve a highly conductive printing pattern, high-temperature sintering conditions are required to remove the insulating organic dispersants from metal NPs and NW ink, which hinders the formation of a uniform conductive structure upon solvent drying in the ink.[70] To solve this problem, various attempts were made by decreasing the NP size and using an appropriate stabilizing agent with controlled proportions.[69] Alternative sintering methods were developed to heat the printed pattern without disrupting the polymeric substrate, such as, post-printing, thermal, photonic, plasma, microwave, and chemical sintering.[8c]

Furthermore, the printing quality is primarily dependent on the wettability and adhesion properties of the polymer substrate. However, the mechanism of adhesion involves various factors, including the substrate features such as the surface topography, chemical composition, porosity, conductive ink properties, surface energy of the substrate, and surface tension of the ink. In general, most polymers exhibit low surface energy, which poses significant limitations to printed electronics. Thus, various treatment methods such as, inducing roughness on the surface by mechanical means, chemical treatment, flame treatment, and plasma treatment are critical to increase the surface energy of the polymer substrate; thus enhancing the adhesion properties.

Screen printing,[7,12,79b,82a,83,111,112,130] inkjet printing,[8c,89,95,101,103,104,106,109,110,113,115–117,119–121,123–125] and transfer printing are several conventional printing methods developed and improved for printing numerous materials, including conductive polymers, onto various nanomaterials; including 0D, 1D, and 2D materials such as Cu, Zn, Sb, Pb, Ni, Sn, Ti, Ag, In, Bi, Pt, and Au for the fabrication of electrically conductive pathways on various substrates.[6] For example, screen printing is a simple, versatile, and inexpensive mass printing technology extensively used to printing various nanomaterial inks, including Ag NPs[71] and NWs,[72] Cu NPs,[73] 2D graphene,[74] and conductive polymer PEDOT:PSS[75] on polymer plastic substrates such as PET,[74,76] PI,[77] PEN,[78] PC,[79] and polymer elastomer substrates such as PDMS,[80] TPU.[81] Similarly, in the inkjet printing process, plastic substrates that exhibit different properties such as high mechanical strengths, in addition to condensing and hydrophobic surfaces, were adopted due to their excellent printing behaviors.[82] Polyesters such as, PC,[83] PET,[84] PEN,[85] and PI[6] have been extensively utilized for the injection printing of numerous materials such as WO_3-PEDOT:PSS, MXene inks, Ag NPs, PEDOT:PSS, and graphene due to their clarity, moisture absorption, chemical resistances, CTEs, and cost (**Figures 3**a,b). Similarly, polymer elastomer substrates and gels were subjected to inkjet printing for stretchable and flexible electronic devices.[86] In addition to the abovementioned printing process, the other printing techniques involve transfer printing, which is applicable to various polymer substrates, and is based on transferring functional materials over a large substrate target area. For example, Ko et al. described a smart printing approach for the transfer printing of semiconducting materials with micro/nanostructure arrays on diverse substrates.[87] Figure 3c presents the damage-free peeling and transfer of honeycomb Si micromembranes onto various rigid and flexible substrates such as SiO_2/Si, PI, and thin PET substrates. Furthermore, by patterning an n-type semiconductor on a semiconductor memory operating system (CMOS) ring oscillator, Marotrao et al. devised a roll-to-roll (R2R) printing technology to bridge quick response (QR) codes in R2R-printed CMOS-based ring oscillators.[88] A poly (ethylene imine)-based n-doping ink was prepared and applied by a R2R gravure printing system.

Fabrication by Functional Coating: Coating is one of the most common methods for accumulating functional inks on various substrates. Due to its simplicity and low cost, this technique is desirable for preparing electrodes for flexible electronic devices. Polymer substrates exhibit a wide range of characteristics, including flexibility, low mass, low cost, and machinability. Moreover, they lack several features such as, stability, active functional groups, conductivity, and the barrier effect. Polymers differ by long polymer chains that constitute their mechanical properties, which have different molecular masses. However, these chains are mostly observed at the surface of the polymer, thus resulting in a reduction in the glass transition temperature near the surface. Hence, a boundary with a weak surface energy is obtained on the surface of the polymer substrate. Furthermore, the surface of the polymer substrate lakes in functional groups and also shows contamination. Therefore, various techniques such as plasma treatment are utilized to activate the surface of the polymer substrate for the subsequent coating process. Short-time plasma exposure results in the generation of free radicals, which facilitates the coating process. For example, in a previous study, after 5 min of N_2 plasma pre-treatment, the PC substrate exhibited excellent adhesion to a SiOx coating. Similarly, the PP substrate exhibited adequate adhesion after 2 min of He plasma treatment.[92]

Dip coating,[93] spray coating,[88,107,126–129] spin coati ng,[8c,105,131,132] and mayor rod coating[91,102] are among the most common coating techniques. Kwon et al. reported a simple dip-coating technique to deposit coating polymer layers onto PET fibers, and revealed the first dip-coated polymer light-emitting displays (PLEDs) on separate fibers with a high luminance of 1000 cd m^{-2} and stable operation under a low bias voltage (<10 V). With the same operation as the dip coating method, infiltrating or soaking is used to coat materials on porous substrates by immersion in a coated material solution. Yu et al. proposed a method using dip-coated conductive sponges to develop a fractured microstructure in a piezoresistive pressure sensor.[90] The typical procedure presented in Figure 3d displays the initial coating of the PU sponge with graphene oxide (GO) nanosheets, as synthesized via a viable dip-coating method. After centrifugation, the GO coated on the PU sponge was reduced into reduced graphene oxide (rGO) by immersion in a hot HI solution, which was further converted to a dense and fractured microstructure by hydrothermal treatment. By increasing the adhesion properties with surface pre-treatment, the spray coating technique was applied to various substrates such as PET,[91,93] poly(methyl methacrylate) (PMMA),[94] PDMS,[95] and other polymer substrates. Moreover, PET has been extensively used in spray coating. Tao et al. reported a facile and scalable spray coating technique to deposit Ag NWs/polyvinyl butyral on PET and glass substrates for protection against radiative heat, to minimize energy consumption.[91] An R2R spray technology is shown in Figure 3e, which allows for the continuous fabrication of flexible Ag NWs with dimensions

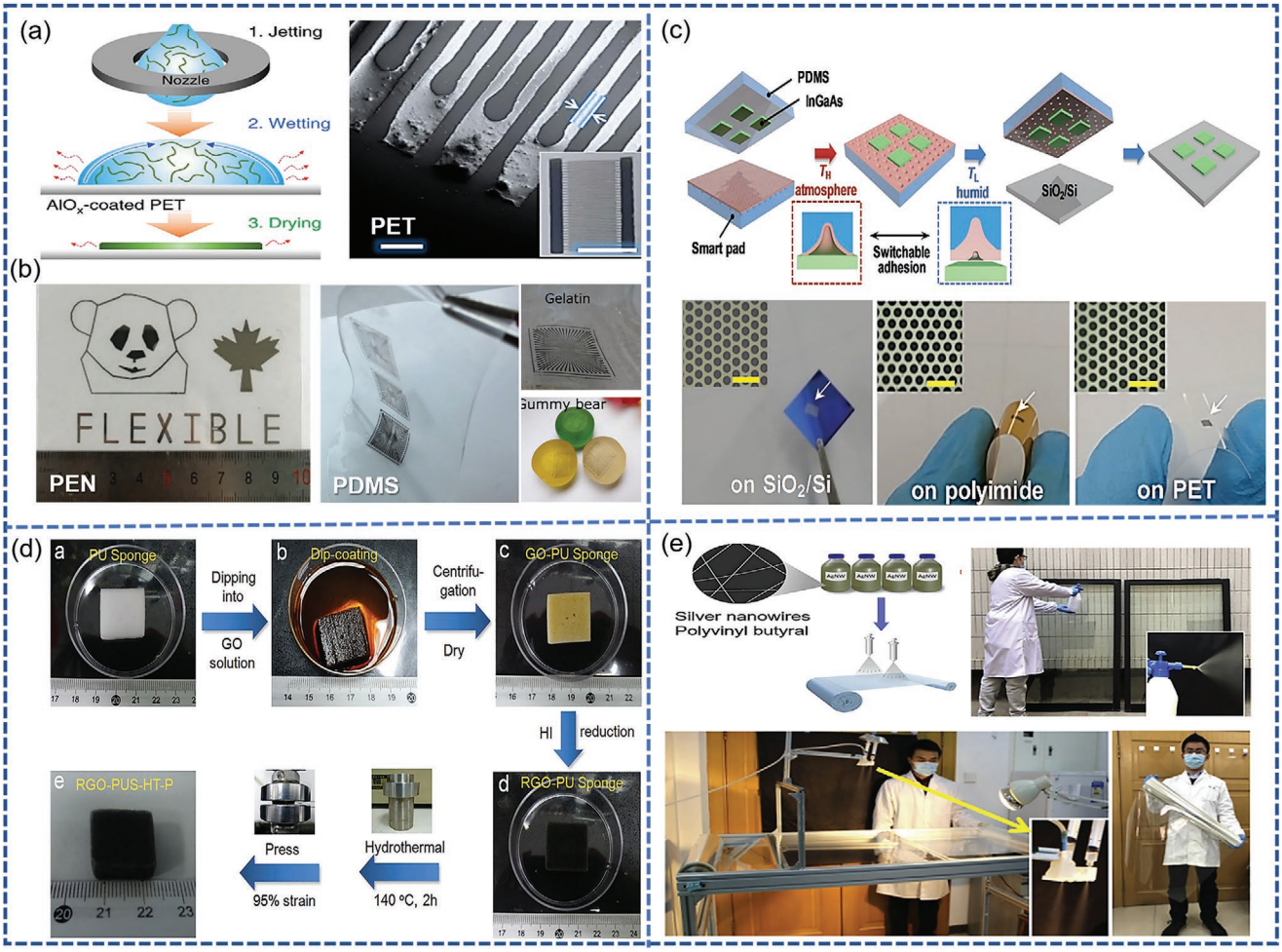

Figure 3. a) Schematic of inkjet printing for MXene with ultrahigh-resolution and its SEM image. b) Image for inkjet printing of AgNPs on flexible PEN substrate with Photograph of printed carbon MEAs on a PDMS, gummy bear, and gelatin substrate. Reproduced with permission.[89] Copyright 2019, Springer Nature; Reproduced with permission.[85] Copyright 2018, Wiley-VCH; Reproduced with permission.[86a] Copyright 2018, Springer Nature. c) Smart printing schematic of InGaAs (square-patterned) onto SiO_2/Si substrates including InGaAs nanomembranes transfer using the smart adhesive pad, consists upon the high and low-adhesion state. An optical and microscope picture of a hexagonally patterned Si membrane is shown at the bottom. SiO_2/Si, PI film, and thin PET substrates were sequentially transferred (from left). Reproduced with permission.[87] Copyright 2016, Wiley-VCH. d) Schematic of synthesis as well as pressure-sensing models of graphene-wrapped PU sponges, RGO–PU, RGO–PU–HT, RGO–PU–HT–P sponges and their SEM images (right side). Reproduced with permission.[90] Copyright 2019, Wiley-VCH. e) Diagram for R2R spray coating of Ag NWs/polyvinylbutyral on PET substrate. Reproduced with permission.[91] Copyright 2019, Elsevier.

of 2 m × 1 m coated on PET films with a high visible range transmittance and low sheet resistance.

An alternative coating method to deposit identical thin films onto flat substrates is the spin coating method, which has been extensively utilized for the deposition of several different materials on various polymer substrates such as PET,[96] PI,[97] PEN,[98] and PDMS.[99] In addition, the Mayer rod method is a widely used technique in which a rod is used to deposit different functional materials in the coating solution and control the coating weight.[100]

3.1.2. Applications of Polymer Electronics in Flexible and Wearable System

There has been a significant increase in research and development for the emerging utilization of flexible substrates, to fabricate electrodes for flexible electronic devices, which can be attributed to their potential applications. The selection of the substrate is dependent on the application. For example, wearable electronic devices require various characteristics for application in fabricated electrodes, such as, softness, stretchability, self-healing capability, comfortability, and multifunctionality. However, for flexible electronic devices, the substrate only requires bendability. In the following section, a discussion is presented on the different applications of polymer substrate based flexible electronic devices, including sensors, energy storage systems, and electronics.

Sensor Devices: For flexible and wearable sensing devices outfitted with a series of simple sensors such as strain sensors, temperature sensors, biosensors, and multifunctional sensors for voice and facial expression detection; polymer substrates with comparatively low range Young's moduli of ≈106–1012 Pa are desirable for the encapsulation layers and skin adhesives. Plastic

Table 3. Properties of flexible paper substrate based devices.

Substrate	Processing method	Material deposited	Transparency	Typical devices	Ref.
Photopaper	Inkjet	Ag NPs	Transparent	Solar cells	[227]
Nano paper	Inkjet	Ag NPs	Transparent	Antennas, OLEDs, solar cells	[107]
Paper	Inkjet	Ag NPs	Transparent	Wires and antennas	[199]
Photo paper	Inkjet	Ag NPs	Transparent	Flexible electronics	[228]
Filter paper	Inkjet	CNTs	Not Transparent	Inkjet printing	[229]
Glassine paper	Screen-printing	Graphene Ink	Not Transparent	Thin-film transistors	[191]
Cellulose paper	Screen-printing	Carbon ink	Not transparent	Self-powered biosensors	[230]
Copy paper	Dry printing process	Ag NWs	Transparent	Patternable electrodes	[231]
Cellulose paper	Dry creeping process	Nitrocellulose membrane	Not transparent	Triboelectric nanogenerators	[232]
Cellulose paper	Dry creeping process	PDMS/Ag paste	Transparent	Strain sensor	[233]
Graphene paper	In situ growth	MnO_2	Not transparent	Supercapacitor	[222]
Printing paper	Laser printing	MXene	Not transparent	Micro-supercapacitors	[234]
Cellulose papers	Sputtering	Ag	Not transparent	Thin-film transistors	[215]
Paper	Electrodeposition	PPy	Not transparent	Energy storage devices	[223]
Filter paper	Filtration	Graphene nanosheet suspension	Not transparent	Energy storage devices	[223]
Whatman filter paper	Solution processed	CNT	Not transparent	Cancer detection	[207f]
Cellulose filter paper	Dip coating	Au NP's	Transparent	Molecular detection	[207a]
Tissue paper	Dip coating	Cu/Au	Not transparent	Triboelectric nanogenerators	[207c]
Printed paper	Gravure printing	Ag NP ink	Not transparent	Heavy metals detection	[235]
Nano-paper	Gravure printing	2,2,6,6-Tetramethylpiperidinyloxy	Not transparent	Radio-frequency identification (RFID) devices	[236]
Nano paper	Inkjet printing	Ag NP	Transparent	Electrical performances	[107]
Paper	Inkjet printing	Cu/Ag	Not transparent	Sensors/nano generators	[237]
Printing paper	Inkjet printing	g10,12-Pentacosadiynoic acid	Transparent	Colorimetric sensing	[196]
Copy paper	Laser printing	Ag NW	Not transparent	Multiresponsive actuators	[203]
Cellulose paper	Laser printing	Pt NP	Not transparent	Functional patterns	[202]
Paper	Laser printing	Silica NPs	Not transparent	Superhydrophobic patterns	[201]
Copy paper	direct laser patterning	Gelatinmediated inks	Not transparent	3D foldable electronics	[204]
Copy paper	Rod-coating	Graphene oxide	Not transparent	Flexible touch screens	[211a]
Paper	3D pen printing	Color dyes	Not transparent	Microfluidic biosensor	[238]
Paper	Screen printing	Ni/MnO_2	Not transparent	Supercapacitors	[239]
Carbon fibers (CNF) paper	Vacuum filtration	Ag NWs	Not transparent	TENG	[205]
Glossy paper	Transfer printing	PEDOT:PSS	Not Transparent	Photovoltaic cell	[240]
Cellulose paper	Spray coating	$CuInSe_2$	Not transparent	Solar cells	[241]
Whatman filter paper	Spray coating	–	Not transparent	Electrochemical devices	[208b]
Nano paper	Spin coating	PEDOT	Transparent	Solar cells	[242]
Copy paper	Pen on paper	Ti_3C_2 MXene	Not transparent	Energy storage	[197a]
Xerox paper	Pen on paper	Silver ink	Not transparent	Flexible electronics	[197d]
Printing paper	Mayer rod coating	rGO	Not transparent	Energy-storage devices	[225]
CNF paper	Electrospinning	CNF	Not transparent	Supercapacitor	[225]

substrates such as PET and PI with high thermal and chemical resistances and inject tattoo paper are a few examples of polymers that can be used in flexible wearable sensors.[132,142] Despite their moduli mismatches with skin, these substrates are utilized due to their high optical transparency, low flexural rigidity, excellent chemical inertness, wide range, and biocompatible formulations. Furthermore, they are compatible with additive printing techniques such as inkjet printing and screen printing. However, the poor breathability and lack of stretchability limit the practical use of these plastic substrates for shrunk designs and applications. For wearable sensing devices, the mechanical compatibility of active and passive device materials is critical.

Passive materials such as substrates and functional materials constitute a major part of the device. Hence, polymer elastomers such as, PDMS,[143] Ecoflex,[144] and TPU are widely used in wearable sensors due to their desirable physical features, including optical transparency, biocompatibility, excellent flexibility, low moduli, and high failure strains. These features allow for a large degree of deformation without tearing and various surface attachment sites, that is, thighs, forearms, and joints.

For the successful integration of these polymer substrates into sensing devices, the first step is the development of a stretchable electrode. The development of numerous nanosized materials with outstanding electrical, chemical, and mechanical properties in conjunction with suitable elastomeric substrates allows for the realization of stretchable electrodes. For example, Pan et al. fabricated high stretchable and transparent electrodes by patterning Ag nanofibers (Ag NFs) on the elastomeric substrate, producing highly conductive and transparent electrode.[145] To produce an excellent conductive network during stretching condition, Ag NFs were assembled in different orientation and only 10% increases in resistance were detected at 100% strain by using random orientation Ag NFs. Goldfield et al. developed strain sensors by embedding a new KI and glycerol solution biocompatible conductive liquid into a silicone elastomer substrate.[137] The strain sensors recorded slight hysteresis at ≈5 Hz, and a gauge factor of 2.2 at 1 Hz, with high flexibility and durability for a minimum of 1000 cycles. Liu et al. recently demonstrated NW-microfluidic (NMH) hybrid strain sensors by combining brittle metal NWs such as, carbon nanotubes (CNTs), Ag NWs, or Cu NWs, and a conductive organic solution (PEDOT:PSS) on an Ecoflex substrate that reacted to strain ranging from 4% to over 400%. Moreover, it exhibited a high sensitivity and durability at low strains, as shown in **Figure 4**a.[146] The strain curve shown in Figure 4b illustrates the mounting of the sensor on the knee skeleton model to stimulate the movement of the ligaments.

The second step is the development of a stretchable design that demonstrates excellent stability under mechanical deformation and prevents fractures in the electrode and performance degradation. Various stretchable platforms have been extensively utilized to realize stretchability, including wavy structures, serpentine interconnect structural configurations, sponge structures, folding patterns based on origami architecture, fiber configurations, and intrinsically stretchable materials. Rogers et al. demonstrated a temperature sensor containing a serpentine trace configuration of gold (Figure 4c,d), in which a thin metal film was laminated between PI and Ecoflex polymer films. Due to its stiffness, the PI layer provides resilience, whereas Ecoflex supports the overall stretchability of the system.[147] In another study, Ren et al. fabricated an Au nanomesh structure with a PDMS electrode, which demonstrated superior conductivity and stretchability. The electrode exhibited a small conductivity change from ≈21 to 67 Ω sq^{-1} at a strain of 160%.[148] Recently, Wang et al. reported skin-inspired stretchable and conformable matrix network by connecting 100 sensory nodes via different wires.[149] The stretchable and expandable structures integrated on a PI network outspread the e-skin sensing functionality to multifunctional sensing including temperature, humidity, in-plane strain, magnetic field, light, proximity, and pressure.

In addition, for implantable skin sensors, the substrate biocompatibility is critical for their successful application to skin or other organs. Despite the numerous factors governing biocompatibility, various substrates such as PDMS, cellulose substrates, and silk-based textile substrates are biocompatible. In addition, to increase biocompatibility, various naturally occurring materials such as, hard gelatin, starches, and caramelized glucose have been demonstrated as suitable substrates for electronic devices. Furthermore, for bodynet and implantable systems, the long-term compatibility of the stretchable electrode is the most critical requirement, and significant research has been conducted to alter existing electronic materials for adaption to organisms, and not for long-term usage. Therefore, cell packaging is desirable due to the accommodation of foreign matter by the organism in vivo.[150] For example, a PDMS cover was developed as a wireless battery-free electronic sensing device that allows for the simultaneous detection of sweat during exercise.[151] Apart from polymer elastomers, hydrogels are used for various implantable biomedical sensors such as, pH and glucose sensors.[152] Wang et al. reported a soft skin type triboelectric nanogenerator (TENG) for biomechanical energy harvesting and touch sensing by utilizing two commonly used elastomers, namely, PDMS or commercial very high bond, and ionic hydrogel as the electrification layer and electrode.[138] The hydrogel was sandwiched between two elastomer films; thus resulting in a highly stretchable (strain of 1160%) and transparent (maximum transparency of 96.2%) soft skin TENG-based tactile sensor, which was used at five different pressure points, as shown in Figure 4e,f.

Hence, for the construction of flexible and stretchable sensors for wearable applications, the critical aspects include flexible and stretchable substrate selection, durable materials, novel and simple processing techniques, and deformable electronic models.

Energy Storage Devices: Compared with other substrates such as metal and carbon-based substrates, polymer substrates are non-conductive and cannot be applied directly as electrodes for energy storage devices. However, due to the large flexibility and simple processability of polymer substrates, they can be modified using various conductive materials for their successive utilization as current collector electrodes for supercapacitors,[153] batteries,[154] nanogenerators,[155] and solar cell devices.[156]

The major mechanical deformation property of flexible energy storage electrodes is their capacity to tolerate the bending state to a certain curvature. Two parameters are typically used to describe the bending conditions of electrodes, namely, the bending angle and radius. In addition, the end-to-end distance (L) is used with the bending direction to represent the bending condition. However, it only demonstrates the qualitative analysis of the bending process, and is not suitable for the comprehensive analysis of the bending states of flexible energy storage electrodes. A schematic description of the θ, R, and L values of flexible energy storage electrodes is presented in **Figure 5**a. The validation of these three parameters follows a pattern in which the length of the device can vary if the bending angle and radius are constant. Longer devices may be less impacted during bending due to the localization of the stress region. Similarly, by maintaining R and L; θ can be varied, thus resulting in different stressed areas. Hence, to

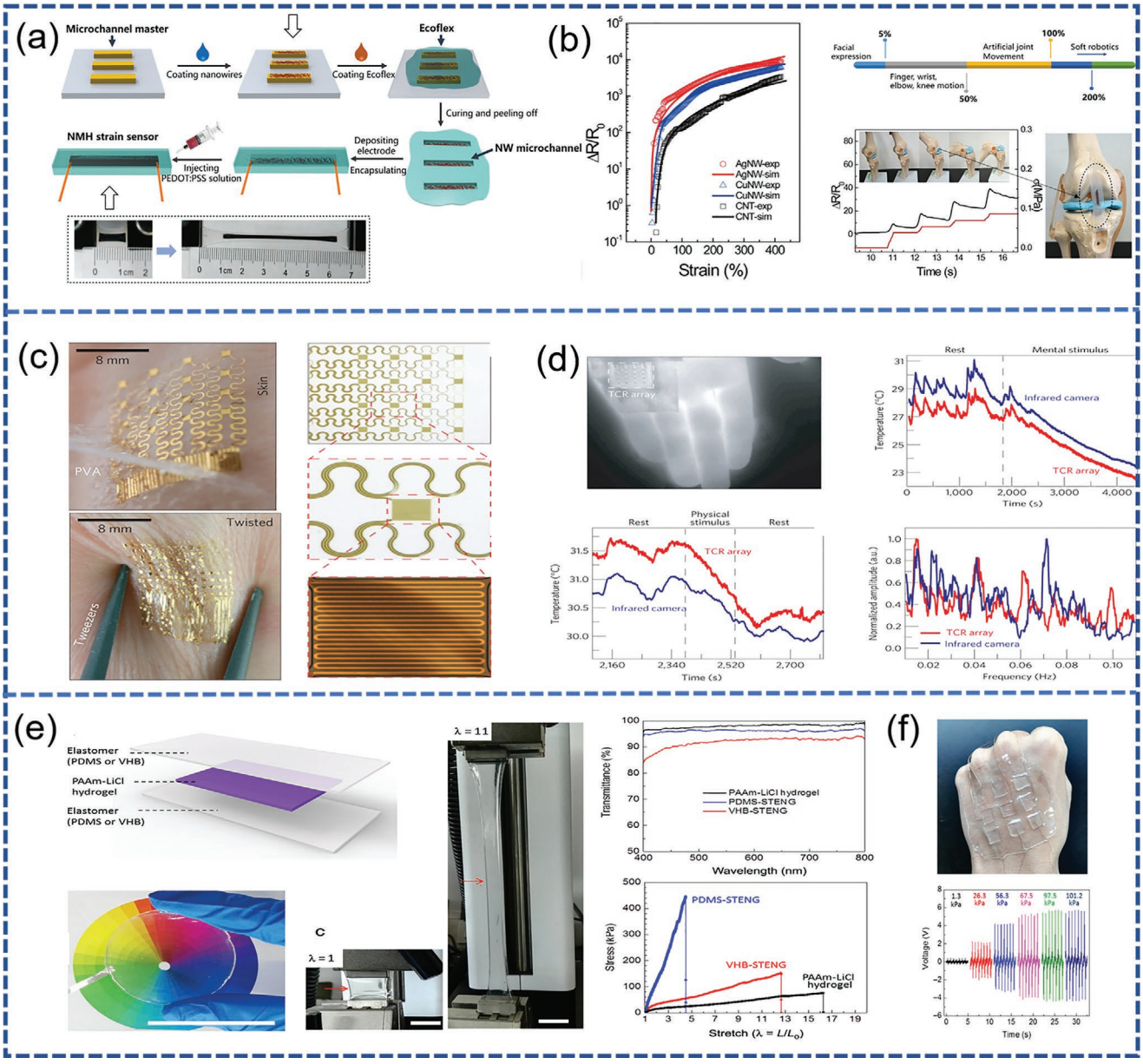

Figure 4. a) Schematic diagram for fabrication of NMH sensors. b) Photograph of under stretched and relax state and its application for the movement detection of skeleton knee model (black), and the tensile strength under different deformations (red). Reproduced with the permission.[146] Copyright 2018, Springer Nature. c,d) Optical and magnified image (single sensor) of 4 × 4 temperature coefficient of resistance integrated on a thin elastomeric substrate and applied on the skin by using water-soluble adhesive. IR image is for palm mounted sensor during stimulus experiments. Infrared camera output graphs represent the temperature of the palm (blue) and a sensor array (red) during mental. Reproduced with permission.[147] Copyright 2013, Springer Nature. e,f) Schematic diagram of sandwich structured TENG and its optical image during the stretched state, attached on hand with 3 × 3 pixels. Graphs illustrate the voltage profiles at 5 different pressures. Reproduced with permission.[138] Copyright 2017, American Association for the Advancement of Science.

estimate the bending strength of flexible electrodes for energy storage applications, θ, L, and R should be provided. To clarify this, Zhi et al. reported changes in the capacity retention due to changes in one parameter while maintaining the other two parameters. This demonstrates the dependency of charge storage properties on the abovementioned parameters under mechanical deformation (Figure 5b).[157]

In addition to flexible electrodes, stretchable electrodes are critical for wearable energy storage devices. In general, stretchable electrodes can store high strains and shape deformations, thus increasing the design and material requirements. For stretchable devices, structural reversibility is critical and considered as challenging, given the degradation in the device performance due to slight irreversible mechanical deformation. Furthermore, an ideal stretchable energy storage device should be operable under high strain conditions, and demonstrate a high recovery of the electrochemical performance upon removal of the external force. To date, numerous attempts have

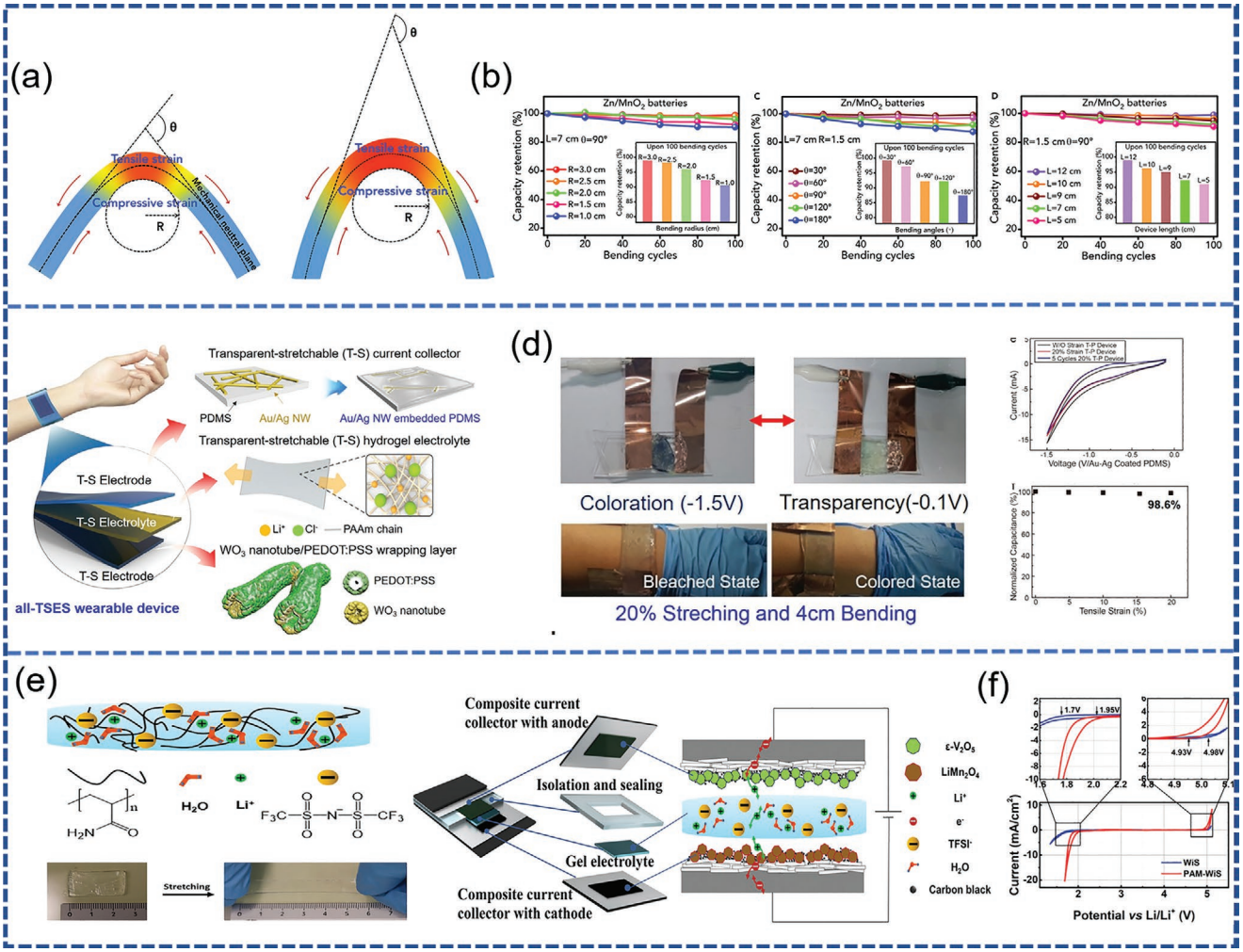

Figure 5. a,b) Key parameters (L, q, and R), used for bending state of flexible and wearable energy storage devices. Reproduced with permission.[157] Copyright 2019, Cell Press. c,d) Schematic diagram of stretchable and transparent electrochromic supercapacitor. Au/Ag core–shell with acute oxidation resistance, flexible and stretchable hydrogel electrolyte, WO_3 nanotube, and wrapping a layer of PEDOT:PSS. Illustration of the arm-wrapped all-TSES device with 20% stress in cyclic voltammetry and variation in capacitance. Reproduced with permission.[137] Copyright 2019, American Chemical Society. e) Schematic illustration with photographs of the unstretched and stretched PAM/WIS gel. f) Schematic figure of stretchable full cell. Reproduced with permission.[158] Copyright 2019, Wiley-VCH.

been made to increase the stretchability of electrodes. However, less focus was directed toward their mechanical recoverability. For example, Kim et al. utilized a core–shell Au/Ag NW embedded PDMS substrate with WO_3 NTs/PEDOT:PSS and a polyacrylamides-based hydrogel electrolyte, as shown in Figure 5c.[137] The WO_3 NTs/PEDOT:PSS bi-stacked active materials exhibited superior electrochromic functioning under mechanical deformations with a maximum specific capacitance of 471.0 Fg^{-1}, and a 92.9% capacity retention after 50 000 charge/discharge cycles. Furthermore, Figure 5d presents the suitability of the device for wearable applications, which demonstrated a 98.6% retention of capacitance under a total strain of 20%, thus confirming its appropriateness for wearable applications. Furthermore, a low-modulus silicone elastomer was used as a substrate, and a stretchable rechargeable lithium-ion battery (LIB) was fabricated using active materials with a segmented design, to develop stretchable batteries with the capacity to deform due to the dynamic motions of the wearable electronics.[165b] The resulting device exhibited a reversible stretchability of up to 300% while retaining a capacity density of 1.1 mAh cm^{-2}.

Moreover, for stretchable energy storage devices, gel electrolytes are critical to withstand high stretchability.[159] Numerous gels such as, sodium polyacrylate (PANA), polyacrylic acid, poly(vinyl alcohol) (PVA)/H_3PO_4, and PAM have been utilized in stretchable energy storage devices after 100 stretching cycles at a maximum strain of 200%. Moreover, all these hydrogels demonstrated exceptional residual strains of ≈24–33%.[152] These gel electrolytes have been used extensively in stretchable energy storage supercapacitors and batteries.[160] For example, Wang et al. fabricated a polymer supercapacitor using a pure polypyrrole (PPy) electrode and a double network (DN) hydrogel as electrolytes. The developed hydrogel demonstrated an excellent mechanical stretchability of up to 500% with a restoration of ≈100% of the original length. Similarly, an aqueous gel electrolyte contains PAM hydrogel membrane into lithium-ion water PAM-water-in-salt (WIS) was prepared and used for a stretchable

aqueous Li-ion battery to broaden the potential window, as shown in Figure 5e.[158] The as-prepared hydrogel demonstrated stretchability at a strain of 300% with a high ionic conductivity of $\approx 10^{-3}$–10^{-2} S cm^{-1}, and an expanded electrochemical window of 1.95–4.3 V with respect to Li/Li+; thus confirming its suitability for stretchable aqueous Li-ion batteries (Figure 5f). Furthermore, to solve the interlayer slippage and delamination problems under high deformations, Zhi et al. recently fabricated a non-laminated structure using an elastic electrode and highly elastic supramolecular hydrogel electrolyte.[161] The intrinsic elasticity of the utilized hydrogel and elastic nature of electrode provide the as-fabricated supercapacitor device with significant mechanical consistency and outstanding electrochemical performances, and an areal capacitance of 0.37 F cm^{-2} and volumetric energy density of 0.082 mW h cm^{-3}. With in situ integration, the pyrrole electrode was covalently and hydrogenally bonded to a silk fibroin-based elastic supramolecular hydrogel sheet, thus resulting in a non-laminated device with high structural integrity. Furthermore, due to the supramolecular design in the hydrogel matrix, an outstanding self-healing competency was demonstrated at ≈95.8% after 30 cutting and healing cycles. In addition, for stretchable energy harvesting TENG devices, double-network ionogel was also reported by Wang and coworkers. For triboelectrification, the IL-locked ionogel was coupled with another layer of patterned PDMS containing one electrification layer that provided excellent stretchability and transparency due to the unique mechanical properties of the ionogels and PDMS. The utilization of TENG devices in tactile sensing demonstrated maximum sensitivity of 1.76 V N^{-1} while detecting impacting forces in the range of 0.1–1 N and excellent linearity with impacting forces at various tensile ratios of 0%, 10%, 50%, and 80% strain.

Other Electronic Devices: With the utilization of flexible polymer substrates; low-cost, lightweight, and transparent electronic devices such as, transistors, photodetectors, and display devices have been widely reported to meet the increasing demand for flexible electronics. The use of polymer substrate-based photodetectors has been widely reported due to their numerous advantages such as accessibility, precise control of thickness, intrinsic flexibility of polymers, and large-scale applications. Polymer substrates such as PET,[162] PEN,[163] PI,[9a,164] and PDMS[165] have been widely reported for their inherent flexibility. Zhang et al. reported a graphdiyne (GDY)-based flexible photodetector, for which GDY nanosheets were spin-coated onto PET substrates, thus exhibiting a high photocurrent at ≈5.98 μA cm^{-2}, photoresponsivity of 1086.96 μA W^{-1}, and excellent long-term stability (**Figure 6**a).[166] The device exhibited pronounced photoresponsivity and stability after 1000 bending and

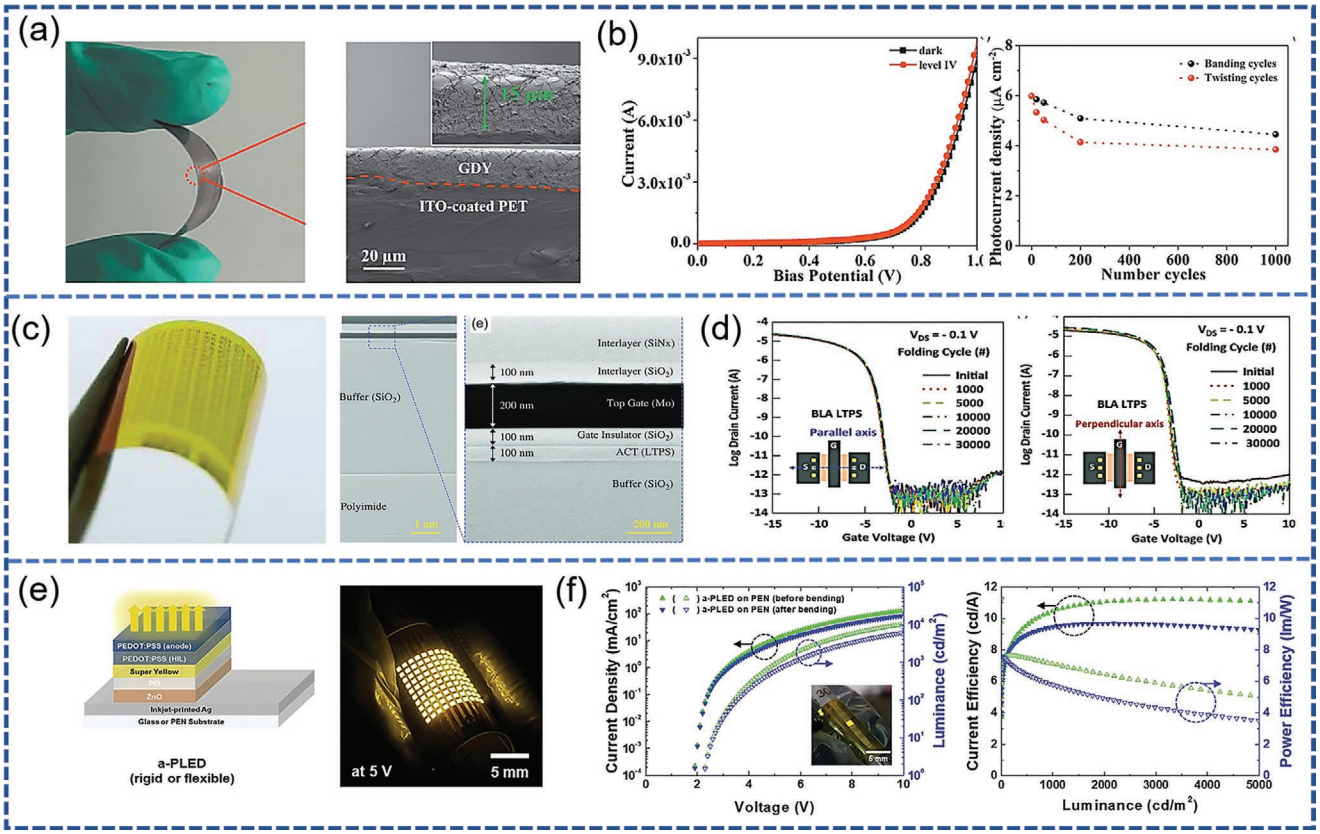

Figure 6. a) Photograph of GDY-based photodetector with SEM images. b) Photo-response of GDY-based photodetector with the mechanical response (bending and twisting cycle). Reproduced with permission.[166] Copyright 2020, Wiley-VCH. c) Optical image of the flexible thin-film transistor (TFT) on PI substrate with corresponding SEM image. d) TFT performances comparison of BLA poly-Si TFT measured parallel and perpendicular to the current path after folding until 30 000 cycles. Reproduced with permission.[169] Copyright 2020, Wiley-VCH. e) Device architectures and photographs of a-PLED arrays with fine lines on glass and PEN substrates. f) Working efficiencies of a-PLEDs on PEN substrates. Reproduced with permission.[170] Copyright 2020, Wiley-VCH.

Table 4. Properties of the flexible textile substrate-based devices.

Substrate	Processing method	Material deposited	Temperature	Typical devices	REF
Cotton textile	Doctor blade coating	Ni, V_2O_5	RT	Flexible batteries	[315]
Polyester cotton fabric	Spray Coating	PEDOT: PSS	RT	Solar cells	[316]
Nylon	Screen printing	Ag	90 °C	e-Textile	[280]
Silk, nylon	Screen printing	CNT	80 °C	TENG sensor	[279]
Polyester/nylon textile	Laser printing	RGO	80°	Microsupercapicitors	[317]
Silk fabric	3D printing	CNT	RT	Energy-storage and harvesting	[287]
Pristine woven textile	Inkjet printing	Ag ink	150 °C	Electronic devices	[281]
Polyester/cotton textile	inkjet-printed	Ag Np ink	130 °C	Tracking device	[318]
Polyamide textile	Inkjet printing	PEDOT: PSS	110 °C	Electrocardiogram devices	[319]
PET textile	Spray coating, dip coating	CNT/RGO	90 °C	Strain sensor	[320]
Silk textile	Spray coating	Ag NWs	RT	Humidity sensor	[288]
Cotton fabric	Spray coating	Graphene	120 °C	Temperature sensor	[321]
Polyester textile	Drop casting	Ag NWs	150 °C	EMI shielding device	[322]
Cotton textile	Dip coating, in situ growth	Co-Al LDH	120 °C	Self-power devices	[323]
Polyester/cotton textile	Dip coating	CNT	RT	Li-ion battery	[324]
PET fabric	Dip coating	Black phosphorus	RT	TENG device	[325]
PET textile	Dip coating	PPy/MXene	100 °C	Heating device	[289]
Nylon fabric	Dip coating	Ag NWs, AuNPs	80 °C	SERS device	[326]
Cotton textile	Dip coating	PEDOT:PSS	70 °C	Triboelectric nanosensors	[327]
Cotton textile	Dip coating	Ag NWs	RT	Passive personal heating	[328]
Polyester fabric	In situ polymerization	PEDOT:PSS	60 °C	Supercapacitors	[329]
Polyester textile	In situ polymerization	rGO, PANI	35 °C	Supercapacitors	[300b]
Cotton textile	In situ polymerization	PPy	80 °C	Self-power electronics	[301]
Cotton textile	In situ polymerization	PANI	RT	Motion sensor	[298]
Carbon textiles	Hydrothermal	$NiMo_3S_4$ nanosheet	80 °C	Sodium-ion batteries	[295]
Carbon textile	Hydrothermal	$NiCo_2S_4$	200 °C	Lithium–oxygen battery	[330]
Carbon textile	Hydrothermal	MnO_2@TiN	95 °C	Supercapacitors	[293]
Carbon textile	Hydrothermal	$Na_2Ti_3O_7$ nanosheet	80 °C	Sodium-ion pseudocapacitors	[294]
Cotton textile	Electrodeposition	NiCo hydroxide and MnO_2	RT	Zn-ion batteries	[331]
Cotton textile	Electrodeposition	Iridium Oxide NPs	RT	Supercapacitor	[332]
Polyester yarn	Electrodeposition	Ni-Co nanosheets	RT	Self-charging power device	[297]
Commercial textile	Electrodeposition	MnO_2 sheets	RT	Supercapacitors	[333]
Silk textile	CVD	PEDOT	80 °C	Conductive fiber	[296]
Cotton yarn	CVD	pEGDMA	130 °C	Fibertronics	[334]
Carbon fiber	CVD	ZnO NWs	300 °C	Water splitting	[335]
Silk fiber	Dip coating	Ag NWs	RT	Temperature–pressure sensor	[336]
Cotton textile	CVD	rGO	250 °C	Pressure sensor	[337]
Polyester Textile	Baking	Nitrile film	70 °C	Nano-energy nano-system	[338]

twisting cycles at ≈4.45 and 3.85 μA cm^{-2}, respectively, due to the excellent GDY structural flexibility and PET substrate with high compatibility (Figure 6b). In addition to polymer plastic substrates, polymer elastomers such as, PDMS have been extensively utilized for flexible and stretchable photodetector devices. Bao et al. reported a PDMS substrate-based wearable photodetector with a unique helical structure, which exhibited a high stretchability at a strain of up to 600%, capacity to accumulate deformation, and is promising for the construction of other wearable devices.[167] Similarly, the use of PDMS as the substrate was demonstrated by Rogers et al. to support 2D active materials such as graphene and MoS_2 on a PDMS substrate for the construction of a 3D flexible photodetector.[168]

In addition, significant research was conducted on the construction of transistor devices on polymer substrates such as, PET,[171] PI,[97,172] PEN,[173] and polymer elastomers such as, PDMS,[174] TPU,[175] and Ecoflex.[176] A PI substrate based thin-film transistor (TFT) was demonstrated by the blue laser

annealing (BLA) of amorphous silicon, as shown in Figure 6c.[169] The integration of the PI substrate resulted in the excellent flexibility and foldability of BLA TFT with a high mechanical stability, which exhibited a slight shift in the threshold voltage (V_{TH}) at ≈0.1 V after 30 000 cycles of folding, as shown in Figure 6d. To demonstrate the high flexibility and excellent mechanical compatibility of transistors, Wang et al. demonstrated the fabrication of a dinaphtho[2,3-b:2,3-f]thieno[3,2-b]-thiophene organic synaptic transistor on an elastic PDMS support, thus resulting in the adhesion of the transistor on the curved surfaces of substrates by the elimination of strain-induced wrinkles. Moreover, other elastomers such as Ecoflex- and TPU-based transistors were reported for flexible device applications.[176]

Polymer flexible substrates provide an excellent platform for the integration of LEDs, to realize wearable electronics, conformal lighting, and bendable displays. Polymer plastic substrates such as, PET and PEN have been widely reported for the fabrication of LEDs due to their high mechanical flexibility and stability.[177] Hong et al. demonstrated polymer-LEDs (a-PLEDs) on a flexible PEN substrate (Figure 6e) and optimized the pixel shape and features, thus demonstrating a high current efficiency of 10.4 cd A^{-1}.[170] The fabricated device exhibited a high mechanical stability after 100 bending cycles with a bending radius of 3.5 mm, as shown in Figure 6f, thus demonstrating a degradation of 10% and 20% in the current efficiency at a lower 1000 cd m^{-2} and higher luminance range. In addition, the integration of the LED devices on polymer elastomers such as PDMS was reported for stretchable and wearable electronic devices.[178] Yu et al. demonstrated stretchable halide perovskite LEDs with a high reachability of up to 40% for 100 cycles without failure, and an excellent mechanical robustness with a large luminance intensity of 15 960 cd m^{-2} at 8.5 V.[179]

Thus, polymer substrates are critical in flexible electronics for bendability, where the device is attached to the bendable layer using the various processing techniques described above. This provides significant versatility in the proposed applications.

3.2. Paper Substrate Based Flexible Electronic Devices

Paper is environmentally friendly and the most widely used flexible substrate with a substantially lower price (0.1% dm^{-2}) than plastic substrates such as PET, which has a cost of ≈2 cents dm^{-2}; and PI, which has a cost of ≈30 cents dm^{-2}. Paper substrates do not demonstrate environmentally friendly and recyclable properties. However, they demonstrate a low mass, accessibility, high biocompatibility, and biodegradability; with a small thermal expansion coefficient value from ≈28–40 ppm K^{-1}.[180] Paper is manufactured in various forms such as writing paper, printing paper, drawing paper, and wrapping paper. Moreover, it is prepared by dewatering a dilute suspension of cellulose fibers and filtration by pressing and heating. The major national manufacturers of paper are China (26.5%), the European Union (22.5%), the United States of America (USA) (17.9%), and Japan (6.5%), with a total manufacturing mass of 420 billion kg per year.[181] More than 50 years ago, paper was proposed as a substrate for electronic applications.[182] However, ≈30 years was required for the development of the first simple smart pixel electronic components on paper.[183] Recently, extensive research has been published on the integration of paper substrates into flexible electronic devices due to their advantages of high flexibility, ease of mass production, cost-effectiveness, and environmental friendliness.[181]

3.2.1. Technologies for Flexible Conductive Paper Electrodes

For flexible device fabrication, paper substrate based electronics signify a major advancement, thus leading to low-cost, highly flexible, and lightweight devices; which fulfill the increasing demand for smart electronic devices. Various processing techniques have been established to modify paper substrates for integration into flexible devices. The utilization of paper substrates in electronic devices is based on two main approaches: i) The direct utilization of paper substrates in devices with printing and other processing techniques, and ii) the addition of certain functions to the cellulose paper-type patterning devices on other flat substrates, or a smooth layer coating on the paper surface due to surface roughness and high porosity and opaqueness. In the following subsections, focus is directed toward the processing of paper substrates for flexible electronic devices by classification into two main categories: Physical and chemical processing techniques.

Fabrication of Conductive Paper Electrode by Additive Techniques: Due to their low cost, simple processing, mild conditions, and no additional materials, additive methods are extensively utilized to process paper substrates. Physical methods involve printing and coating methods, which are commonly considered as the reproductive processes for the attachment of a large variety of materials.

Printed Paper Electrodes: The single-paper concept cannot be used as the definition of paper for printed electronics. The selection of the paper substrate mainly depends on the functional material deposited on the substrate. However, to print functional materials on a paper substrate, several general characteristics such as, the surface smoothness, barrier properties, and print definition are pre-requisites. In general, paper substrates have a rough surface and absorbing nature because of which some functional coating or lamination with plastic substrates such as PE or PET, aluminum, and wax are applied to the paper surface. Emamian revealed that during the printing process, the paper substrate is more absorptive, thus resulting in the low distribution of ink after printing.[184] The coating of aqueous dispersions of pigments and binders onto recyclable paper substrates with excellent barrier characteristics and high smoothness is an alternative approach to the tuning of the surface attributes such as the roughness, surface energy, and porosity. The scanning electron microscopy (SEM) image presented in **Figure 7**a displays the various layers of the paper substrate coatings, namely, the top layer, barrier layer, smoothing layer, and paper base.[185] The top coating layer comprising mineral pigments allows for uniform ink distribution via controlled porosity and thickness. Furthermore, this barrier layer prevents the diffusion of ink solvents and functional materials, thus resulting in the improvement of the functional properties and elimination of fiber swelling. In addition, this technique enhances the heat stability of the paper, thus allowing for infrared sintering at high temperatures.[186] Feng et al. recently

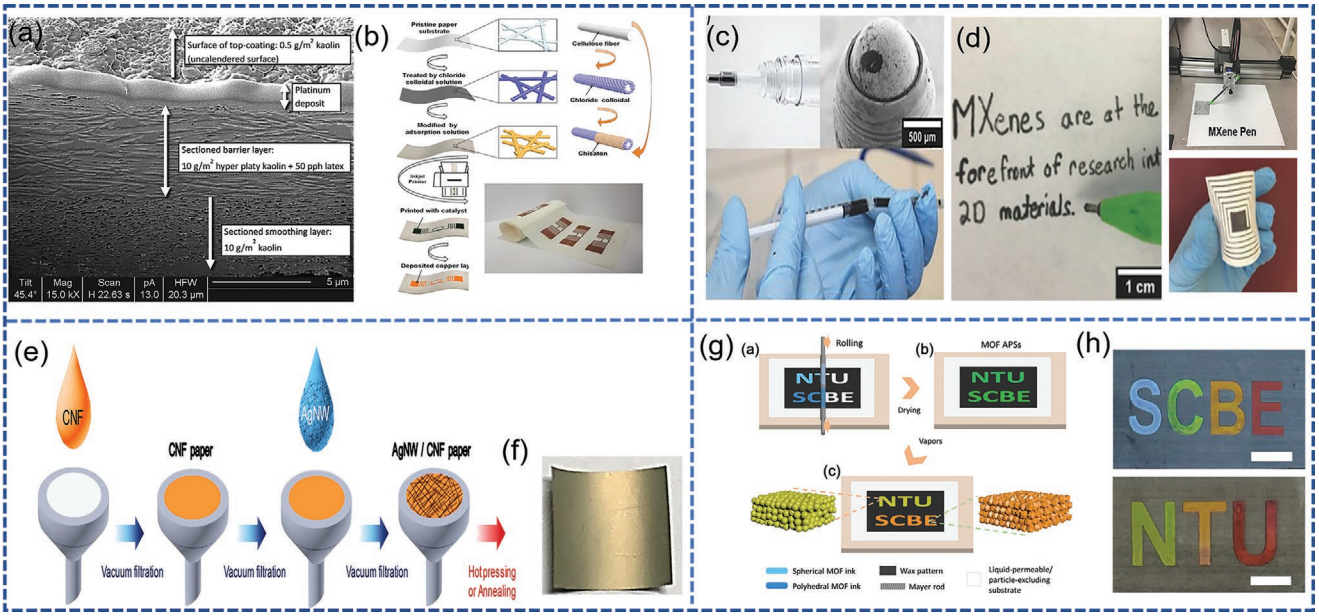

Figure 7. a) Focused ion beam etched cross-section image. Reproduced with permission.[185] Copyright 2012, Elsevier. b) Schematic diagram of flexible RFID tags on paper substrates by surface modification, inkjet printing, and electroless deposition, respectively. Reproduced with permission.[187] Copyright 2019, Wiley-VCH. c) Optical image of rollerball pen representing direct writing of Ti_3C_2 inks. d) Water dissolved Ti_3C_2 for paper writing with computer-controlled drawing apparatus (AxiDraw) and versatile patterning of AxiDraw at the right side. Reproduced with permission.[197a] Copyright 2019, Wiley-VCH. e) Schematic of step by step fabrication for Ag NWs/CNF paper by vacuum filtration method. f) An optical image of Cellulose-based TENG. Reproduced with permission.[205] Copyright 2018, Elsevier. g) Precise illustration for Mayer rod coating of MOF APS patterns with h) selective wetting (hydrophilic area of the substrate), ii) formation of APS patterns (after water removal), iii) vapor-responsive color changes by spherical/polyhedral MOF inks, and multicolored photographs of letters respectively. Reproduced with the permission.[206] Copyright 2019, Wiley-VCH.

reported a solution-processing procedure combined with inkjet printing to produce inkjet high-quality patterns.[187] The paper substrate was modified by immersion in an $SnCl_2$ colloidal solution to prevent ink penetration, followed by immersion in a chitosan solution to enhance the absorption ability of the paper substrate for the inkjet-printed catalytic ion, as shown in Figure 7b. The resulting printed paper exhibited an excellent copper layer with an improved conductivity of ≈70%, as shown in Figure 7b. Furthermore, during the printing process, functional materials are typically dissolved in solvents such as toluene or dichlorobenzene. During the direct contact of these solvents with the paper substrate, rapid evaporation occurred, thus indicating short-term barrier properties. However, for sensing and other biomedical applications, acidic or basic analytes may be lost for a period of time. Thus, long-time barrier properties are critical for controlling the absorption of ink during device fabrication and confirming the end-use function.

For high-resolution devices, narrow and uniformly printed lines are critical to the actual functionality of the printed material, which is typically determined as electrical conductivity. The practical determination of the volumetric resistance on an absorbing surface cannot be achieved. Therefore, the surface resistivity is selected as the main parameter for measuring conductivity. However, when printing electrical components on a paper substrate, ink formulation is a key phase that is significantly influenced by variables such as the concentration of the ink, presence of binders, defining viscosity, ink evaporation rate, and surface tension. As a result, the printing technique is influenced by the ink qualities and paper substrate parameters such as the pore volume, porosity, surface energy thickness, and roughness. However, the optimization of these properties can be achieved by selecting the pigment size, shape, and distribution.[188] Another factor influencing the printing of paper substrates is the dimensional stability of the fiber network, given that the printing of functional material on a paper substrate involves solvent utilization based on harsh drying methods, which has a significant influence on dimensional stability. Thus, the maintenance of functionality in an alternating environment is critical. However, using a paper substrate with a barrier layer minimizes fiber expansion by limiting the solvent and humid penetration.

Various printing methods such as screen printing,[189,191,230,239] inkjet printing,[107,196,199,227,228,237] pen on paper,[190,197a,d] and laser printing[201–203,234] have been used to print a variety of ink materials. Frisbie et al. demonstrated foldable organic thin-film transistors (TFTs) by screen-printing high-viscosity graphene ink with improved resolution on glassine paper with a smooth surface.[191] Similarly, there have been reports on the inkjet printing of numerous precursor inks, including inorganic nanoparticles such as, Ag, Au, and Cu NPs,[192] quantum dots,[193] 2D materials containing graphene,[194] metal-organic frameworks,[195] and conjugated polymers.[196] Another printing approach specific to the paper substrate is the pen-on-paper paradigm, which provides a simple and rapid method for depositing conductive materials such as graphite; CNT inks; Ag, Au, and Cu nanomaterial inks; MXene ink; and liquid metal ink[197] on paper substrates to fabricate devices for emerging applications of electronic components,[198] energy storage devices,[199]

and electrochemical sensing.[200] Gogotsi et al. demonstrated the direct writing of Ti_3C_2 MXene inks with different concentrations using a commercially available pen.[197a] Figure 7c presents the direct-writing implementation of a rollerball pen filled with MXene inks. To study the rheological properties, direct-writing was established by loading the MXene pen into a computer-controlled robotic arm, as presented in Figure 7d. This indicates that at a controlled concentration and writing speed, depending on the smoothness of the substrate platform, lines with thicknesses and widths of ≈0.5–10 μm and 0.3–1 mm, respectively, can be patterned. In addition to these techniques, laser printing has been utilized to print a variety of materials on paper substrates, such as, hydrophobic fumed silica NPs,[201] peptides,[202] Ag NWs,[203] and Zn nanoparticles.[204]

Conductive Materials Coated Paper Substrate: In physical methods, various coating techniques such as, dip coating,[207a,c] spray coating,[208b,241] vacuum filtration,[205,223] and drop-casting are utilized extensively for the processing of paper substrates. The dip coating technique, which involves the immersion and drawing of the substrate from a liquid reservoir, has been utilized for the processing of paper. Moreover, in this technique, the optimization of various parameters such as the functionality of the substrate, ink properties, dipping cycle, submersion time, and humidity of films with controlled thickness and reproducibility is conducted. Various materials such as, CNTs, graphene, Au/Ag NWs, conductive polymers, and other composite structures have been coated onto paper substrates using this technique.[207] Wu et al. coated Ag NWs onto commercial tissue paper by immersion in an Ag NW suspension for 10 s, followed by drying at 90 °C for 1 min after solvent evaporation. The thickness of the coated Ag NWs was changed by repeating the immersion process for different time-periods. Similarly, Han and coworkers demonstrated mulberry tree-derived paper (MP) as a substrate, and coated it with active carbon followed by a PEDOT:PSS coating using a scalable dip-coating method for the fabrication of mechanically and chemically strong supercapacitors.[207b] Spray coating, which involves the spraying of coating materials on the substrate through the air, has been utilized for the fabrication of electronic component structures on paper substrates. Significant research has been conducted on the spraying of coatings onto paper substrates.[208] Based on this operation, Edman et al. demonstrated LEDs on paper by depositing all layers of the device, including the anode, cathode, and active materials, using a spray coating technique on specialty paper and copy paper.[209] The morphology of the coated film was determined by maintaining three parameters, namely, the solvent vapor pressure, solute concentration, and substrate temperature.

To realize free-standing paper electronics, vacuumed filtration is considered as the simplest and most preferred technique due to its rapid and scalable properties. In this technique, the paper can be used as a filter due to its 3D porous structure, thus exhibiting the capacity to block materials with sizes greater than the pore sizes. At the same time, materials were directly coated onto the surface of the fiber and filled with these materials. This technique has been utilized extensively to prepare paper electrodes by depositing a wide range of materials, including various graphene composites with nanomaterials such as, Si, Co_3O_4, Fe_2O_3, MnO_2, SnO_2, MoS_2, and TiO_2; and CNT composites with polyaniline (PANI), PEDOT, Ti_3C, MoO_3–x, In_2O_3 and V-MnO_2, and Ag NWs.[210] Kim et al. demonstrated a vacuum filtration technique for the fabrication of a paper substrate as a contact surface for use in TENGs.[205] The fabrication process presented in Figure 7e displays the deposition of Ag NWs on cellulose nanofibril (CNF) paper via vacuum filtration, in which the cellulose suspension was poured on the membrane filter and filtered through a solvent. Furthermore, by adjusting the amount and concentration of the Ag NW solution, vacuum filtration was performed to coat the electrode material (Figure 7f).

In the coating industry, Mayer rod coating, which involves the drawing of the solution over the surface of the substrate by a metal rod wrapped with wire, is considered as a common coating technique for the fabrication of thin films in a continuous and controlled manner. This technique has been utilized for the large-scale production of films from a variety of materials such as, carbonaceous materials (graphene and CNTs),[211] Ag NWs,[212] conductive polymers,[213] metal–organic frameworks,[206] and MXenes[214] on paper substrates. Duan et al. recently reported the scalable construction of responsive amorphous photonic structure (APS) patterns employing spherical metal organic framework (MOF) particles via the infiltration-assisted (IFAST) Mayer rod coating method.[206] Figure 7g presents the initial infiltration of the dispersing liquid of colloidal particles into the permeable substrates, thus allowing for the immobilization of particles on the substrates. However, the further deposition of aqueous MOF inks by Mayer rod coating allowed for the wetting of exposed substrates, and not the patterns covered by wax, thus resulting in the deposition of the IFAST colloidal assembly on the designated part of the paper substrate. Furthermore, isotropic structural colors of APSs such as, polyhedral ZIF-8, particle-APS, and MOF APS are presented in Figure 7h, which exhibited different colors of blue, green, yellow, and red.

Other techniques, such as sputtering, thermal evaporation, and drop-casting, have been commonly used for the processing of paper substrates. The thermal evaporation method requires expensive equipment and high-vacuum conditions when compared with the sputtering technique. Wan et al. fabricated TFTs using the various techniques of drop-casting, immersion, thermal evaporation, and sputtering.[215] The fabrication process involves the drop-casting of the cellulose nanofiber solution on the weighing paper in the first step, followed by immersion in a CNF solution for 30 s. Following the sputtering of the indium tin oxide source/drain electrode on the opposite side of the immersed paper sheet by one-step radiofrequency (RF) magnetron sputtering, a thin layer of Ag was thermally deposited on the CNF-immersed paper sheet surface, thus resulting in flexible TFTs.

Conductive Paper Electrode by Chemical Methods: Due to the lower physical adsorption contacts between the active components and cellulose fibers in the typical techniques employed for the manufacturing of paper substrates, the realization of flexible electronics under a high mechanical stress is not reliable. Thus, chemical approaches can be used to extend the usefulness of paper substrates in addition to physical approaches. This process involves the chemical transformation of chemical substances and the formation and breaking of chemical bonds between the atoms without influencing the nuclei. A discussion is presented on the general chemical techniques for the

processing of the paper substrate, including in situ seed-mediated growth, chemical vapor deposition (CVD), electrospinning, and polymerization.

Focusing solely on the growth process for regulating morphology and improving material interactions with the paper substrate, in situ seed-mediated growth is regarded as an effective technique. By utilizing this technique, numerous reports were published on the decoration of active nanomaterials such as, Ag,[216] Au,[217] alloy,[218] Pt,[219] and metal oxides[220] on paper substrates. Moreover, during this process, no actual difference in the structure of the paper was observed. Zhao et al. reported the seed-mediated coating of Au NPs on cellulose paper, thus revealing no apparent structural difference with a coating of small-sized Au NPs.[221] Due to the self-catalytic effect, the gold seeds rapidly increased in size as the reaction time increased, thus resulting in porous gold electrodes with a larger effective surface area. The same group also recently demonstrated an isolated hierarchical PANI/G/MnO_2 paper substrate using a layer-by-layer in situ growth method.[222] **Figure 8**a presents the schematic procedure, thus exhibiting the polymerization of PANI on printing paper in the first step, followed by the deposition of the graphene sheet on the composite paper. Finally, MnO_2 was produced in situ on PANI/G paper via the oxidation of the cellulose fiber and graphene by immersing the composite paper in a $KMnO_4$ solution. Moreover, Figure 8b presents no apparent structural changes in the paper cellulose during the deposition process.

In addition, CVD techniques have been commonly used to prepare conductive paper-type single-walled (SWCNTs), multi-walled CNTs (MWCNTs), and their composites (Fe_2O_3/SWCNTs) on paper substrates;[223] in addition to graphene and its composites (graphene/PANI, Mn_3O_4/RGO composite).[224] Similarly, electrospinning is used for the fabrication of nanofibers and microfiber paper with hollow peripheral fibers and solid fibers with a high aspect ratio. Zhou et al. produced a porous, flexible, N-doped carbon nanofiber arrangement by the carbonization of electrospun polyacrylonitrile/polyvinylpyrrolidone/thermoplastic polyamide hybrid composite fibers (Figure 8c).[225]

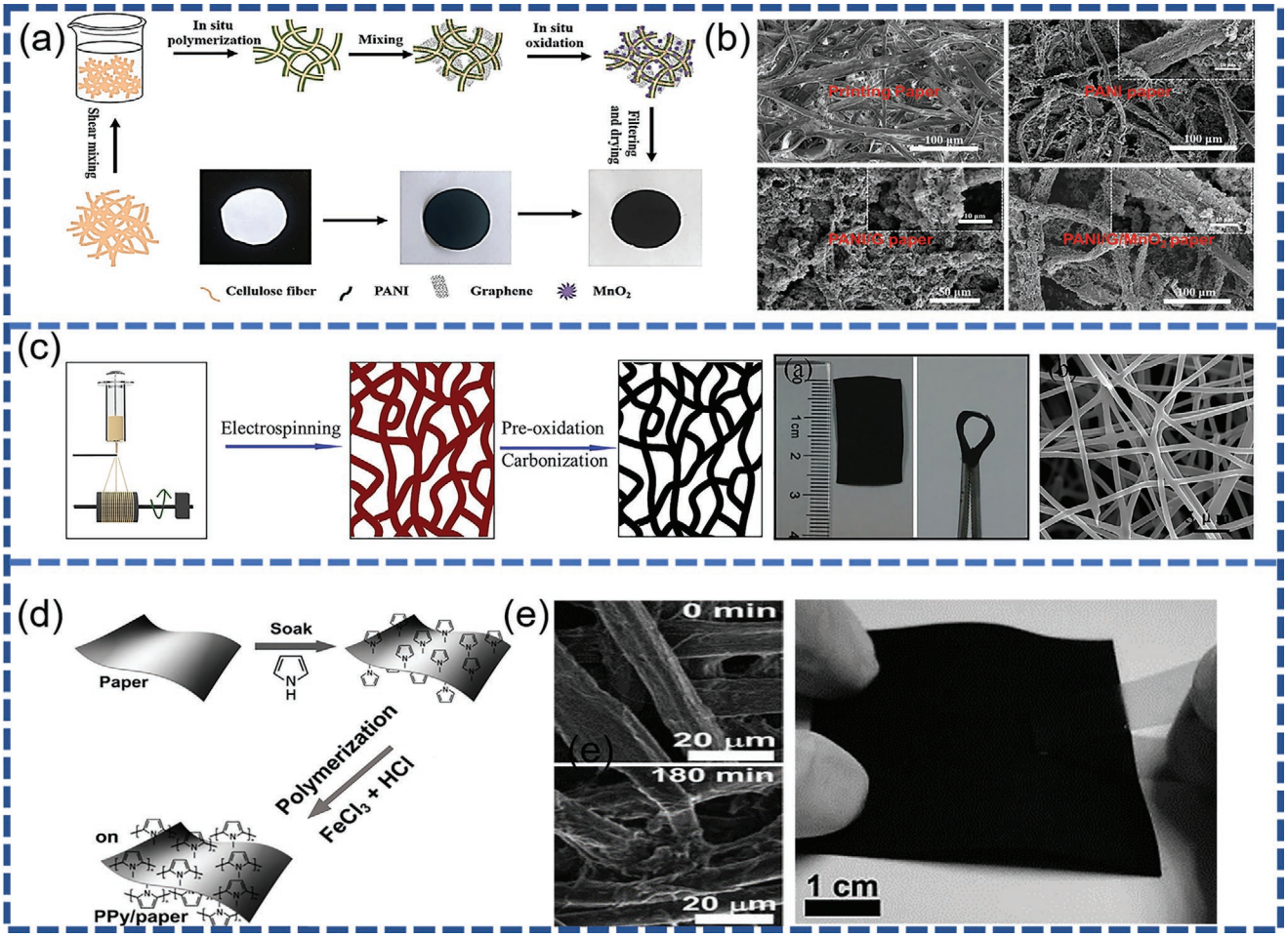

Figure 8. a) Schematic procedure, exhibiting the polymerization of PANI on printing paper to form PANI/G/MnO_2 hybrid. b) SEM images of Printing paper, PANI paper, PANI/G paper, and PANI/G/MnO_2 paper, respectively. Reproduced with permission.[222] Copyright 2019, Elsevier. c) Schematic for the fabrication process of cross-linked carbon nanofibers. Right side optical image of the cross-linked N-doped carbon nanofiber network before and under folding. Reproduced with permission.[225] Copyright 2015, Elsevier. d) Schematic diagram of the fabrication of polypyrrole-coated paper. e) SEM images for polypyrrole-coated paper at 0 and 180 min after polymerization. Tape test showing very strong mechanical property of the final prepared polypyrrole-coated paper. Reproduced with permission.[226] Copyright 2013, Elsevier.

For various applications in paper electronics, conductive polymers have been established as a substitute for metal growth, as they demonstrate excellent features such as, high electrical and optical stabilities, a high energy density, and high flexibility. During the immersion process, the cellulose paper with rough and porous architecture can be readily coated with a conjugated polymer by the development of the hydrogen bond with the added polymer monomers. By the polymerization of monomers into the polymer, the 3D porous architecture acts as an active layer for paper electronics applications. Zhou et al. demonstrated the immersion of daily printing paper into a PPy monomer solution and the polymerization of PPy onto the paper substrate in the presence of ferric chloride with a hydrochloric acid solution, which acted as oxidizing and dopant agents, respectively.[226] Figure 8d reveals that, in comparison with the blank paper substrate, there was an increase in the roughness and connections between fibers in accordance with a change in the color to black in the case of the polymerized paper substrate. Moreover, the resulting paper exhibited the excellent adhesion of PPy with the paper substrate in the mechanical adhesion test with tape (Figure 8e).

3.2.2. Applications of Paper Electronics in Flexible and Wearable Systems

There has been a recent increase in the research and development of paper modification with a various materials due to their potential applications in sensing devices, energy storage devices, and other electronic devices. The integration of nanomaterials on paper results in unique physical and chemical properties such as, a low mass, high flexibility, environmental friendliness, disposability, low cost, electrical and thermal conductivity, high mechanical strength, and electrochemical behavior; in addition to optical properties. In this selection, a brief discussion is presented on the potential applications of paper substrate based flexible electronic devices.

Sensor Devices: Due to the numerous characteristics of paper substrates such as, their 3D fibrous structure, mechanical properties, biocompatibility and biodegradability, and ease of production and modification, they are excellent candidates for integrated sensing platforms. There was a recent increase in the development of paper-based sensing platforms, including glossy paper,[243] filter paper,[244] abrasive papers,[245] and printing paper;[246] as signified by the fabrication of paper-based sensors devices such as strain sensors, pressure sensors, biomedical sensors, and chemical sensors (pH sensors and gas sensors).[7] The commonly utilized paper substrates in the fabrication of sensor devices are glossy paper, abrasive paper, and printing paper. Cellulose paper containing 98% α-cellulose with no additives is mostly used in sensor devices due to its uniformity, smooth surface, thickness of 0.18 mm, and medium flow rate. In addition, commercially available cation-exchange and anion-exchange papers can be modified with various functional groups to demonstrate different properties such as, color development uniformity, chromatographic separation, and immobilized molecule binding.[247] Xu et al. demonstrated a flexible strain sensor by applying cellulose to crêpe paper and converting it into a conductive carbon fiber network.[233] **Figure 9**a presents the schematic diagram for the development of strain sensors, thus revealing the carbonization of crêpe paper by thermal treatment in N_2 atmosphere to conductive crêpe paper with a color change from white to black, and encapsulation in PDMS to fabricate flexible strain sensors. Moreover, Figure 9b presents the sensing response of the device under physical motions of bending and stretching, thus revealing the applicability of the sensor to the multidimensional monitoring of human body motions as a wearable device. Furthermore, paper-based skin sensors were reported for the manufacture of implantable devices.[197b] Similarly, for the first time, Gu et al. demonstrated the simultaneous detection of wrist pulse and three sweat indicators using a gecko-inspired, wearable, nanotentacle substrate (G-sensor) coupled with a microfluidic system and a polyvinylidene fluoride (PVDF)-based piezoelectric nanogenerator (PENG).[248] Figure 9c illustrates a microfluidic system coupled with a PENG for sweat sensing and wrist pulse monitoring during jogging, where each end of the channel was employed for the detection of different parameters such as, the pH, lactate, and urea levels. In addition, the changes in current of the skin sensor were recorded by measuring the wrist pulse frequency at ≈132 BMP, as shown in Figure 9d. In addition, a paper-based chemical sensor was demonstrated by Zhu et al. by fabricating organic self-powered chemical sensing elements with a paper substrate based organic thermoelectric (OTE) platform, as shown in Figure 9e.[249] The high power generation capacity demonstrated by the OTE device resulted in an ultralow operating voltage, and the device was operated at a temperature gradient of 35 K for NH_3 sensing at a low concentration of 1 ppm, as shown in Figure 9f.

In addition, biomolecular office paper with a smooth surface and low cost is commercially used as a flexible support for sensing devices. This paper mostly discusses its hydrophobic nature, as it contains 10% alkyl ketene dimer and a low filler percentage.[250] However, although used in processing techniques, the selection of the filler should be considered, given that the calcium carbonate signal can lead to inaccurate data for several methods (X-ray diffraction).[251] Numerous reports were published by utilizing copy paper substrate in sensing devices.[252] Jung et al. fabricated a AuNP-decorated paper surface-enhanced Raman spectroscopy (SERS) substrate sensor for label-free molecular detection by using a simple dip-coating method, and controlled the AuNP size with respect to the pH change of the Au-precursor solution (Figure 9g).[207a] The SERS activity was applied for the detection of bipyridylium pesticides after detachment from the apple peels, and concentration-dependent Raman spectra were observed from the tested SERS substrate at a low concentration of 1 ppm, as shown in Figure 9h; thus demonstrating its applicability to various label-free chemical SERS sensors.

Energy Storage Devices: The common properties of paper substrates, such as, rough surfaces, are considered as drawbacks in thin-film devices. However, for energy storage devices, these properties have significant potential due to the high aspect ratio of paper fibers (length of several tens of micrometers, and width of 20 μm) and high porosity with a diameter at the micrometer-scale. To use paper substrates in flexible energy storage devices as current collectors, they should exhibit a high and stable conductivity under flexible

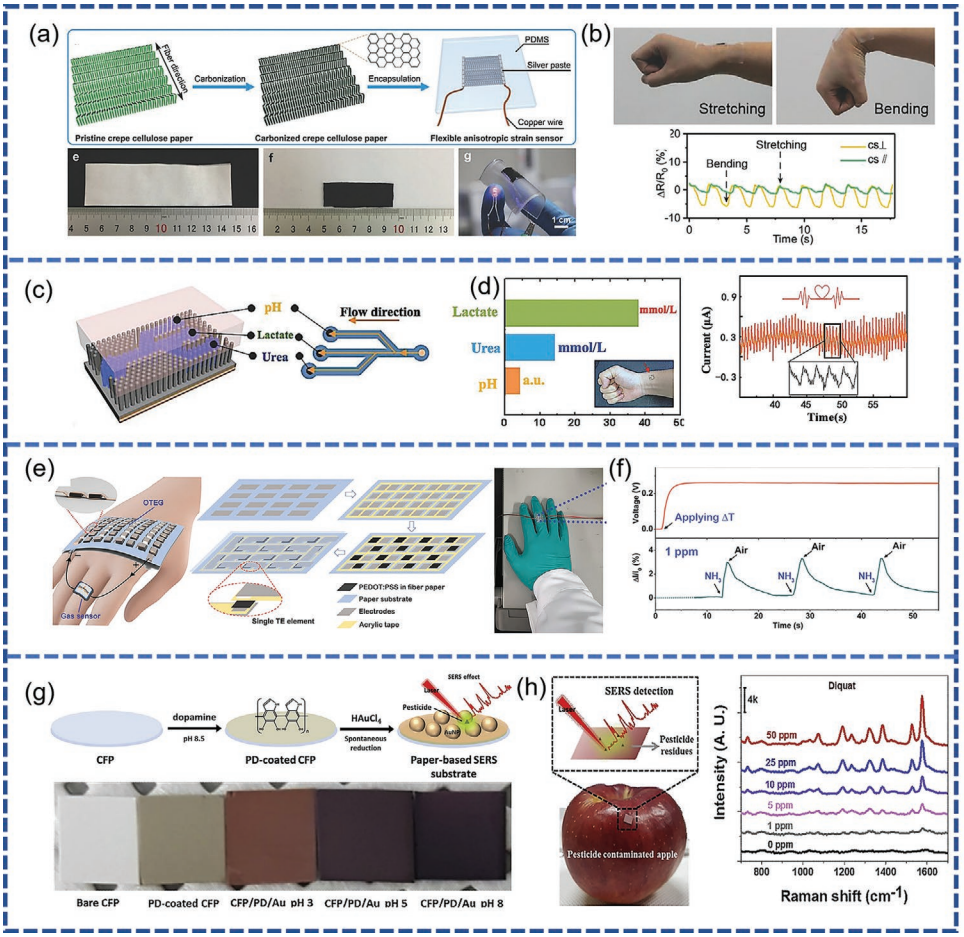

Figure 9. a) Schematic diagram for the fabrication mechanism of the flexible carbonized crepe paper (CCP) strain sensor. Photograph at lower side representing the carbonization of CCP before and after the treatment. The final image is in working condition of the flexible CCP strain sensor. b) Working of CCP sensor during stretching and bending of the wrist. The graph shows the resistance change during stretching–bending of the wrist. Reproduced with permission.[233] Copyright 2018, Wiley-VCH. c) Schematic representation of artificial skin based on integrated microfluidic and nanogenerator for simultaneous monitoring of sweat and pulse during running. d) Detection of lactate and urea concentrations during running by artificial skin. Graphical representation of current changes in artificial skin during pulse sensing and the inset shows the image of artificial skin attached to a human wrist. Reproduced with permission.[248] Copyright 2019, Wiley-VCH. e) Schematic diagram for the fabrication mechanism of OTE generator with PEDOT:PSS legs. Working photograph of an OTE array powered chemical sensor attached on hand. f) Optical image of an OTE array powered chemical sensor attached on the middle finger. The right side graph represents the monitoring of voltage output caused by a temperature difference between a heating plate and a cooling flow. Reproduced with permission.[249] Copyright 2019, Wiley-VCH. g) Schematic diagram of synthesis mechanism for paper-based SERS substrate. Surface morphology and optical property observations of bare cellulose filter paper (CFP), PD-coated CFP, and SERS substrates from left to right at different pH values. h) Schematic illustration of pesticide observation with a paper-based SERS substrate on an apple surface. Graphical representation of Raman spectra of DQ with pesticides at various concentrations. Reproduced with permission.[207a] Copyright 2019, Elsevier.

conditions. The high porosity provides a high absorption activity by exploiting the capillary action, which allows for the fabrication of flexible, highly conductive, and mechanically resistant materials. Numerous approaches were developed to functionalize paper substrates with Ag NWs,[205] CNTs,[253] and graphene[254] to obtain a high conductivity. Furthermore, the charge storage in energy devices depends on the surface area. The CNFs present in a paper substrate with high porosity contain a high amount of surface hydroxyl groups, which demonstrate the capacity to increase self-assembly with conductive inks. Various metal oxides materials and conductive polymers have been deposited on paper substrates for applications in energy storage devices such as supercapacitors, electrochemical batteries, nanogenerators, and biofuel cells based on their underlying operational principles, as clarified in the following sections.[255] For example, by incorporating various materials such as, MoO_3, MoS_2, α-MnO_2, PEDOT films, SWCNTs and composites (MnO_2-CNT film PANI-CNT MnO_2-CNT film), N-carbon fiber and composites (V_2O_5-carbon fiber and PANI-carbon fiber);[223] a large variety of supercapacitor devices were fabricated. Chen et al. achieved completely printed, in-plane, flexible micro-supercapacitors (MSCs) by screen-printing thixotropic nanocomposite inks containing RuO_2xH_2O@ Ti_3C_2Tx (MXene) nanosheets and Ag NWs.[256] The prepared thixotropic nanocomposite inks presented in **Figure 10**a were screen-printed onto a paper substrate, and by drop-casting a gel electrolyte onto the project area of the microelectrodes for the construction of flexible MSCs. Figure 10b presents the capacitance

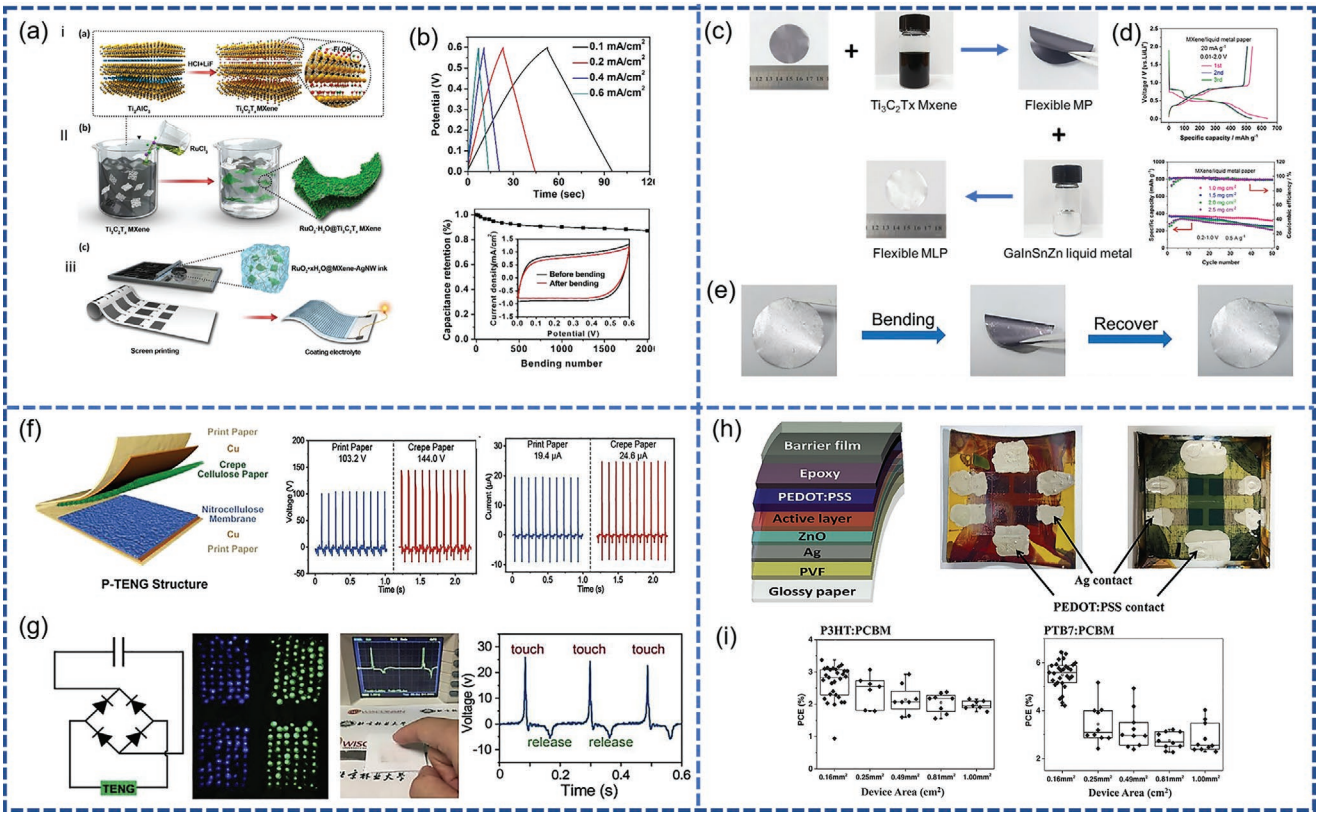

Figure 10. a) Schematic diagram for the synthesis process of i) Ti_3C_2Tx MXene, ii) $RuO_2{\cdot}xH_2O$@MXene nanocomposite, and iii) flexible MSC devices. b) Electrochemical response of R@M-A0.75:1 micro-supercapacitors:galvanostatic charge/discharge profiles from 0.1 to 0.6 mA cm^{-2} (four different current densities). The graph at the bottom represents capacitance change during multiple bending cycles under the constant strain of 5.0% (inset: contrastive CV curves recorded at 100 mV s^{-1} before and after 2000 bending cycles). Reproduced with permission.[256] Copyright 2019, Wiley-VCH. c) Schematic diagram consisting of optical images of MLP synthesis. d) Graphs represents the charge–discharge curves (in 0.01–2.0 V at 20 mA g^{-1}) and cycling response of MLP at multiple mass loading (in 0.2–1.0 V at 0.5 A g^{-1}) at top and bottom, respectively. e) Optical images of mechanical test for MLP showing complete recovery after bending cycle. Reproduced with the permission.[265] Copyright 2019, Wiley-VCH. f) Structural diagram of PTENG and its triboelectric response under constant stress (at a frequency of 10 Hz) in the form of load voltage output and short-circuit current output (Isc), respectively. g) Circuit diagram of P-TENG attached in the bridge rectifier. Optical image of P-TENG during the lightening of multiple green and blue LEDs under repeatedly pressure stress (9.6 kPa at a frequency of 10 Hz). Graphical verification of P-TENG self-powered touch sensing. Reproduced with the permission.[232] Copyright 2019, Elsevier. h) Structural diagram of the paper-based solar cell. Optical images of final devices with PEDOT: PSS and Ag contacts i) P3HT: PCBM, and ii) PTB7:PCBM devices from left to right, respectively. i) Box plot diagram of normalized median value i) P3HT:PCBM and ii) PTB7:PCBM at different area paper devices. Reproduced with permission.[69] Copyright 2019, Wiley-VCH.

properties of the resultant screen-printed MSCs, which demonstrated a volumetric capacitance of 864.2 F cm^{-3} at a scan rate of 1 mV s^{-1}; with a high cycle stability, high rate capacity, and high flexibility (87.3% retention after 2000 bending cycles with a bending strain of 5%). Furthermore, for the realization of fully flexible electronic devices with higher areal energy densities, paper substrate-based LIBs have been extensively reported due to the mechanical flexibility of lightweight cellulose fibers. Nanostructured active materials with high theoretical capacities such as V_2O_5,[257] CuO,[258] SnO_2,[259] MoO_2,[260] Co_3O_4,[261] Fe_2O_3,[262] Ge,[263] and Si,[264] are homogeneously dispersed in the 3D conductive networks of paper substrates for flexible and wearable battery applications. Qian et al. recently reported a lightweight, flexible, and freestanding MXene/liquid metal paper (MLP) as an anode for LIBs by restricting the 3 °C GaInSnZn liquid metal in the matrix of MXene paper without a binder or conductive additive.[265] Figure 10c presents an image of MLP, as fabricated by the processing of an aqueous suspension of Ti_3C_2Tx MXene into a flexible paper based on a vacuum filtering method, followed by the coating of GaInSnZn liquid metal onto MP to form an MLP with a silvery metallic luster. The as-fabricated paper electrode exhibited excellent mechanical properties such as bendability and foldability without damage (Figure 10d). Moreover, the capacitance properties presented in Figure 10e reveal a high discharge capacity of 638.79 mAh g^{-1} at 20 mA g^{-1} by satisfying the cycling performance of the MLP with the loading of different masses within the potential window of 0.2–1.0 V at 0.5 A g^{-1}.

The paper substrate with properties of low mass, low cost, environmental friendliness, and thermal stability has emerged as an excellent substrate for nanogenerator devices.[266] Gong et al. demonstrated a paper-based TENG (P-TENG), as presented in Figure 10f, using commercially available crêpe cellulose paper and a nitrocellulose membrane with significantly different tribopolarities. The P-TENG exhibited excellent triboelectric performances, including an output voltage and current

of 196.8 V and 31.5 µA, respectively, in addition to a power density of 16.1 W m^{-2} with high durability of over 10 000 cycles.[232] In addition, Figure 10g reveals that P-TENGs can serve as a sustainable energy source for the powering of electronic devices (illumination of 240 LEDs via a bridge rectifier) and have significant potential for applications in self-powered touch sensing and human–machine interfaces.

The incorporation of solar cells into portable electronic devices is based on the stringent requirements for various characteristics such as the mass, mechanical properties, and cost. To meet these requirements, a low-cost, flexible, and porous paper substrate provides a solution for abundant, recyclable, renewable, and environmentally friendly future electronics.[181,267] Iyer et al. reported a paper-substrate organic solar cell with a power efficiency of 3.37% with poly(3-hexylthiophene) and [6,6]-phenyl C61 butyric acid methyl ester (PCBM) (P3HT:PCBM) blends as photoactive layer (PAL), and 6.44% with poly({4,8-bis[(2-ethylhexyl)oxy]benzo[1,2-b:4,5-b] dithiophene-2,6-diy{3-fluoro-2-[(2ethylhexyl)carbonyl]thieno[3,4-b]thiophenediyl) (PTB7:PCBM) blends as PAL, as presented in Figure 10h,i.[69]

Other Electronic Devices: Electronic gadgets with high flexibility, low mass, and high transparency are increasingly manufactured and developed. There are numerous reports on the fabrication of electronic devices on soft substrates, such as, transistors, photodetectors, and display devices. There has been an increase in the research conducted on the manufacture of transistors on paper substrates for flexible electronics applications. The paper substrate has been extensively utilized in transistor devices as a substrate,[268] tunnel layer for memory transistors,[269] and transistor component.[208a] Moreover, it has been used as a dual-functional layer operating concurrently as a substrate and a transistor component.[270] With respect to transistors, several studies have been conducted on the use of a paper substrate as an insulator with eco-friendly electrolytes made from cellulose. Wan et al. reported TFTs on paper substrates impregnated with CNFs, which were used as a gate dielectric and substrate.[215] During fabrication, the paper substrate was immersed in a CNF solution for 30 s, and a thin Ag layer was thermally evaporated on the surface of the CNF-impregnated paper. In the final step, the source and drain electrodes were sputtered onto the other side of the CNF-impregnated paper. **Figure 11**a presents the large specific electrical double-layer capacitance (2.3 µF cm^{-2}) of the paper substrate without apparent electrical degradation at different bending radii. In addition, flexible TFTs with two in-plane gates were used to demonstrate a NAND logic operation, as shown in Figure 11b.

The fabrication of paper-based wearable photodetectors has attracted significant research attention due to the low cost, availability, biocompatibility, and mechanical flexibility of paper

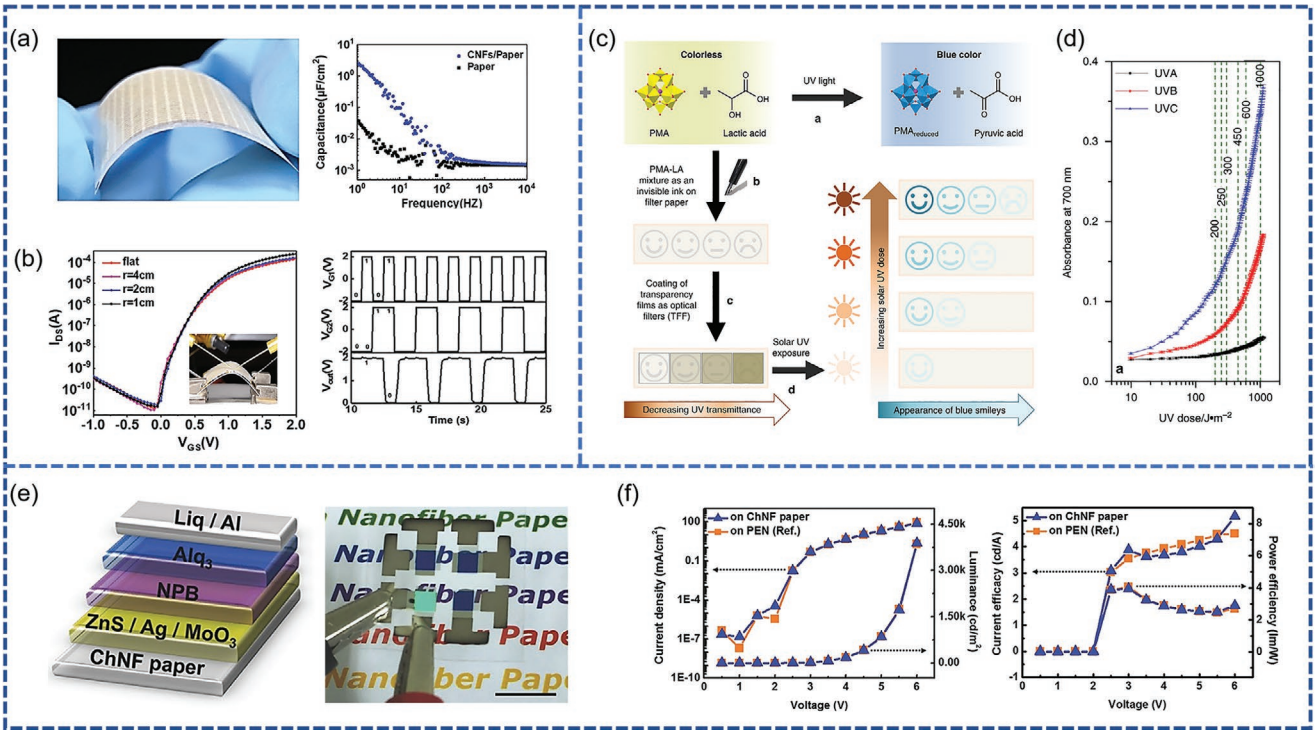

Figure 11. a) Optical image of the flexible TFTs and capacitance changes under different frequencies of CNFs-soaked and the regular paper. b) TFTs responsive curve at different bending radii with an optical image of the bent device during measurements (inset). Logical measurement demonstration of NAND logics in flexible TFT. Reproduced with permission.[215] Copyright 2019, Wiley-VCH. c) Schematic for synthesis mechanism of paper-based colorimetric UV sensor. d) PMA–LA response for UVR dose showing its ability to make difference between UVA, B, and C. Three plots represents responses for UVB MED (200, 250, 300, 450, 600, and 1000 J m^{-2}, respectively). Reproduced with permission.[271c] Copyright 2018, Springer Nature. e) Structural diagram of OLED and optical image of flexible OLED build on ChNF paper. Working of OLEED in flat and flexed state on the left and right side at 1 cm scale bar. f) Graphical representation of OLED's J–L–V characteristics, fabricated on a ChNF paper for analysis and a PEN film for reference. Reproduced with permission.[272] Copyright 2016, Wiley-VCH.

substrates. Paper-based photodetectors have various advantages such as intrinsic flexibility, hygroscopicity, environmental friendliness, disposability, and improved adhesion between paper and materials due to their porous structure. Significant research has been conducted on the development of paper-based photodetector devices.[271] Bansal et al. reported paper-based UV photodetectors using photoelectrochromic ink as the photoactive material to measure the UV type and intensity of UV light.[271c] Figure 11c presents the drawing of a phosphomolybdic acid and lactic acid (LA) invisible aqueous solution on a paper substrate containing transparent films as the coating filters. Upon exposure to UV light, the color of the smileys on the paper changed, as presented in Figure 11d, and was highly dependent on the dosage of UV light, thus demonstrating a capacity to change the number of transparent films above the ink by the absorption of UV light at different dosages. Furthermore, the device demonstrated a high distinguishing capacity with the absorption of the active material for UV-A, UV-B, and UV-C; which indicates a high capacity to discern three types of UV light with a significant difference in the effects on the human body.

The use of paper in the manufacture of flexible displays as a component of LEDs has attracted considerable research attention. Several studies were recently conducted on paper-based LEDs for flexible, lightweight, and thin displays.[272,273] For the use of paper substrates in LEDs, it is necessary to improve the resistance to organic solvents, increase dimensional stability, and minimize surface roughness, among other enhancements. Bae et al. developed transparent paper from self-assembled chitin nanofibers for flexible green electronics.[272] Using a centrifugal casting process, a homogeneous large-area sheet with a diameter of 5 in was produced, with excellent bendability and foldability, and a 92% optical transmittance. In addition, Figure 11e presents an OLED device developed from chitin nanofibers (ChNF) paper with a thickness of 40 m, and surface planarization layer made from PMMA. Figure 11f presents the current density–luminance–voltage (*J–L–V*) curve and efficiency plot, thus revealing a maximum luminance of 3890 cd m^{-2} at a turn-on voltage of 2.5 V. Wang et al. recently fabricated a paper electrode with a high flexibility and conductivity by the electroless deposition (ELD) of Cu NPs using a dopamine monomer with a planar and hydrophobic surface, high reflection, and excellent mechanical flexibility and stabilities.[274] Furthermore, the fabricated paper electrode was effectively utilized as a mechanical support and electrode in an OLED, thus demonstrating a maximum luminance of 700 cd m^{-2} at a turn-on voltage of 2.5 V.

The recent developments in paper-based flexible electronic devices led to the advancement of numerous applications, including energy storage devices and sensing systems for biomedical applications, among other electronic applications. Moreover, the increasing preference for paper substrates over conventional substrates is due to their ease of use, low cost, availability, high flexibility, ease of modification, and disposability. In addition, due to the ease of processing paper substrates using various processing techniques, paper substrates can be modified with numerous materials, including conductive polymers and nanomaterials. Despite these advantages, the stability and durability of paper substrates limit their applicability to commercial flexible electronic devices. However, the integration of specialized materials on paper substrates with distinct characteristics can serve as a basis for the development of paper-based electronic devices with various applications.

3.3. Fiber/Textile Substrate Based Flexible Electronic Devices

Textiles are flexible, stretchable, porous materials composed of fibers with high aspect ratios (higher than 103). The fiber materials are made up of filaments that are knitted together to form a continuous architecture with lengths of 15–150 mm and thicknesses of 10–50 μm.[275] Several manufacturing techniques are utilized for effective textile production, such as yarn spinning, knitting, weaving, dyeing, printing, and washing using fibers with stretchability and a slight recoverable extensibility.[276] Textile materials should be able to absorb a significant amount of water, withstand light and heat, and be chemically resistant, among other characteristics; for practical use. Natural fibers are composed of macromolecules with a high molecular mass and high fiber alignment, with cotton exceeding 1500 kDa and silk exceeding 600 kDa. For the production of fibers, the molecular mass of the polymer determines the processability and mechanical properties of the resulting fiber. For example, in the case of a hydrogen-bonded polyamide, a molecular mass of ≈20 kDa is sufficient for textile applications due to the strong intermolecular interactions, whereas a minimum molecular mass of 60 kDa is required for polypropylene polymers due to the weak forces involved.

Textiles with integrated electronic components (e-textiles) provide advantages to flexible, wearable, and conformable large-area electronic systems, thus innovating applications in various industries such as communication, entertainment, sports, healthcare, space, and security.[277] Moreover, compared with other substrates, textile substrates allow for the distribution of large electronic systems, and facilitate the development of body-worn or wearable technologies. In terms of ultra-flexibility, stretchability, and patchability to the skin, electronic textiles are highly desirable due to their unique characteristics, including flexibility, low mass, wearability, and inherent warm and snug properties. Therefore, to foster substantial industrialization, electronic textiles have evolved as excellent candidates for wearable electronics, to enhance the electronic functionality and connectivity over the next few years. The current market for e-textiles results in sales of ≈100 million USD per year, and is predicted to reach 1.4 billion USD by 2030.[278]

3.3.1. Fabrication Techniques for E-Textiles

For flexible and wearable device applications, conventional textile materials such as, silk, cotton, synthetic polyester, and wool should be conductive due to their electrically insulating nature, and demonstrate high flexibility and stretchability while withstanding mechanical deformations such as, bending, twisting, and stretching. Numerous techniques were recently developed to realize e-textiles while maintaining stability and preventing performance degradation in large-scale manufacturing. The processing techniques for textile substrates are classified into three approaches: 1) The physical coating method, which includes the

direct coating of functionalized material based on various techniques of printing (screen printing and inkjet printing) and coating (dip coating, blade coating, and infiltration) onto fiber/yarn/textile substrates; 2) the chemical in situ growth of various active materials onto fiber/yarn/textile substrates using chemical methods such as hydrothermal synthesis, microwave synthesis, and electrodeposition; and 3) the fabrication of fibers/yarns/textiles on a large scale with intrinsic properties by spinning techniques, the removal of the interfaces between the substrates and active materials, and the solving of the contact problems, which result in poor conductivity. In the following section, a brief discussion is presented on the processing techniques employed for textile substrates in flexible electronic devices.

Physical Coating Techniques: In general, most textile materials such as silk, cotton wool, and synthetic polyester have an electrically insulating nature. However, for successful utilization in wearable electronics, a high conductivity, flexibility, and stretchability are desirable. In addition, high stability during bending, stretching, and twisting is critical. In addition to the functionalization of the textile substrate with conductive materials, polymer binders, or other additives; the inclusion of adhesion promoter, colorant, plasticizer, and biocide coatings are required. Thus, textile coatings can be of different types depending on the nature of the components used, such as organic and inorganic coatings, hydrophobic and hydrophilic coatings, functional coatings, and metallic and nonmetallic coatings. For the fabrication of e-textiles, various techniques were developed for the integration of conductive materials such as metal NPs, NWs, CNTs, and graphene on fibers; deposition of metal filaments with yarns; and the patterning of conductive materials on textiles using screen printing,[279,280] inkjet printing,[281,318,319] and 3D printing. Using the screen-printed method, various conductive inks such as Ag NWs, CNTs, and PEDOT:PSS have been printed on textile substrates.[279] Someya et al. demonstrated the screen printing of textile-permeable viscous ink on textile substrates, thus allowing for the highly stretchable and conductive deposition on textiles via a simple and inexpensive method.[280] **Figure 12**a presents a schematic illustration of the screen printing of Ag flack ink directly on a tricot-knitted textile of nylon and PU. After screen printing, a capillary process was conducted to absorb and dry the ink from the surface to the interior of the textile, thus resulting in elastic conductors with inherently flexible conductive pathways and knitted textile structures. Moreover, Figure 12b presents the SEM images of fiber bundles occupied with elastic conductors before and after printing, which filled a significantly small gap with the stretchable conductor composite. Before printing, the textile substrate requires the coating of a thick ink-receptive layer due to the high porosity and surface roughness of the textile. Jur et al. fabricated e-textiles by the inkjet printing of Ag inks onto woven textiles based on Kirigami patterns.[281] Figure 12c presents a schematic diagram of the kirigami patterning process, thus demonstrating the inkjet printing of reactive Ag inks onto pristine woven fabrics comprising 100% PET fibers in both directions. In the subsequent curing step, Ag ions were reduced to elemental Ag by annealing at 150 °C, which produced conformal Ag with excellent adhesion to the polyester woven fabrics, as shown in Figure 12d. This confirmed the presence of cured Ag after printing, and the improvement of the washing durability of the printed e-textiles. To date, several reports have been published on the inkjet printing of conductive materials such as conductive polymers,[282] 2D conductive materials,[283] and NWs[284] on textile substrates.

Furthermore, for electronic textile manufacturing, 3D printing provides three methods for different hierarchical levels: i) The integration of printed fiber or yarn structures into the fabric for e-textile manufacturing, ii) the combination of 3D printing with other techniques such as electrospinning for the printing of the entire textile, and iii) the utilization of textiles as a substrate for printing hybrid structures, thus imparting new properties to the textile substrate. For example, Yang et al. reported a thermally conductive fibrous structure by combining 3D printing techniques with wet spinning using a suspension of PVA with boron nitride nanosheets.[285] Similarly, Yao et al. fabricated a hybrid fiber-shaped supercapacitor and temperature sensor by utilizing a 3D printing material extrusion setup.[286] Zhang et al. recently fabricated an energy management textile by directly 3D printing smart patterns of core-sheath fibers on textiles using a 3D printer assembled with a coaxial spinneret.[287] The 3D printing patterns fabricated by the extrusion of core-sheath fibers from a coaxial spinneret on a textile substrate are presented in Figure 12e. In particular, a core-sheath structured fiber was fabricated by the uniform injection of CNT ink, in addition to SF ink from the inner spinneret, into the outer spinneret; and uniformly distributed on the textile by matching the speed motion of the coaxial spinneret with the extrusion rate of the fiber (Figure 12f).

However, the printing process results in poor adhesion between the conductive material and parent elastomer fiber; thus, the bonding energies require improvement. Among other methods, the most commonly utilized process involves the application of plasma treatment, which generates reactive groups and radicals. Recently, Yu et al. reported the layer-by-layer spray coating of Ag NWs and MXene nanosheets on a multifunctional silk textile substrate for the development of a highly conductive biomimetic leaf-like nanostructure on porous textiles, as illustrated in Figure 12g.[288] In the first step, after the plasma treatment and polyethyleneimine deposition, the textile substrate was spray-coated with MXene nanosheets and Ag NWs, which was repeated for different durations; thus resulting in highly conductive networks on the silk substrate (Figure 12g). Furthermore, Jia et al. reported a drop-casting technique to deposit Ag NWs, and a composite solution containing Ag CNTs, polytetrafluoroethylene nanoparticles, and a fluoroacrylic polymer. On a 100% pre-strained textile substrate, Ag NW solution was deposited dropwise and dried at 25 °C for 120 min. The composite solution was added dropwise to decorate the textile with a superhydrophobic coating, as illustrated in Figure 12h. Similarly, Yu et al. demonstrated a dip-coating approach for the decoration of PPy/MXene onto a PET textile, as presented in Figure 12i,j, thus realizing uniform textile deposition by the MXene sheets due to the hydrogen bonding and van der Waals forces between the PPy/MXene sheets and fibers.[289] To improve the environmental stability, the coated textile was further decorated with a silicone layer, which prevented oxidation and the degradation of its MXene component. Moreover, in dip coating, the surface properties of the textile substrate have a significant influence on the amount of active materials

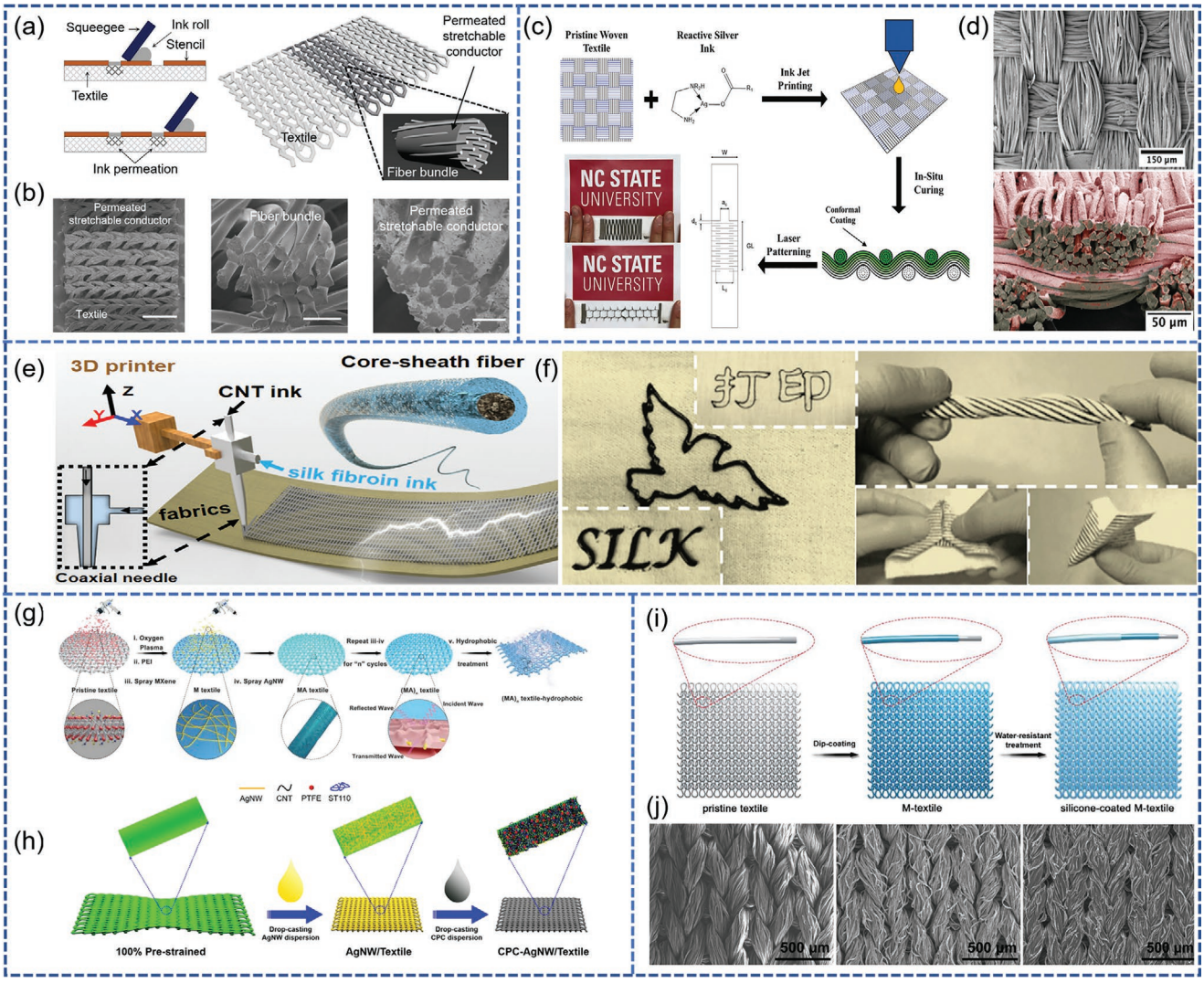

Figure 12. a) Schematic of direct stencil printing on textile and illustration of permeated composite in a single fiber bundle. b) Surface and cross-section SEM images of printed wiring and textile before and after printing, respectively. Reproduced with permission.[280] Copyright 2017, Wiley-VCH. c) Schematic diagram for synthesis and characterization of laser cutting printed e-textiles. d) Surface SEM of pristine woven at 150 μm and cross-sectional SEM image of a printed woven indicating red (silver coating) on grey (individual fibers). Reproduced with permission.[281] Copyright 2019, Wiley-VCH. e) Schematic elaboration of 3D printing mechanism utilizing the coaxial spinneret. f) Images of patterns designed on textile, English word SILK, flying pigeon, and Chinese characters. Twisted and folded images showing flexible behavior of smart textile. Reproduced with permission.[287] Copyright 2019, Cell Press. g) Schematic diagram indicating manufacturing process of conductive, hydrophobic, and permeable silk textile by layer-by-layer fabrication approach. h) Schematic for deposition of Ag NWs and CPC to form CPC-AgNW textile. Reproduced with permission.[288] Copyright 2019, Wiley-VCH. i) Schematic of manufacturing PPy/MXene-decorated and silicone-coated PET and M-textile respectively. j) SEM images of pristine, M-textile, and silicone-coated M-textile (from left to right). Reproduced with permission.[289] Copyright 2019, Wiley-VCH.

coated, and vary significantly from the type of fabric materials.[298,324–328,336] Multicoating dip and dry coating methods were reported with multiple dipping cycles (5–35 cycles).[290]

Chemical In Situ Growth onto Fiber/Yarn/Textile Substrates: In addition to physical coating methods for textile substrates, chemical in situ growth approaches were developed for the direct synthesis of various materials on the surface of textile substrates via various chemical reactions such as hydrothermal reactions,[293–295,323,330] CVD reactions,[296,334,335,337] in situ polymerization,[298,300b,301,329] and electrodeposition.[297,331–333]

The in situ hydrothermal synthesis of the textile substrate involves chemical reactions above the ambient temperature and pressure in a sealed heated solution. For in situ hydrothermal synthesis, carbon fiber textiles are the most favorable and widely used substrates due to their stability under ambient conditions. Various materials, including metals or metal oxides with unique structures such as nanosheets,[291] NWs,[292] nanorods,[293] and cluster-type structures have been synthesized on textile surfaces. Zhang et al. decorated $Na_2Ti_3O_7$ nanosheet arrays on carbon textiles using a simple hydrothermal process with strong adhesion.[294] Thereafter, Yang et al. constructed a 3D hierarchical nanosheet of $NiMo_3S_4$ nanoflakes on flexible carbon cloth by a simple hydrothermal growth process, as presented in **Figure 13**a, thus demonstrating anion adsorption on

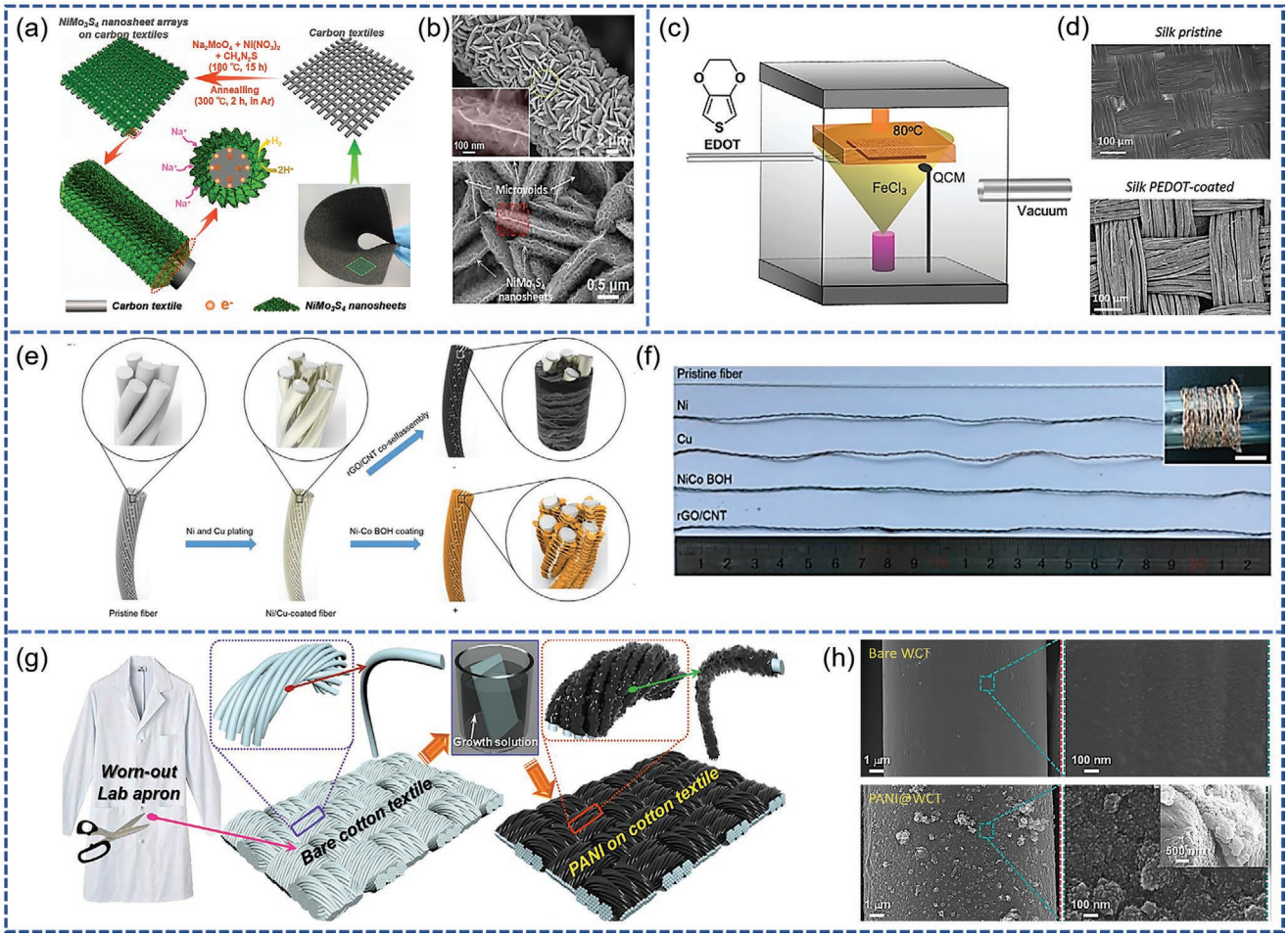

Figure 13. a) Schematic diagram of fabricating 3D hierarchical nanosheet ($NiMo_3S_4$) patterns on carbon textiles. b) SEM images of NiMo3S4/CTs at different magnifications. Reproduced with permission.[295] Copyright 2018, Elsevier. c) Structural diagram of the vapor deposition system. d) SEM images of pristine silk textile and PEDOT-coated silk textile. Reproduced with the permission.[296] Copyright 2017, Wiley-VCH. e) Schematic of the manufacturing mechanism of Y-ASC. f) Optical image of yarns for multiple coatings (Ni, Cu, Ni-Co BOH, rGO/CNT). Reproduced with permission.[297] Copyright 2019, Wiley-VCH. g) Schematic illustration for PANI deposition on WCT surface. h) High-magnification SEM results of pristine and PANI coated onto the WCTs. Reproduced with permission.[298] Copyright 2018, Elsevier.

the $NiMo_3S_4$ surfaces during the hydrothermal process. This accelerated the oriented growth of nanocrystals, thus leading to a 3D hierarchical nanosheet array formation.[295] Figure 13b presents the SEM image, which reveals the uniform distribution of $NiMo_3S_4$ nanosheet arrays on the surface of the carbon textiles.

In situ CVD involves the exposure of the substrate to a single or multiple volatile precursors, which react or deposit on the substrate surface with the removal of by-products by gas flow through the reaction chamber. Typically, this technique has been extensively utilized for the preparation of silicon materials such as carbide, dioxide, and nitride; carbon materials such as, nanotubes, nanofibers, graphene, diamond; and 2D materials such as, MoS_2 and MXene on different flexible and rigid substrates.[9a] Andrew et al. coated conductive polymer PEDOT films on various fibers such as, silk, linen, and bast fiber fabrics using a reactive vapor deposition compartment, as presented in Figure 13c, thus demonstrating the uniform distribution of $FeCl_3$ vapor from the electrical furnace to a sample stage positioned 7 in above the furnace.[296] The stainless-steel tubing transported 3,4-ethylenedioxythiophene (EDOT) vapor from outside the chamber based on an in-line mass flow controller. The EDOT vapor flux coincided with the $FeCl_3$ vapor plume, thus resulting in the polymerization of EDOT into EDOT oligomers, which were deposited on different fiber fabrics placed in the intersectional regions. Figure 13d presents the SEM images of the silk fabric before and after the coating of PEDOT by CVD, thus resulting in uniform and conformal coatings on the silk surface.

In addition, electrodeposition is an effective technology for synthesizing a film of solid materials from a solution of ions onto electrically conductive substrates. This process involves a three-electrode system comprising of Ag/AgCl as the reference electrode and Pt mesh/wire as the counter electrode by applying a suitable potential and current for the formation of reduced on the working electrode. Moreover, this technique has been utilized extensively for the electrodeposition of transition metal oxides such as MnO_2 and Co_3O_4, iridium oxide, and

conductive polymers PPy and PANI on conductive textiles such as metal-coated textiles and carbon textiles.[276,299] Recently, Wang et al. reported the ELD of Ni and Cu on polyester yarn, as illustrated in Figure 13e.[297] The Ni-Co bimetallic oxyhydroxide was electrodeposited on the Cu surface acting as a positive electrode, whereas the redox reaction between the Cu and GO/CNT suspensions resulted in an RGO/CNT hybrid film on the negative electrode, as shown in Figure 13e. The optical image presented in Figure 13f reveals the coating of Ni, Cu, NiCo BOH, and RGO/CNT on the polyester yarn.

In situ polymerization, which is a simple single-step, large-scale, and cost-effective method, has been extensively employed to deposit conductive polymers such as PPy, PANI, and PEDOT on textile substrates.[300] Yu et al. utilized an in situ polymerization technique to deposit PPy on a cotton textile by a two-step polymerization method, which involved the immersion of the cotton textile in a solution of 0.5 M pyrrole for 20 min, and further proceeded through the absorption of oxidant solution at 0–4 °C. This resulted in a change in color into greenish-black color, which indicated the deposited pyrrole on the textile.[301] Similarly, the same group recently demonstrated a low-temperature and cost-effective in situ polymerization method for depositing PANI on a cotton substrate with a high flexibility.[298] As presented in Figure 13g, portions of cotton textiles were cut from a worn-out lab apron and immersed in the polymerization solution for 0–3 h, thus resulting in PANI nanoarchitectures on the cotton textiles. Figure 13h presents the low-and high-magnification SEM images of the bare and coated textiles, thus revealing no materials on the surface of the bare textile. However, after the polymerization process, the conductive polymer PANI was uniformly distributed in the form of particles on the microfiber surfaces, as shown in Figure 13h.

Fabrication of Fibers/Yarns/Textiles with Intrinsic Properties by Spinning Techniques: In addition to the physical and chemical processing techniques of textile substrates, the development of yarns and fabrics with intrinsic properties by the spinning process is considered a promising strategy. In general, the spinning process is categorized into dry, wet, and electrospinning techniques. The wet spinning and dry spinning techniques are used to extrude the filaments into a solvent tank or a stream of air, respectively. In these methods, spinning solutions are prepared that contain an individual or active nanomaterial mixture such as GO, CNTs, pyrrole, and PANI, where electrode materials demonstrate superior mutual compatibility.[302]

The wet spinning method has been extensively used for the preparation of numerous fibers, for example, conductive polymer fibers such as, PEDOT:PSS fibers,[303] GO fibers,[304] MXene/GO fibers,[305] CNT fibers;[306] and other composite fibers such as, Ag NWs/PU composite fibers.[307] Gao et al. proposed a wet spinning technique to produce non-woven graphene fiber fabrics (GFFs) from graphene staple fibers in aqueous solvents, followed by integration into the entire fabric via strong inter-fiber bonding.[308] Moreover, the annealing process resulted in flexible, strong, lightweight, and highly conductive interfused GFFs. Thereafter, Kim et al. reported a 1D graphene fibrous structure by the wet spinning method illustrated in **Figure 14**a, thus revealing that upon the exposure of the pre-aligned GO to a flowing environment (Step II), it can be aligned in a uniform direction (Step I).[304b] Moreover, the third coagulation step stabilized and densified the aligned GO sheets into a fibrous arrangement during the coagulation process. After washing and drying, freestanding continuous GO fibers were obtained, as presented in Figure 14a. The optical and SEM images presented in Figure 14b reveal the winding of GO fibers on a bobbin with uniform morphology, which contained well-aligned GO sheets along the fiber axis.

Dry spinning is considered as an environmentally friendly method and an important technique in the chemical fiber industry that does not require a coagulation bath, which simplifies the spinning process and reduces the production cost. In the dry spinning process, the solidification of the fiber occurs because of the evaporation of volatile solvents. Buehler et al. developed a simple bioinspired spinning approach to group regenerated silk fibers (RSFs) under acoustic environmental conditions by pulling a silk microfibril solution from a mixing chamber without post-processing, based on the dry-spinning characteristics.[309] The fabricated as-spun RSFs exhibited natural silk properties with a hierarchical architecture and excellent mechanical properties. Cheng et al. recently reported a novel dry spinning method for the fabrication of AuNW/SEBS stretchable fiber conductors, as shown in Figure 14c.[310] After mixing AuNWs with a SEBS block copolymer in tetrahydrofuran (THF) solution, the viscous and volatile spinning solution was extruded into the air from a needle, thus resulting in THF evaporation and the formation of dry-spun fibers longer than 10 m on a metal bobbin. Figure 14d presents optical images of the fiber before and after the deposition of gold nanoparticles, thus revealing the color change after the deposition process.

The spinning techniques mentioned above only reveal the capacity to fabricate spun fibers with diameters at the micrometer scale. However, fabricating nanometer-scale fibers has attracted significant research attention due to the large surface-to-volume ratio. Electrospinning is a versatile approach, and is considered as efficient for the fabrication of ultrafine fibers with diameters ranging from <0.003–1 μm. Numerous attempts are evident for abdicating electrospun fibers for textile applications.[312] Buehler et al. reported graphene reinforced silk fibers by electrospinning from the dispersion of graphene/silk fibroin suspensions.[313] Furthermore, Lee et al. demonstrated the electrospinning of a PDMS ion gel core and PVDF coatings for the fabrication of a core–shell fiber mat.[314] Tan et al. recently fabricated seaweed-derived nanofibrous membranes by a cost-effective strategy that involves the electrospinning of polyethylene oxide (PEO5000k) with a high molecular mass and a sodium alginate (SA) composite solution, followed by crosslinking and washing with water, thus resulting in a SA/nanofibrous membrane (SA-NFM) with excellent morphology, as presented in Figure 14e,f.[311]

3.3.2. Applications of E-Textiles in Flexible and Wearable Systems

Sensor Devices: The investigation of textile-based wearable sensory systems was first conducted in the 1980s with initial focus on the use of bulky inorganic devices in textiles, which increased the mass and discomfort of textiles. Over time, textile-based wearable sensor devices such as strain/motion sensors, touch/pressure sensors, temperature sensors, electrochemical

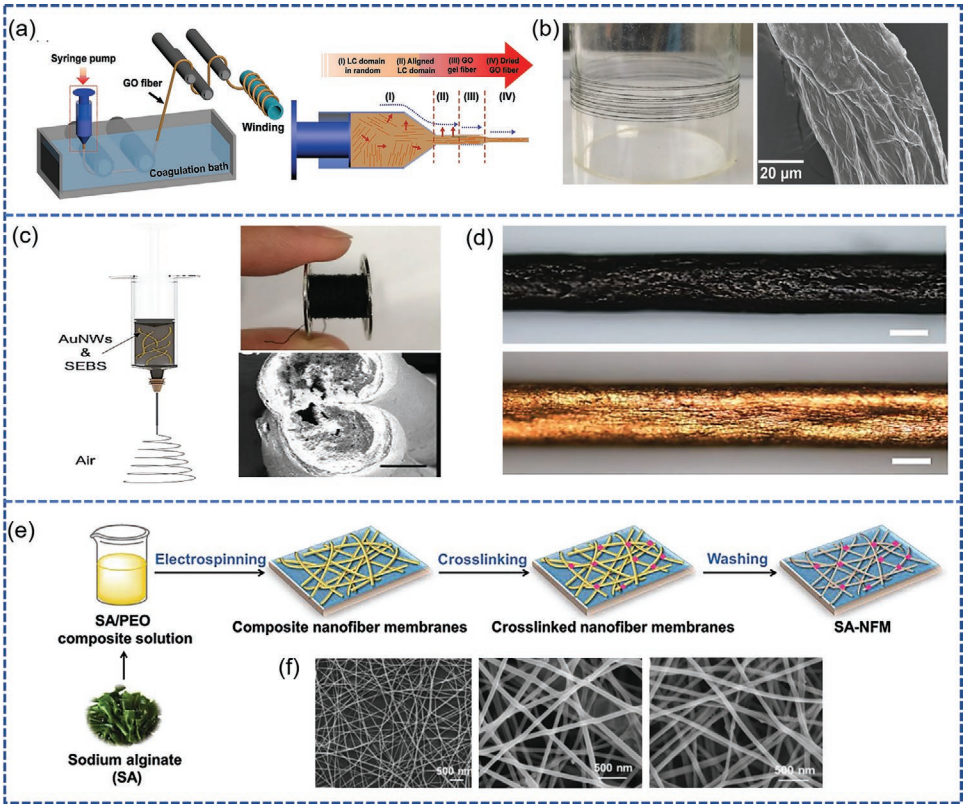

Figure 14. a) Synthesis schematic of graphene oxide (GO) fiber formation. b) GO wrapped on the bobbin and its SEM image. Reproduced with permission.[304b] Copyright 2018, Wiley-VCH. c) Schematic for the fabrication of AuNWs/SEBS. Optical image of 10 m long AuNWs/SEBS fiber wrapped on the metal bobbin and EDX analysis. d) Photographs of the AuNWs/SEBS before and after the growth of Au film. Reproduced with permission.[310] Copyright 2019, Wiley-VCH. e) Schematic for synthesis steps of 2D electrospun membranes. f) SEM images after crosslinked by Ca^{2+}, and removal of PEO at 500 nm scale bars. Reproduced with the permission.[311] Copyright 2019, Wiley-VCH.

sensors, and gas sensors have been extensively investigated by fabricating electrically conductive fibers for the detection of physical and chemical changes, and conversion into electrical signals. In general, e-textiles require the superficial attachment of electronic elements such as integrated circuit chips or resistors to the fabric. The coating techniques discussed above change several properties of the fabric such as the shear, tensile, and bending properties, due to the changes in the mobility of the yarn after coating. The modification of various fabric/textile substrates to different levels of structural hierarchy can be realized for the fabrication of sensing devices. The first level of modification necessitates the development of conductive fibers for the construction of e-textiles. The second level involves the replacement of a simple yarn with a sensitized yarn. The third level entails the modification of the textile surface by coating it with a sensing material to realize sensing properties. The final level involves the utilization of multiple fabrics to fabricate the sensing composite. However, the modification of these sensing properties can be achieved in the fabric structure at any level. For example, at the first level of developing fibers to realize sensing properties, significant research has been conducted.[339] For example, Lewis et al. fabricated soft capacitive strain sensor fibers for the determination of elongational strains for specific applications in soft robotics and human–machine interfaces.[339c] Additionally, Anikeeva et al. reported a flexible and stretchable probe with the capacity to combine optical stimulation and electrophysiological recordings for successful implantation into mouse spinal cords.[340] Polymer fibers were produced by the thermal drawing process, and further coated with conductive Ag NWs, as shown in **Figure 15**a. The constructed probe was tested for electrical impedance and optical transmission under deformations similar to those observed in mouse spinal cords, thus demonstrating the excellent resilience of the polymer fiber cores and concentric mesh electrodes to strain. Finally, the optically evoked neural activity and sensory-evoked activity were measured in the spinal cord of mice, thus demonstrating the excellent usage of these probes in the spinal cord sensory system (Figure 15b,c).[340]

In addition to fiber sensors, textile/fabric substrate sensors coated with sensory material were reported. Ren et al. demonstrated a wearable textile strain sensor by coating GO on a polyester fabric substrate, and applied it to different parts of the body such as the knee, wrist, finger, and elbow for the detection of large motions.[341] Chen et al. recently utilized e-textile technology to fabricate a flexible and wireless pressure sensor array for the remote measurements of human-interactive pressure distribution.[342] The performance dependence of the pressure sensor under various mechanical loads demonstrated an outstanding sensitive response to cyclic loads, and signal repeatability for over 20 000 cycles of external loads. Furthermore, textile-based

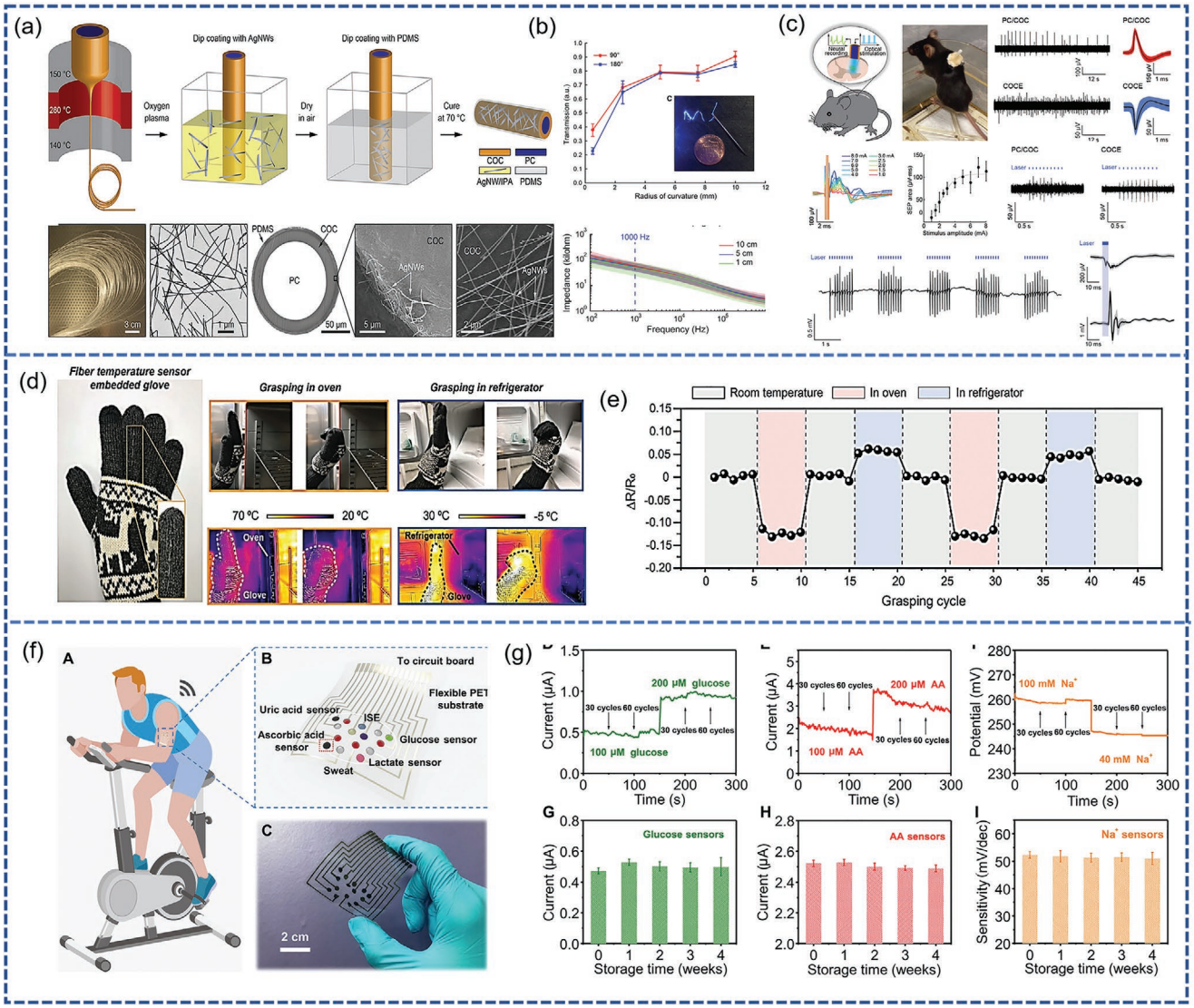

Figure 15. a) Fabrication schematic of the fiber probe with corresponding SEM and TEM images. b) Transmission and impedance spectra of fiber probes. c) Probing spinal cord electrophysiology with flexible and stretchable neural probes. Reproduced with permission.[340] Copyright 2017, American Association for the Advancement of Science. d) Optical and IR images of smart gloves for temperature sensing. Grasping responses under different temperatures were recorded in a refrigerator and oven. e) Graphical representation of continuing grasping movements for smart gloves sensing at two different temperatures (oven and refrigerator). Reproduced with permission.[345] Copyright 2020, Wiley-VCH. f) Schematic image of flexible Silk NCT-based sensor and after attaching on arm for sweat examination of a volunteer under constant physical activity. g) Electrochemical measurement results of the SilkNCT-based glucose sensors as AA Na and glucose sensors at multiple storage times. Reproduced with permission.[346] Copyright 2019, American Association for the Advancement of Science.

temperature sensors with the capacity to measure temperature via electrical signals have been widely reported.[276,343] Jia et al. fabricated thermally drawn multi-material fibers for temperature and pressure sensing with pressure and temperature sensitivities of 4 kPa and 2 °C, respectively.[344] In the case of deformable e-textiles for temperature monitoring in diagnostics, strain-induced interference limits the device upon various movements. To overcome this limitation, Pang et al. recently published a paper describing an inherent strain-insensitive temperature sensor fiber with a high sensitivity of 0.93% and low strain sensitivity at a tensile strain of 60%.[345] Figure 15d presents the fiver sensor integrated into a smart glove with a wireless transmitter for temperature monitoring, which exhibited a resistive response to various temperatures when the glove was placed in an oven or refrigerator. Moreover, the resistive response during repeated grasping correlates with the thermal images presented in Figure 15e, thus demonstrating the high heat sensitivity and low strain sensitivity of the device.

There has been a recent increase in research conducted on wearable sensors for the measurement of physiological parameters in medical diagnoses. Meanwhile, for wearable textile sensors, moisture and water absorption property may lead to decline in conductive and sensing performance. So waterproof property of electrode endows the sensors with brilliant

anticorrosion performances toward harsh environment like acid/alkaline environment, ultraviolet radiation, stain, and humid environment.[347] For example, Wang et al. fabricated a superhydrophobic strain sensor with enhanced sensing stability and anti-corrosion property by partially embedding perfluorosilane-coated graphene into TPU.[348] Later on, Shen et al. developed tunable wearable nonwoven fabrics strain sensor by dip coating of conductive cellulose nanocrystal/graphene. For creating superhydrophobicity, the prefabricated electrode was further coated with HF-SiO_2 in ethanol dispersion.[349]

Among other sensors, textile-based electrochemical sensors exhibit a capacity for the detection of toxic agents or the concentration of specific compounds in body fluids for medical therapeutic and diagnostic applications. In a wearable chemical sensor, a sweat sensor has significant value for diagnostic applications. Choi et al. reported highly sensitive sweat sensing threads with a high self-healing efficiency (>97%) and ease of integration into fabric used for K^+/Na^+ sensing.[350] Subsequently, Zhang et al. reported a silk fabric derived carbon textile flexible sweat analysis patch for the instantaneous detection of six health-related biomarkers such as, lactate, glucose, ascorbic acid, uric acid, Na^+, and K^+.[346] Figure 15f presents an image of a SilkNCT-based flexible sensor array prepared by a laser processing strategy; and its application onto a volunteer arm during physical activity to measure biomarkers in the sweat is presented in Figure 15g, thus demonstrating the instantaneous detection of biomarkers with high selectivity, high sensitivity, and long-term stability.

Energy Storage Devices: Textile-based energy storage devices have been systematically categorized into three approaches: fiber devices, woven and knitted textile devices, and coated textile devices. The first report on the fabrication of fiber or yarn-like energy storage devices was published between 2011 and 2012 by transforming materials into 2D or 3D fabrics.[351] Additionally, numerous production problems were thereafter addressed by coating a fabric with several layers of the current collector, electrode, or separator; or by encapsulation within a single portion of fabric or a multi-layered garment. However, there are several problems with respect to the applied materials, methods, and characterization of textile-based energy storage devices. These include the device ranking (in terms of the device performance with respect to the electrochemical activity, flexibility, stretchability, and testability), electrode characterization, performance matrix consideration (in terms of linear, gravimetric, volumetric, or areal capacitance), criteria for material selection, and targeted performance indicators.

The most critical component in energy storage devices is fiber electrodes due to their high flexibility and strength, and their capacity to be wearable and knittable with no decrease in electrochemical performance. The design of fiber devices can be single or multiple, depending on the power generation requirement. Furthermore, these devices can be readily integrated into textile designs. The single-fiber design mostly contains coating layers, which serve as electrodes and electrolytes. For example, as a single-fiber device, a hybrid smart fiber was fabricated containing a supercapacitor at the core and a triboelectric energy harvester at the shell (**Figure 16**a), thus exhibiting a high efficiency in the spontaneous self-charging process without an external power supply.[352] The potential difference was due to the generation of surface charges by the triboelectric effect, and enhanced by employing an asymmetric coaxial structure. Furthermore, the electrochemical performance of the fabricated supercapacitors before and after coating with a poly(vinylidenefluoride-trifluoroethylenechlorotrifluoroethylene) (P(VDF-TrFE-CTFE)) terpolymer yielded a rectangular curve, as shown in Figure 16b, thus indicating ideal energy storage with specific capacitances of 157 and 155 F cm^{-2} for the supercapacitors, and a corresponding high coulombic efficiency. Peng et al. reported the first fiber-based LIB by twisting an aligned CNT fiber and lithium wire.[353] Thereafter, extensive research was conducted on fiber/yarn-base flexible batteries.[354] A cable-shaped LIB was developed on CNT woven microfilms, thus resulting in an ultrahigh density fiber electrode of ≈10 mg cm^{-2}. Furthermore, manufactured fiber-shaped LIBs demonstrated a high flexibility and volumetric energy density of 215 mWh cm^{-3}, thus indicating a high capacity to supply power to light devices under various deformations while retaining a stable performance after weaving into textiles. Similarly, other fiber-shaped batteries such as fiber-shaped Li−S batteries were reported by Kim et al., by coupling a hybrid fiber electrode (prepared by a wet spinning technique) with a lithium wire, which resulted in a high volumetric capacity of 0.44 × 106 mAh L^{-1}, a high energy density of ≈917 Wh L^{-1}, and a long cycle lifespan.[355] Moreover, high mechanical flexibility and stability were achieved while sustaining a linear displacement of 50% for 30 cycles of bending. In addition to fiber-based supercapacitors and batteries, a flexible fiber-based dye-sensitized solar cell (DSSC) was developed by Zou et al. A cell with a diameter of 200 μm was designed by twisting two electrodes into a single fiber-type device.[356] In a cell, a TiO_2 coated stainless steel fiber acted as the working electrode, and Pt wire acted as the counter electrode. The charge transport from the photoanode to the counter electrode was transferred via a liquid electrolyte. Furthermore, the weaving structure allowed for the light to reach the working electrode from almost all directions. This study initiated the weaving of solar cells into various shape. Another contribution of this study was the integration of a fiber-type supercapacitor with a fiber DSSC for the fabrication of a novel power device with a process cycle efficiency of ≈2.1%.[357]

The single-fiber design demonstrates the capacity to enhance the weaving and knitting properties of fiber-shaped devices. However, excellent compatibility is required between the different layers to realize mechanical properties such as flexibility and tenacity. Differences in these properties may lead to difficulties in balancing the various factors of the system. Peng et al. recently published a critical review on the development of fiber-based energy storage devices with a slight emphasis on the interface between the active materials and electrodes.[358] Coating highly curved fibers with a thin uniform film is challenging, given that under significant mechanical deformation, breakage may occur. In addition, numerous studies were conducted on the stretchability of 1D energy devices with various stretchable systems.[359] The long-term stability of these devices is limited. Furthermore, liquid electrolytes cause a reduction in the stability of these devices, given that the active long-term encapsulation of liquids in a fiber system is challenging.

The second category is the weaving or knitting of fiber into textiles. Mai et al. fabricated a thread-type fiber supercapacitor

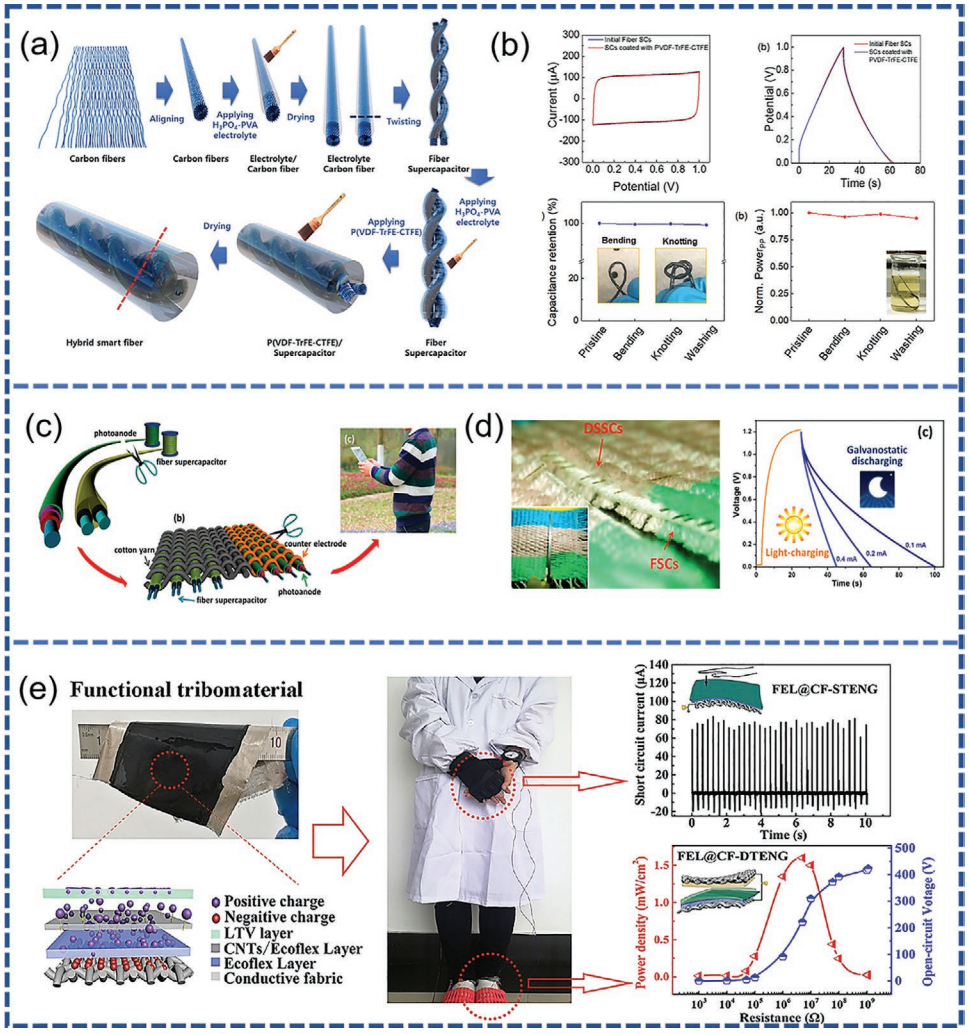

Figure 16. a) Brief fabrication schematics for a hybrid smart fiber. b) CV curves at of 10 mV s^{-1} scan rate under 0.0–1.0 V applied potential sweep. The second graph represents galvanostatic charge–discharge at −2 0.05 mAcm current density. Reproduced with permission.[352] Copyright 2020, Wiley-VCH. c) Structural schematic for fiber supercapacitor (FSC) or DSSC tailored into multiple components. Optical image showing the wearing future of smart energy to power small electronics. d) Image showing tailorability of the integrated textile cloth with DSSC and FSCs functions. Graphical representation of light-charge and galvanostatic discharge responses. Reproduced with permission.[360] Copyright 2016, American Chemical Society. e) Optical image and structural schematic for functional tribomaterial with responses when attached to different body parts. Reproduced with permission.[361] Copyright 2019, Elsevier.

(FSC) and DSSC photoanode to produce a solid tailorable energy textile by weaving, sewing, and tailoring.[360] The as-fabricated device demonstrated the capacity to harvest solar energy and store it, as presented in Figure 16c. Moreover, it was a single layer energy textile with integrated functions of simultaneous solar energy harvesting and storage, as provided by a ZnO-based DSSC and TiN-based FSC, respectively. Figure 16d presents an optical image of the energy textile with DSSC and FSC functions, which demonstrated a high light-charge and galvanostatic discharge performance; with a full charge cycle to 1.2 V in 17 s, and a discharge current 0.1 mA in 78 s by self-harvesting solar energy.

In addition, functional material-coated textiles were widely reported for energy storage devices. Zheng et al. fabricated composite fabric electrodes by the vacuum filtration of RGO and MWCNTs onto Ni-coated cotton fabric, thus exhibiting a double-layer capacitor behavior by reaching an areal capacitance up to 6.2 F cm^{-2} at a high areal current density of 20 mA cm^{-2}. Moreover, the as-fabricated fabric-type supercapacitor with a composite electrode demonstrated a capacitance of 2.7 F cm^{-2} at 20 mA cm^{-2} at the first charge–discharge cycle, and 3.2 F cm^{-2} after 10 000 charge–discharge cycles without capacitive decay after 10 000 bending tests.[362] Furthermore, the high mechanical flexibility and integration feasibility (medical, clothing, and household applications) of functional coated textiles make them ideal candidates for implementation in the energy supply systems of wearable applications. In addition to these characteristics, the most critical property is softness, which is necessary for human comfort. In general, decorating an insulating cloth with functional materials decreases the softness of the cloth. To solve this problem, Wang et al. evaluated the flexibility of a functionally coated textile in terms of softness. A highly flexible cloth current collector was decorated, and it demonstrated

a high conductivity of ≈4–200 kS m^{-1} and softness of 8 mm. With a high capacity of ≈1.0 mAh cm^{-2} and high energy density of 1.7 mWh cm^{-2} at a power density of 8.5 mW cm^{-2}, the as-fabricated metal cloth demonstrated a high performance in Zn batteries.[363] Furthermore, the device exhibited a high flexibility for 2000 folding cycles. In addition, Guo et al. fabricated negative TENGs using a composite fabric (Figure 16e), thus yielding high outputs (≈490 V, ≈43 µA, ≈70 nC, and 1.6 mW cm^{-2}) a small force and frequency.[361] Moreover, based on this output performance, wearable electronics such as charge capacitors, LEDs, scientific calculators, and drive quartz watches were powered and further subjected to mechanical energy harvesting by various common object contacts, by the fabrication of a glove based on flexible functional elastomer layers (FEL@CF-STENG), as presented in Figure 16e.

Other Electronic Devices: Various approaches were developed for textile-based electronic devices, and are mainly demonstrated by two different approaches: the embedment of simple electronic devices into textile substrates, and the use of 1D functional fibers in woven textile electronics. Numerous textile-based electronic devices such as transistors, displays, photodetectors, and memory devices have been reported for potential applications in flexible and wearable electronic devices.

To realize high-performance electronic devices, textile- or fiber-based transistors are considered as the most critical components; and are frequently reported for numerous applications such as wireless biosensors, photosensors, and memory devices, among other electronic applications.[165a,364] Yan et al. fabricated nylon fiber based organic electrochemical transistors (OECTs) by depositing a Cr/Au/PEDOT:PSS multilayer electrode on fiber that was woven with cotton yarns onto a flexible and stretchable fabric, for implementation as biosensors (**Figure 17**a).[365] Figure 17b presents an image of the relaxed and stretchable fabric sequentially woven with two OECTs with glucose sensors from a urine, glucose, and uric acid solution; thus realizing the integration of multifunctional devices into a non-invasive wearable electronic system. Lee et al. recently proposed a fiber organic transistor fabricated using a double-stranded assembly of electrode microfibers (DSA-fiber TFT),

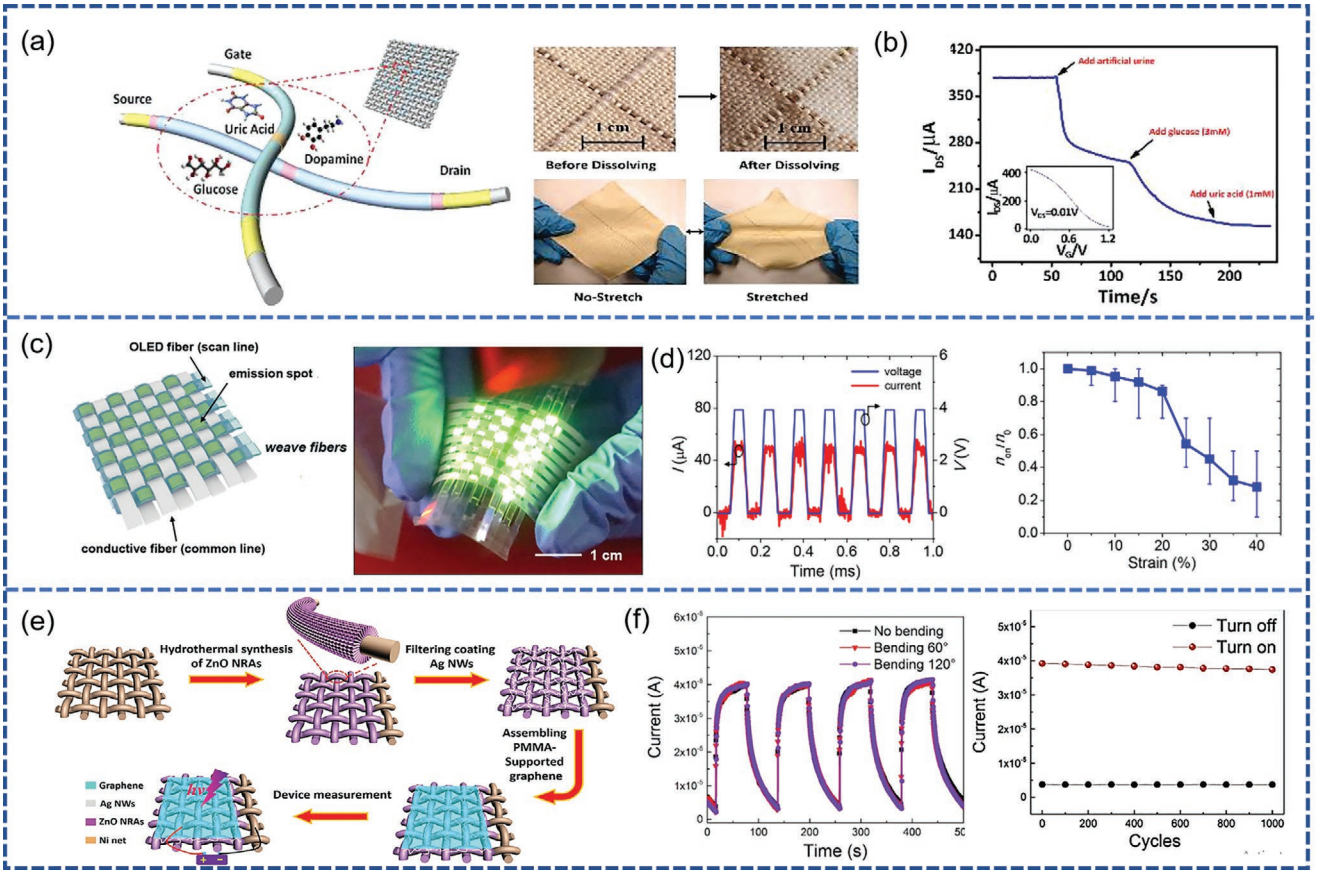

Figure 17. a) Structural diagram for OECT sensors by weaving fiber-based devices. Optical image of fabric devices before and after the removal of PVA. The bottom right images show stretched and upstretched states of the device. b) Current output curve of a smart diaper integrated with glucose sensor to detect glucose, uric acid, and artificial urine. Reproduced with permission.[366] Copyright 2018, Wiley-VCH. c) Structural diagram textile-based OLED. Bright OLED image showing its practical application. d) Luminance (L) curves indicating blue, green as bare and red, orange as passivated OLED at ambient conditions (air and DI water). The blue graph indicates the ratio between many working OLEDs to the initial value (n0) under constant strain. Reproduced with permission.[367] Copyright 2017, Wiley-VCH. e) Fabrication schematic for a textile-based wearable photodetector (Ni/ZnO NRAs/Ag NWs/graphene). f) *I*–*t* measurements at 1 V bias of PDT and its photoresponse under 1000 bending cycles. Reproduced with permission.[367] Copyright 2020, American Chemical Society.

thus demonstrating a high output current of over −5 mA at a low operation voltage of −1.3 V.[176] Moreover, the resulting fibrous transistors exhibited high performances after washing, bending, and deformation; thus demonstrating the successful application of fibrous organic transistors to the detection of electrocardiography signals from a human body and the switching of current-driven LED devices.

The development of textile-based display devices has attracted significant research attention, with earlier focus on the incorporation of standard LEDs onto the fabrics. However, in terms of materials and the most advanced processing technologies, there has been significant progress in the development of textile based polymer light-emitting electrochemical cells, OLEDs, and wearable displays.[368] Lee et al. fabricated high-performance, durable, and wearable fiber-based e-textile displays by depositing OLED materials onto rectangular stripe fibers with periodical passivation, thus resulting in woven textiles with perpendicularly arranged conductive fibers interlaced with interconnectable OLEDs, as presented in Figure 17c.[366] The as-fabricated OLEDs demonstrated a high brightness of ≈4300 cd m^{-2} at 5 V and efficiency of 46 cd A^{-1}, ≈58 lm W^{-1}; with negligible delays in the ON/OFF responses of the OLED pixels in terms of the rising and falling transitions of the current flow, in addition to a high mechanical stability (Figure 17d). Sun et al. recently fabricated highly flexible and efficient fabric OLEDs with a polarization layer with a thickness of ≈3 μm, and a high electroluminescent performance and flexibility.[369] The maximum current efficiency of 78 cd A^{-1} was achieved with a small variation in the current efficiencies of ≈8% after 1000 bending cycles with a bending radius of 1 mm, thus demonstrating the high bending stability of the fabric OLEDs. Hence, they are suitable for wearable displays by sewing onto clothes.

In addition, textile- and fiber-substrates have been frequently used for the fabrication of wearable photodetectors due to their mechanical flexibility and biocompatibility.[370] Several studies have been conducted on the fabrication of substrate-based wearable photodetectors by utilizing nanomaterials and organic materials with the advantage of intrinsic flexibility. Zeng et al. utilized an Ni textile as a substrate for the fabrication of a highly bendable photodetector by growing ZnO nanowire arrays on the Ni textile via the hydrothermal method, to facilitate electron-hole separation.[367] Additionally, the filter coating of Ag NWs was realized on the surface of ZnO nanorod arrays, which were further subjected to the assembly of a PMMA-supported graphene film with a thickness of 70 μm for photodynamic therapy, as presented in Figure 17e. The device performance of the fabricated photodetector (Figure 17f) indicated a high stability with no current degeneration under high bending conditions (120°) and over 1000 bending cycles. Similarly, a fiber-shaped self-powered p-CuZnS/n-TiO_2 UV photodetector was fabricated by Fang et al., thus demonstrating a high responsivity of 640 A W^{-1}, photocurrent of ≈4 mA at 3 V, and quantum efficiency of ≈2.3×10^5%.[371] Furthermore, due to the ultrahigh photocurrent, the as-fabricated photodetector was integrated into commercial electronics for real-time wearable UV radiation sensors, thus providing a universal strategy for the fabrication of smart wearable electronic devices.

The development of textiles replicate human civilization to an extent and has attracted significant research attention for the integration of electronic devices into textiles, to realize practical wearable applications such as sensing, display devices, and other electronic devices due to their high absorption capacity, light resistance, heat exposure, and high chemical resistance. At the end of the 20th century, the increased fabrication of e-textiles was due to a series of developments in material science and electronics, which further expanded the application scope of embedded electronics in clothing. However, there are several limitations to the advancement of textile electronics, although there has been significant progress in recent years.

4. Conclusions and Future Prospects

Compared with rigid electronics, flexible electronics demonstrate superior performances and are more practical for implementation, in addition to their advantages of varying flexibility, low mass, portability, and mechanical strength. The worldwide flexible electronics market is expected to grow at a CAGR of 10.6% from 17.47 billion USD in 2017 to 43.26 billion USD in 2026.[14] In flexible electronics, in addition to imparting a degree of flexibility, flexible substrates play a critical role in providing mechanical flexibility, low mass, low thickness, mechanical strength, and low cost. The research advances highlighted in this review elaborate the significance of flexible substrates for the fabrication of flexible and bodynet systems, which serve as a basis for the construction of low-cost, efficient electronic devices ranging from basic electronic components to integrated platforms. Based on this technology, numerous applications can be realized with significant advantages. However, there are several limitations to be overcome, as presented below.

1) One of the critical challenges is the selection of substrates with suitable thermal, chemical, electrical, mechanical, and morphological (surface) properties; as is required to achieve different properties such as user comfort, flexibility, fashion, and miniaturization. An ideal substrate should exhibit thermal and chemical stability during processing. Moreover, high mechanical flexibility and excellent adhesion properties are desirable for realizing flexible devices in practical applications. 2) For substrate processing, the selection of suitable fabrication techniques with the characteristics of a simple operation and cost-effectiveness is critical, depending on the substrate behavior. Optimal conditions such as the operating temperature should match the thermal properties of the desired substrate, given that the thermal stability of the substrate induces dimensional stability. Therefore, low-temperature physical methods such as printing and coating methods are more suitable for the processing of flexible substrates. However, poor contact between the substrate and deposition material resulting from physical methods may lead to performance degradation. Therefore, several chemical methods with mild reaction conditions have been extensively implemented for specific substrates such as fabric substrates and carbon paper substrates, thus providing the large-area deposition of more complex structures with excellent surface contact. 3) During the functional modification of the substrate, the availability of nanomaterials has

a significant effect on the physical characteristics such as the resolution, structural accuracy, and functionality. Thus, the development of advanced materials with enhanced properties is desirable for the realization of new functional properties for flexible electronic devices on various substrates. 4) For the fabrication of flexible and wearable devices, the fabrication design of the device is critical for the high stability under mechanical deformation, in addition to the prevention of fractures in the electrode and performance degradation. Additional factors can serve as a basis for further research, such as, a fully miniaturized construction, portability, and outstanding bodynet systems. 5) A comprehensive evaluation of flexible and wearable designs is user-centered and considers all potential commercial opportunities. The systematicness, gradation, and comprehensiveness of the index system development process should be considered, and a scientific and fair assessment of the index system should be established for flexible/wearable product design. Three criteria constitute the requirements for the evaluation of flexible/wearable device design. The first is the 'user requirement,' which states that flexible devices should fulfill a minimum of one rigorous criterion, to ensure and improve human well-being. For 'user requirement,' five users have impact criteria that are considered as necessary, such as time, quality, service, design, and perceived value; each with a distinct score to assess the extent to which wearable and stylish goods can satisfy user requirements. The second component, which is the 'user scenario,' presents a case wherein wearable smart devices are used frequently for a long period of time, and in an irreplaceable manner. The product should be developed to match the outcome of the multiple regression and assessment procedures, including different influencing factors of the frequency, length, and irreplaceable characteristics. Similarly, the third component is 'user experience,' which includes esthetics and emotional experience, while determining whether to purchase a product. Hence, these three components are related to the initial design objective and evaluate the association of flexible/wearable devices. Product design efficacy and dependability improve the product performance, thus allowing for it to fulfill the three criteria of the requirement scenario.

6) In addition, the environmental risks and hazards of flexible devices are critical points of interest. Due to the rapid upgradation of electronic devices, several devices are discarded, thus leading to hazardous environmental contamination, which increases environmental threats. Due to the low cost, low mass, and durable nature of polymer substrates, they are widely used in electronic devices for a wide range of applications. However, the significant increase in the production capacity induces problems with respect to the discarded end-of-life plastic devices due to the low degradation of plastic substrates in soil and natural habitats. To reduce these environmental threats, the construction of electronic systems consisting of renewable and biodegradable substrates and a minimal amount of potentially toxic materials is required. In addition, the cellulose-based paper and textile substrate provide a platform for biodegradable digital electronics that consume a small amount of potentially toxic materials on biodegradable and flexible cellulose-based nanofibril papers and textile substrates, which clearly confirms the feasibility of fabricating high-performance flexible electronic devices using eco-friendly materials. 7) The rapid increase in electronic waste threatens life on earth and causes irreversible damage to the environment. Thus, it is necessary to alleviate the significant effects of non-degradable electronic devices, and to regenerate the environment for future generations. An effective method considered by scientists and professionals involves the recycling of electronic devices, given that alternative methods such as high-temperature burning are undesirable due to the production of toxic gases (e.g., CO_2 and residue), which are harmful to the environment. In sustaining the environment, recycling requires less energy for the production of raw materials, and minimizes the requirement for raw material, thus helping to preserve natural sources. The recycling process demonstrates a substantial increase in the rate of recovery based on the collection, cleaning, sorting, and size reduction of waste materials; thus confirming the practical significance of eliminating environmental pollution waste. 8) Further, implantable smart electronic devices will trigger a revolution in the field of Point-of-Care healthcare and Human-Machine-Interfaces in the near future. With the continuous advancement of wireless charging technologies and flexible Nanogenerators, these long-term stable and self-powered implanted biomedical systems will become important modern clinic diagnostics and therapeutic tools. Among which, the development of novel materials and device configuration integrated with flexible substrates will be the most crucial technologies in the field of implantable smart electronics. However, the compatibility of current flexible substrates for implantable electronics are far from ideal, lacking the abilities to perfectly adhere and conform to the shape of human tissues or organs, to exhibit excellent bioabsorbability which eliminates the need of later surgeries to remove the electronics, and to have antibacterial and anti-inflammatory properties etc. Future work in this field may focus on the development of flexible, bio-functional substrates from novel natural and synthetic polymers and polymer composites with flat, fabric and even textile structures, integrated with energy generation and storage system, to intelligently monitor and control the implantable medical devices in vivo.

Based on the above discussion, it provides an overview of the emerging utilization of flexible substrates in a flexible and implantable system while reviewing three different types of flexible substrates, namely, polymer substrates, paper substrates, and textile substrates. These flexible substrates impart numerous characteristics such as, wettability, density, mechanical flexibility, heat resistance, surface smoothness, low thickness, low cost, and even transparency to flexible electronic devices. Moreover, in the near future, the development of functional integration in flexible electronics will be realized for commercialization. For the scaling of laboratory research to a commercial level, significant research is required to produce cost-effective and robust natural devices for practical commercial applications. Thus, further research is required to select suitable substrates to achieve the desired properties under various parameters such as thermal stability, chemical stability, mechanical flexibility, surface smoothness, and adhesion. Furthermore, functional treatment on a substrate requires a suitable manufacturing technique to ensure the feasibility of flexible electronics applications. Hence, cooperation is necessary between the research community and industry to better adopt a state-of-the-art manufacturing process for the large-scale

production of flexible electronic devices and realization of practical applications.

Acknowledgements

This work was supported by the Science and Technology Innovation Commission of Shenzhen (KQTD20170810105439418, JCYJ20200109114237902) and the National Natural Science Foundation of China (61805004 and 51775351). The authors thank Dr. Na Li from MilliporeSigma, the Life Science business of Merck KGaA Darmstadt for the valuable discussion of the prospects.

Conflict of Interest

The authors declare no conflict of interest.

Keywords

electronic skins, flexible electronic devices, flexible substrates, implantable devices, printed electronics

Received: June 26, 2021
Revised: October 4, 2021
Published online:

[1] J. L. Wang, M. Hassan, J. W. Liu, S. H. Yu, *Adv. Mater.* **2018**, *30*, 1803430.
[2] A. Poor, *HealthTech insider* **2014**.
[3] J. Chen, C. T. Liu, *IEEE Access* **2013**, *1*, 150.
[4] E. Commission, *Directorate-General for Communications Networks*, Content and Technology Brussels, **2016**.
[5] S. Wang, P. Xiao, Y. Liang, J. Zhang, Y. Huang, S. Wu, S.-W. Kuo, T. Chen, *J. Mater. Chem. C* **2018**, *6*, 5140.
[6] Y.-Z. Zhang, Y. Wang, T. Cheng, L.-Q. Yao, X. Li, W.-Y. Lai, W. Huang, *Chem. Soc. Rev.* **2019**.
[7] Y. Gao, L. Yu, J. C. Yeo, C. T. Lim, *Adv. Mater.* **2020**, *32*, 1902133.
[8] a) W. A. D. M. Jayathilaka, K. Qi, Y. Qin, A. Chinnappan, W. Serrano-García, C. Baskar, H. Wang, J. He, S. Cui, S. W. Thomas, *Adv. Mater.* **2019**, *31*, 1805921; b) S. Kumar, C. M. Pandey, A. Hatamie, A. Simchi, M. Willander, B. D. Malhotra, *Global Challenges* **2019**, *3*, 1900041; c) A. Kamyshny, S. Magdassi, *Chem. Soc. Rev.* **2019**, *48*, 1712; d) S. Gong, W. Cheng, *Adv. Electron. Mater.* **2017**, *3*, 1600314.
[9] a) Y. Wang, Q. Yang, Y. Zhao, S. Du, C. Zhi, *Adv. Mater. Technol.* **2019**, *4*, 1900083; b) P. Li, Y. Zhang, Z. Zheng, *Adv. Mater.* **2019**, *31*, 1902987.
[10] X. Wang, L. Dong, H. Zhang, R. Yu, C. Pan, Z. L. Wang, *Adv. Sci.* **2015**, *2*, 1500169.
[11] A. Sumboja, J. Liu, W. G. Zheng, Y. Zong, H. Zhang, Z. Liu, *Chem. Soc. Rev.* **2018**, *47*, 5919.
[12] D. Li, W.-Y. Lai, Y.-Z. Zhang, W. Huang, *Adv. Mater.* **2018**, *30*, 1704738.
[13] A. Malik, B. Kandasubramanian, *Polym. Rev.* **2018**, *58*, 630.
[14] *Markets and Markets* **2018**.
[15] Q. W. Wang, H. B. Zhang, J. Liu, S. Zhao, X. Xie, L. Liu, R. Yang, N. Koratkar, Z. Yu, *Adv. Funct. Mater.* **2019**, *29*, 1806819.
[16] a) X. Chen, W. Guo, L. Xie, C. Wei, J. Zhuang, W. Su, Z. Cui, *ACS Appl. Mater. Interfaces* **2017**, *9*, 37048; b) M. Morales-Masis, F. Dauzou, Q. Jeangros, A. Dabirian, H. Lifka, R. Gierth, M. Ruske, D. Moet, A. Hessler-Wyser, C. Ballif, *Adv. Funct. Mater.* **2016**, *26*, 384.
[17] C. S. Haines, M. D. Lima, N. Li, G. M. Spinks, J. Foroughi, J. D. Madden, S. H. Kim, S. Fang, M. J. De Andrade, F. J. s. Göktepe, *Science* **2014**, *343*, 868.
[18] D. Sengupta, S.-H. Chen, A. Michael, C. Y. Kwok, S. Lim, Y. Pei, A. Kottapalli, *npj Flexible Electron.* **2020**, *4*, 9.
[19] M. Lepicka, M. Gradzka-Dahlke, *Rev. Adv. Mater. Sci.* **2019**, *58*, 50.
[20] D. Lipomi, *Adv. Mater.* **2016**, *28*, 4180.
[21] A. I. Fedorchenko, A.-B. Wang, H. H. Cheng, *Appl. Phys. Lett.* **2009**, *94*, 152111.
[22] a) N. Kazem, T. Hellebrekers, C. Majidi, *Adv. Mater.* **2017**, *29*, 1605985; b) H.-Y. Cheung, K.-T. Lau, M.-P. Ho, A. Mosallam, *J. Compos. Mater.* **2009**, *43*, 2521.
[23] Y. Khan, A. E. Ostfeld, C. M. Lochner, A. Pierre, A. C. Arias, *Adv. Mater.* **2016**, *28*, 4373.
[24] X. Yu, W. Shou, B. K. Mahajan, X. Huang, H. Pan, *Adv. Mater.* **2018**, *30*, 1707624.
[25] H. R. Lim, H. S. Kim, R. Qazi, Y. T. Kwon, J. W. Jeong, W. H. Yeo, *Adv. Mater.* **2020**, *32*, 1901924.
[26] a) C. Yang, Z. Suo, *Nat. Rev. Mater.* **2018**, *3*, 125; b) V. Chabot, D. Higgins, A. Yu, X. Xiao, Z. Chen, J. J. E. Zhang, E. Science, *Energy Environ. Sci.* **2014**, *7*, 1564.
[27] Y. Zhang, S. Wang, X. Li, J. A. Fan, S. Xu, Y. M. Song, K. J. Choi, W. H. Yeo, W. Lee, S. N. Nazaar, *Adv. Funct. Mater.* **2014**, *24*, 2028.
[28] J. A. Fan, W.-H. Yeo, Y. Su, Y. Hattori, W. Lee, S.-Y. Jung, Y. Zhang, Z. Liu, H. Cheng, L. Falgout, M. Bajema, T. Coleman, D. Gregoire, R. J. Larsen, Y. Huang, J. A. Rogers, *Nat. Commun.* **2014**, *5*, 3266.
[29] Z. Wang, L. Zhang, J. Liu, C. Li, *ACS Appl. Mater. Interfaces* **2018**, *11*, 5316.
[30] Z. Lv, Y. Luo, Y. Tang, J. Wei, Z. Zhu, X. Zhou, W. Li, Y. Zeng, W. Zhang, Y. Zhang, *Adv. Mater.* **2018**, *30*, 1870008.
[31] a) T. C. Shyu, P. F. Damasceno, P. M. Dodd, A. Lamoureux, L. Xu, M. Shlian, M. Shtein, S. C. Glotzer, N. A. Kotov, *Nat. Mater.* **2015**, *14*, 785; b) Y. S. Guan, Z. Zhang, Y. Tang, J. Yin, S. Ren, *Adv. Mater.* **2018**, *30*, 1706390.
[32] E. Roh, H. B. Lee, D. I. Kim, N. E. Lee, *Adv. Mater.* **2017**, *29*, 1703004.
[33] J. Song, H. Jiang, Y. Huang, J. Rogers, *J. Vac. Sci. Technol., A* **2009**, *27*, 1107.
[34] a) S. Choi, S. I. Han, D. Jung, H. J. Hwang, C. Lim, S. Bae, O. K. Park, C. M. Tschabrunn, M. Lee, S. Y. Bae, *Nat. Nanotechnol.* **2018**, *13*, 1048; b) C. Zhu, A. Chortos, Y. Wang, R. Pfattner, T. Lei, A. C. Hinckley, I. Pochorovski, X. Yan, J. W.-F. To, J. Y. Oh, *Nat. Electron.* **2018**, *1*, 183.
[35] X. Shi, S. Liu, Y. Sun, J. Liang, Y. Chen, *Adv. Funct. Mater.* **2018**, *28*, 1800850.
[36] Y. Huang, Y. Huang, W. Meng, M. Zhu, H. Xue, C.-S. Lee, C. Zhi, *ACS Appl. Mater. Interfaces* **2015**, *7*, 2569.
[37] K. Zulkowski, *Adv. Skin Wound Care* **2017**, *30*, 372.
[38] J. Lewis, *Mater. Today* **2006**, *9*, 38.
[39] T. Kim, T. Lee, G. Lee, Y. W. Choi, S. M. Kim, D. Kang, M. Choi, *Appl. Sci.* **2018**, *8*, 367.
[40] E. Song, H. Fang, X. Jin, J. Zhao, C. Jiang, K. J. Yu, Y. Zhong, D. Xu, J. Li, G. Fang, *Adv. Electron. Mater.* **2017**, *3*, 1700077.
[41] A. Miyamoto, S. Lee, N. F. Cooray, S. Lee, M. Mori, N. Matsuhisa, H. Jin, L. Yoda, T. Yokota, A. Itoh, *Nat. Nanotechnol.* **2017**, *12*, 907.
[42] a) J. Zhang, Y. Cheng, M. Tebyetekerwa, S. Meng, M. Zhu, Y. Lu, *Adv. Funct. Mater.* **2019**, *29*, 1806407; b) H. Chang, Z. Sun, Q. Yuan, F. Ding, X. Tao, F. Yan, Z. Zheng, *Adv. Mater.* **2010**, *22*, 4872.
[43] W. Du, J. Nie, Z. Ren, T. Jiang, L. Xu, S. Dong, L. Zheng, X. Chen, H. Li, *Nano Energy* **2018**, *51*, 260.
[44] a) F. Yi, J. Wang, X. Wang, S. Niu, S. Li, Q. Liao, Y. Xu, Z. You, Y. Zhang, Z. Wang, *ACS Nano* **2016**, *10*, 6519; b) W. H. Yeo, Y. S. Kim, J. Lee, A. Ameen, L. Shi, M. Li, S. Wang, R. Ma, S. H. Jin, Z. Kang, *Adv. Mater.* **2013**, *25*, 2773; c) G. Xu, C. Cheng, Z. Liu,

W. Yuan, X. Wu, Y. Lu, S. S. Low, J. Liu, L. Zhu, D. Ji, *Adv. Mater. Technol.* **2019**, *4*, 1800658; d) X. Zhou, L. Zhu, L. Fan, H. Deng, Q. Fu, *ACS Appl. Mater. Interfaces* **2018**, *10*, 31655.
[45] J. T. Reeder, J. Choi, Y. Xue, P. Gutruf, J. Hanson, M. Liu, T. Ray, A. J. Bandodkar, R. Avila, W. Xia, *Sci. Adv.* **2019**, *5*, eaau6356.
[46] Y. Jin, L. Li, Y. Cheng, L. Kong, Q. Pei, F. Xiao, *Adv. Funct. Mater.* **2015**, *25*, 1581.
[47] a) I.-C. Cheng, S. Wagner, in *Flexible Electronics* (Eds: A. Salleo, W. S. Wong), Springer, Berlin **2009**, p. 1; b) A. Plichta, A. Habeck, S. Knoche, A. Kruse, A. Weber, N. Hildebrand, *Flexible Flat Panel Disp.* **2005**, *3*, 35.
[48] W. A. MacDonald, M. Looney, D. MacKerron, R. Eveson, R. Adam, K. Hashimoto, K. Rakos, *J. Soc. Inf. Disp.* **2007**, *15*, 1075.
[49] S. Duan, Z. Wang, L. Zhang, J. Liu, C. Li, *Adv. Mater. Technol.* **2018**, *3*, 1870020.
[50] P. Feng, H. Ji, L. Zhang, X. Luo, X. Leng, P. He, H. Feng, J. Zhang, X. Ma, W. J. N. Zhao, *Nanotechnology* **2019**, *30*, 185501.
[51] D. Lee, J. Kim, H. Kim, H. Heo, K. Park, Y. J. N. Lee, *Nanoscale* **2018**, *10*, 18812.
[52] M. Irimia-Vladu, P. Troshin, M. Reisinger, L. Shmygleva, Y. Kanbur, G. Schwabegger, M. Bodea, R. J. A. F. M. Schw, *Adv. Funct. Mater.* **2010**, *20*, 4069.
[53] S. Ling, D. L. Kaplan, M. Buehler, *Nat. Rev. Mater.* **2018**, *3*, 18016.
[54] C. Wang, S. Wang, G. Chen, W. Kong, W. Ping, J. Dai, G. Pastel, H. Xie, S. He, S. Das, *Chem. Mater* **2018**, *30*, 7707.
[55] L. Tang, L. Mou, W. Zhang, X. Jiang, *ACS Appl. Mater. Interfaces* **2019**, *11*, 7138.
[56] Y. Yoon, S. Kim, D. Kim, S. K. Kauh, J. Lee, *Adv. Mater. Technol.* **2019**, *4*, 1800379.
[57] D.-H. Kim, Y.-S. Kim, J. Amsden, B. Panilaitis, D. L. Kaplan, F. G. Omenetto, M. R. Zakin, J. Rogers, *Appl. Phys. Lett.* **2009**, *95*, 133701.
[58] J. Viventi, D.-H. Kim, L. Vigeland, E. S. Frechette, J. A. Blanco, Y.-S. Kim, A. E. Avrin, V. R. Tiruvadi, S.-W. Hwang, A. Vanleer, *Nat. Neurosci.* **2011**, *14*, 1599.
[59] a) D.-H. Kim, J. Viventi, J. J. Amsden, J. Xiao, L. Vigeland, Y.-S. Kim, J. A. Blanco, B. Panilaitis, E. S. Frechette, D. Contreras, *Nat. Mater.* **2010**, *9*, 511; b) T.-i. Kim, J. G. McCall, Y. H. Jung, X. Huang, E. R. Siuda, Y. Li, J. Song, Y. M. Song, H. A. Pao, R.-H Kim, *Science* **2013**, *340*, 211.
[60] A. Salleo, W. S. Wong, *Flexible Electronics: Materials and Applications*, Springer, Berlin **2009**.
[61] W. Si, C. Yan, Y. Chen, S. Oswald, L. Han, O. G. Schmidt, *Energy Environ. Sci.* **2013**, *6*, 3218.
[62] Z. Lv, Y. Luo, Y. Tang, J. Wei, Z. Zhu, X. Zhou, W. Li, Y. Zeng, W. Zhang, Y. Zhang, *Adv. Mater.* **2018**, *30*, 1704531.
[63] Y. Ding, T. Xu, O. Onyilagha, H. Fong, Z. Zhu, *ACS Appl. Mater. Interfaces* **2019**, *11*, 6685.
[64] M. Rawat, E. Jayaraman, S. Balasubramanian, S. S. K. Iyer, *Adv. Mater. Technol.* **2019**, *4*, 1900184.
[65] V. Zardetto, T. M. Brown, A. Reale, A. Di Carlo, *J. Polym. Sci., Part B: Polym. Phys.* **2011**, *49*, 638.
[66] M. Layani, X. Wang, S. Magdassi, *Adv. Mater.* **2018**, *30*, 1706344.
[67] D. J. Burke, D. J. Lipomi, *Energy Environ. Sci.* **2013**, *6*, 2053.
[68] S. Wünscher, R. Abbel, J. Perelaer, U. S. Schubert, *J. Mater. Chem. C* **2014**, *2*, 10232.
[69] J. Perelaer, A. W. De Laat, C. E. Hendriks, U. S. Schubert, *J. Mater. Chem.* **2008**, *18*, 3209.
[70] a) A. Kamyshny, S. Magdassi, *Small* **2014**, *10*, 3515; b) S. Magdassi, A. Kamyshny, *Nanomaterials for 2D and 3D Printing*, John Wiley & Sons, Technology & Engineering, Hoboken, NJ **2017**.
[71] W. Shao, G. Li, P. Zhu, Y. Zhang, Q. Ouyang, R. Sun, C. Chen, C.-P. Wong, *J. Mater. Sci.* **2018**, *29*, 4432.
[72] S. H. Ke, P. W. Guo, C. Y. Pang, B. Tian, C. S. Luo, H. P. Zhu, W. Wu, *Adv. Mater. Technol.* **2020**, *5*, 1901097.
[73] a) Y. Zhang, C. Cui, B. Yang, K. Zhang, P. Zhu, G. Li, R. Sun, C. Wong, *J. Mater. Sci.* **2018**, *53*, 12988; b) M. Joo, B. Lee, S. Jeong, M. Lee, *Thin Solid Films* **2012**, *520*, 2878.
[74] S. Bellani, E. Petroni, A. E. Del Rio Castillo, N. Curreli, B. Martín-García, R. Oropesa-Nuñez, M. Prato, F. Bonaccorso, *Adv. Funct. Mater.* **2019**, *29*, 1807659.
[75] a) B. Wang, M. Baeuscher, X. Hu, M. Woehrmann, K. Becker, N. Juergensen, M. Hubl, P. Mackowiak, M. Schneider-Ramelow, K.-D. Lang, *Micromachines* **2020**, *11*, 474; b) Z. Liu, L. Wu, J. Qian, J. Peng, R. Liu, Y. Xu, X. Shi, C. Qi, S. Ye, *J. Electron. Mater.* **2021**, *50*, 2356.
[76] a) L. Zhou, M. Yu, X. Chen, S. Nie, W.-Y. Lai, W. Su, Z. Cui, W. Huang, *Adv. Funct. Mater.* **2018**, *28*, 1705955; b) K. Arapov, E. Rubingh, R. Abbel, J. Laven, G. De With, H. Friedrich, *Adv. Funct. Mater.* **2016**, *26*, 586.
[77] W. J. Hyun, E. B. Secor, M. C. Hersam, C. D. Frisbie, L. Francis, *Adv. Mater.* **2015**, *27*, 109.
[78] a) S. Duan, X. Gao, Y. Wang, F. Yang, M. Chen, X. Zhang, X. Ren, W. Hu, *Adv. Mater.* **2019**, *31*, 1807975; b) W. Yang, N. W. Li, S. Zhao, Z. Yuan, J. Wang, X. Du, B. Wang, R. Cao, X. Li, W. Xu, *Adv. Mater. Technol.* **2018**, *3*, 1700241.
[79] a) Y. Kusaka, T. Kawamura, M. Nakagawa, K. Okamoto, K. Tanaka, N. Fukuda, *Adv. Powder Technol.* **2021**, *32*, 764; b) N. Peřinka, B. Pozo, E. F. de Gorostiza, C. Mendes-Felipe, J. L. Vilas-Vilela, S. Lanceros-Méndez, *Flexible Printed Electron.* **2021**, *6*, 015004.
[80] W. Li, S. Yang, A. Shamim, *npj Flexible Electron.* **2019**, *3*, 19.
[81] J. Suikkola, T. Björninen, M. Mosallaei, T. Kankkunen, P. Iso-Ketola, L. Ukkonen, J. Vanhala, M. Mäntysalo, *Sci. Rep.* **2016**, *6*, 25784.
[82] M. Gao, L. Li, Y. Song, *J. Mater. Chem. C* **2017**, *5*, 2971.
[83] a) E. Kuusisto, J. J. Heikkinen, P. Järvinen, T. Sikanen, S. Franssila, V. Jokinen, *Sens. Actuators, B* **2021**, *336*, 129727; b) V. Beedasy, P. J. Smith, *Materials* **2020**, *13*, 704.
[84] a) T. Biswas, J. Yu, V. Nierstrasz, *Adv. Mater. Interfaces* **2021**, *8*, 2001882; b) L. Liu, Y. Pei, S. Ma, X. Sun, T. J. Singler, *Adv. Eng. Mater.* **2020**, *22*, 1901351; c) C. J. Zhang, L. McKeon, M. P. Kremer, S.-H. Park, O. Ronan, A. Seral-Ascaso, S. Barwich, C. Ó. Coileáin, N. McEvoy, H. C. Nerl, B. Anasori, J. N. Coleman, Y. Gogotsi, V. Nicolosi, *Nat. Commun.* **2019**, *10*, 1795.
[85] C. E. Knapp, J. B. Chemin, S. P. Douglas, D. A. Ondo, J. Guillot, P. Choquet, N. Boscher, *Adv. Mater. Technol.* **2018**, *3*, 1700326.
[86] a) N. Adly, S. Weidlich, S. Seyock, F. Brings, A. Yakushenko, A. Offenhäusser, B. Wolfrum, *npj Flexible Electron.* **2018**, *2*, 15; b) S. Chen, M. Su, C. Zhang, M. Gao, B. Bao, Q. Yang, B. Su, Y. Song, *Adv. Mater.* **2015**, *27*, 3928.
[87] H. Lee, D. S. Um, Y. Lee, S. Lim, H. j. Kim, H. Ko, *Adv. Mater.* **2016**, *28*, 7457.
[88] J. Sun, K. Shrestha, H. Park, P. Yadav, S. Parajuli, S. Lee, S. Shrestha, G. R. Koirala, Y. Kim, K. Marotrao, *Adv. Mater. Technol.* **2020**, *5*, 1900935.
[89] C. J. Zhang, L. McKeon, M. P. Kremer, S.-H. Park, O. Ronan, A. Seral-Ascaso, S. Barwich, C. Ó. Coileáin, N. McEvoy, H. Nerl, B. Anasori, J. N. Coleman, Y. Gogotsi, V. Nicolosi, *Nat. Commun.* **2019**, *10*, 1795.
[90] H. B. Yao, J. Ge, C. F. Wang, X. Wang, W. Hu, Z. J. Zheng, Y. Ni, S. H. Yu, *Adv. Mater.* **2013**, *25*, 6692.
[91] S. Lin, H. Wang, X. Zhang, D. Wang, D. Zu, J. Song, Z. Liu, Y. Huang, K. Huang, N. J. N. E. Tao, *Nano Energy* **2019**, *62*, 111.
[92] H. Biederman, D. Slavınská, *Surf. Coat. Technol.* **2000**, *125*, 371.
[93] Y. Guo, W. Li, H. Yu, D. F. Perepichka, H. Meng, *Adv. Energy Mater.* **2017**, *7*, 1601623.
[94] Y. Ding, S. Dong, J. Han, D. He, Z. Zhao, R. H. Dauskardt, *Adv. Mater. Interfaces* **2018**, *5*, 1701433.
[95] L. Veeramuthu, B.-Y. Chen, C.-Y. Tsai, F.-C. Liang, M. Venkatesan, D.-H. Jiang, C.-W. Chen, X. Cai, C.-C. Kuo, *RSC Adv.* **2019**, *9*, 35786.
[96] S. Song, K. T. Lee, C. W. Koh, H. Shin, M. Gao, H. Y. Woo, D. Vak, J. Y. J. E. Kim, E. Science, *Energy Environ. Sci.* **2018**, *11*, 3248.

[97] C. Park, M. Koo, G. Song, S. M. Cho, H. S. Kang, T. H. Park, E. H. Kim, C. Park, *ACS Nano* **2020**, *14*, 755.
[98] D. H. Jung, J. H. Park, H. E. Lee, J. Byun, T. H. Im, G. Y. Lee, J. Y. Seok, T. Yun, K. J. Lee, S. O. Kim, *Nano Energy* **2019**, *61*, 236.
[99] S. Noimark, R. J. Colchester, R. K. Poduval, E. Maneas, E. J. Alles, T. Zhao, E. Z. Zhang, M. Ashworth, E. Tsolaki, A. Chester, *Adv. Funct. Mater.* **2018**, *28*, 1704919.
[100] a) S. Cho, S. Kang, A. Pandya, R. Shanker, Z. Khan, Y. Lee, J. Park, S. L. Craig, H. Ko, *ACS Nano* **2017**, *11*, 4346; b) S. Kang, T. Kim, S. Cho, Y. Lee, A. Choe, B. Walker, S.-J. Ko, J. Y. Kim, H. Ko, *Nano Lett.* **2015**, *15*, 7933; c) L. Hu, H. S. Kim, J.-Y. Lee, P. Peumans, Y. Cui, *ACS Nano* **2010**, *4*, 2955.
[101] T. T. Nge, M. Nogi, K. Suganuma, *J. Mater. Chem. C* **2013**, *1*, 5235.
[102] S. Kim, S. Won, G.-D. Sim, I. Park, S.-B. Lee, *Nanotechnology* **2013**, *24*, 085701.
[103] Y.-H. Son, J.-Y. Jang, M. K. Kang, S. Ahn, C. Lee, *Thin Solid Films* **2018**, *656*, 61.
[104] L. Huang, Y. Huang, J. Liang, X. Wan, Y. Chen, *Nano Res.* **2011**, *4*, 675.
[105] J. Liang, Y. Chen, Y. Xu, Z. Liu, L. Zhang, X. Zhao, X. Zhang, J. Tian, Y. Huang, Y. Ma, *ACS Appl. Mater. Interfaces* **2010**, *2*, 3310.
[106] B. Bachmann, N. Y. Adly, J. Schnitker, A. Yakushenko, P. Rinklin, A. Offenhäusser, B. J. F. Wolfrum, P. Electronics, *Flexible Printed Electron.* **2017**, *2*, 035003.
[107] H. J. Park, Y. Jo, M. K. Cho, J. Y. Woo, D. Kim, S. Y. Lee, Y. Choi, S. Jeong, *Nanoscale* **2018**, *10*, 5047.
[108] E. B. Secor, S. Lim, H. Zhang, C. D. Frisbie, L. F. Francis, M. Hersam, *Adv. Mater.* **2014**, *26*, 4533.
[109] E. B. Secor, P. L. Prabhumirashi, K. Puntambekar, M. L. Geier, M. Hersam, *J. Phys. Chem. Lett.* **2013**, *4*, 1347.
[110] C.-L. Lee, C.-H. Chen, C.-W. Chen, *Chem. Eng.* **2013**, *230*, 296.
[111] K. Arapov, K. Jaakkola, V. Ermolov, G. Bex, E. Rubingh, S. Haque, H. Sandberg, R. Abbel, G. de With, H. Friedrich, *Phys. Status Solidi RRL* **2016**, *10*, 812.
[112] E. B. Secor, M. Hersam, *J. Phys. Chem. Lett.* **2015**, *6*, 620.
[113] N. Karim, S. Afroj, A. Malandraki, S. Butterworth, C. Beach, M. Rigout, K. S. Novoselov, A. J. Casson, S. G. Yeates, *J. Mater. Chem. C* **2017**, *5*, 11640.
[114] Y. Gao, H. Ota, E. W. Schaler, K. Chen, A. Zhao, W. Gao, H. M. Fahad, Y. Leng, A. Zheng, F. Xiong, *Adv. Mater.* **2017**, *29*, 1701985.
[115] A. Capasso, A. D. R. Castillo, H. Sun, A. Ansaldo, V. Pellegrini, F. Bonaccorso, *Solid State Commun.* **2015**, *224*, 53.
[116] M. Krivec, M. Lenzhofer, T. Moldaschl, J. Pribošek, A. Abram, M. Ortner, *Microsyst. Technol.* **2018**, *24*, 2673.
[117] G. Hassan, J. Bae, C. Lee, *J. Mater. Sci.* **2018**, *29*, 49.
[118] M. Layani, S. Magdassi, *J. Mater. Chem.* **2011**, *21*, 15378.
[119] M. Layani, M. Grouchko, S. Shemesh, S. Magdassi, *J. Mater. Chem.* **2012**, *22*, 14349.
[120] K. Y. Shin, J. Y. Hong, J. Jang, *Adv. Mater.* **2011**, *23*, 2113.
[121] M. Rogala, I. Wlasny, P. Dabrowski, P. Kowalczyk, A. Busiakiewicz, W. Kozlowski, L. Lipinska, J. Jagiello, M. Aksienionek, W. Strupinski, *Appl. Phys. Lett.* **2015**, *106*, 041901.
[122] M. H. Overgaard, M. Kühnel, R. Hvidsten, S. V. Petersen, T. Vosch, K. Nørgaard, B. W. Laursen, *Adv. Mater. Technol.* **2017**, *2*, 1700011.
[123] Y. Su, J. Du, D. Sun, C. Liu, H. Cheng, *Nano Res.* **2013**, *6*, 842.
[124] Q. He, S. R. Das, N. T. Garland, D. Jing, J. A. Hondred, A. A. Cargill, S. Ding, C. Karunakaran, J. Claussen, *ACS Appl. Mater. Interfaces* **2017**, *9*, 12719.
[125] I. Wlasny, M. Rogala, P. Dabrowski, P. Kowalczyk, A. Busiakiewicz, W. Kozlowski, L. Lipinska, J. Jagiello, M. Aksienionek, Z. Sieradzki, *Mater. Chem. Phys.* **2016**, *181*, 409.
[126] P. N. Nirmalraj, P. E. Lyons, S. De, J. N. Coleman, J. Boland, *Nano Lett.* **2009**, *9*, 3890.
[127] B. B. Parekh, G. Fanchini, G. Eda, M. Chhowalla, *Appl. Phys. Lett.* **2007**, *90*, 121913.
[128] D.-W. Shin, J. H. Lee, Y.-H. Kim, S. M. Yu, S.-Y. Park, J.-B. Yoo, *Nanotechnology* **2009**, *20*, 475703.
[129] T. G. Yun, M. Park, D.-H. Kim, D. Kim, J. Y. Cheong, J. G. Bae, S. M. Han, I.-D. Kim, *ACS Nano* **2019**, *13*, 3141.
[130] Q. Huang, Y. Zhu, *Adv. Mater. Technol.* **2019**, *4*, 1800546.
[131] C. Pang, G.-Y. Lee, T.-i. Kim, S. M. Kim, H. N. Kim, S.-H. Ahn, K.-Y. Suh, *Nat. Mater.* **2012**, *11*, 795.
[132] T. Someya, M. Amagai, *Nat. Biotechnol.* **2019**, *37*, 382.
[133] J. Perelaer, R. Jani, M. Grouchko, A. Kamyshny, S. Magdassi, U. Schubert, *Adv. Mater.* **2012**, *24*, 3993.
[134] J. Perelaer, R. Jani, M. Grouchko, A. Kamyshny, S. Magdassi, U. S. Schubert, *Adv. Mater.* **2012**, *24*, 3993.
[135] J. H. Park, S. Jeong, E. J. Lee, S. S. Lee, J. Y. Seok, M. Yang, Y. Choi, B. Kang, *Chem. Mater.* **2016**, *28*, 4151.
[136] S.-J. Oh, T. G. Kim, S.-Y. Kim, Y. Jo, S. S. Lee, K. Kim, B.-H. Ryu, J.-U. Park, Y. Choi, S. Jeong, *Chem. Mater.* **2016**, *28*, 4714.
[137] S. Xu, D. M. Vogt, W. H. Hsu, J. Osborne, T. Walsh, J. R. Foster, S. K. Sullivan, V. C. Smith, A. W. Rousing, E. C. Goldfield, *Adv. Funct. Mater.* **2019**, *29*, 1807058.
[138] X. Pu, M. Liu, X. Chen, J. Sun, C. Du, Y. Zhang, J. Zhai, W. Hu, Z. L. Wang, *Sci. Adv.* **2017**, *3*, e1700015.
[139] J. Oliveira, V. Correia, H. Castro, P. Martins, S. Lanceros-Mendez, *Addit. Manuf.* **2018**, *21*, 269.
[140] S. Gong, W. Schwalb, Y. Wang, Y. Chen, Y. Tang, J. Si, B. Shirinzadeh, W. Cheng, *Nat. Commun.* **2014**, *5*, 3132.
[141] K. Jost, D. Stenger, C. R. Perez, J. K. McDonough, K. Lian, Y. Gogotsi, G. J. E. Dion, E. Science, *Energy Environ. Sci.* **2013**, *6*, 2698.
[142] K. Kim, B. Kim, C. H. Lee, *Adv. Mater.* **2019**, *32*, 1902051.
[143] a) Y.-W. Cai, X.-N. Zhang, G.-G. Wang, G.-Z. Li, D.-Q. Zhao, N. Sun, F. Li, H.-Y. Zhang, J.-C. Han, Y. Yang, *Nano Energy* **2021**, *81*, 105663; b) K. H. Ke, C. K. Chung, *Small* **2020**, *16*, 2001209.
[144] a) S. Mondal, B. K. Min, Y. Yi, V. T. Nguyen, C. G. Choi, *Adv. Mater. Technol.* **2021**, *6*, 2001039; b) J. Lee, S. Pyo, D. S. Kwon, E. Jo, W. Kim, J. Kim, *Small* **2019**, *15*, 1805120.
[145] X. Wang, Y. Zhang, X. Zhang, Z. Huo, X. Li, M. Que, Z. Peng, H. Wang, C. Pan, *Adv. Mater.* **2018**, *30*, 1706738.
[146] S. Han, C. Liu, H. Xu, D. Yao, K. Yan, H. Zheng, H.-J. Chen, X. Gui, S. Chu, C. Liu, *npj Flexible Electron.* **2018**, *2*, 16.
[147] R. C. Webb, A. P. Bonifas, A. Behnaz, Y. Zhang, K. J. Yu, H. Cheng, M. Shi, Z. Bian, Z. Liu, Y.-S. Kim, *Nat. Mater.* **2013**, *12*, 938.
[148] C. F. Guo, T. Sun, Q. Liu, Z. Suo, Z. Ren, *Nat. Commun.* **2014**, *5*, 3121.
[149] Q. Hua, J. Sun, H. Liu, R. Bao, R. Yu, J. Zhai, C. Pan, Z. L. Wang, *Nat. Commun.* **2018**, *9*, 244.
[150] Y. J. Hong, H. Jeong, K. W. Cho, N. Lu, D. Kim, *Adv. Funct. Mater.* **2019**, *29*, 1808247.
[151] A. J. Bandodkar, P. Gutruf, J. Choi, K. Lee, Y. Sekine, J. T. Reeder, W. J. Jeang, A. J. Aranyosi, S. P. Lee, J. Model, *Sci. Adv.* **2019**, *5*, eaav3294.
[152] B. Guo, Z. Ma, L. Pan, Y. Shi, *J. Polym. Sci., Part B: Polym. Phys.* **2019**, *57*, 1606;
[153] a) N. Kurra, M. K. Hota, H. Alshareef, *Nano Energy* **2015**, *13*, 500; b) X. Shi, F. Zhou, J. Peng, R. a. Wu, Z. S. Wu, X. Bao, *Adv. Funct. Mater.* **2019**, *29*, 1902860.
[154] a) J. Liang, S. Wang, H. Yu, X. Zhao, H. Wang, Y. Tong, Q. Tang, Y. Liu, *Sustainable Energy Fuels* **2020**, *4*, 2718; b) S. Xu, Y. Zhang, J. Cho, J. Lee, X. Huang, L. Jia, J. A. Fan, Y. Su, J. Su, H. Zhang, H. Cheng, B. Lu, C. Yu, C. Chuang, T.-I. Kim, T. Song, K. Shigeta, S. Kang, C. Dagdeviren, I. Petrov, P. V. Braun, Y. Huang, U. Paik, J. A. Rogers, *Nat. Commun.* **2013**, *4*, 1543.
[155] H. Guo, Q. Leng, X. He, M. Wang, J. Chen, C. Hu, Y. Xi, *Adv. Energy Mater.* **2015**, *5*, 1400790.
[156] a) L. Sun, W. Zeng, C. Xie, L. Hu, X. Dong, F. Qin, W. Wang, T. Liu, X. Jiang, Y. Jiang, *Adv. Mater.* **2020**, *32*, 1907840; b) I. Jeon, K. Cui, T. Chiba, A. Anisimov, A. G. Nasibulin, E. I. Kauppinen, S. Maruyama, Y. Matsuo, *J. Am. Chem. Soc.* **2015**, *137*, 7982.
[157] H. Li, Z. Tang, Z. Liu, C. Zhi, *Joule* **2019**, *3*, 613.

[158] X. Chen, H. Huang, L. Pan, T. Liu, M. Niederberger, *Adv. Mater.* **2019**, *31*, 1904648.
[159] Y. Wang, F. Chen, Z. Liu, Z. Tang, Q. Yang, Y. Zhao, S. Du, Q. Chen, C. Zhi, *Angew. Chem.* **2019**, *131*, 15854.
[160] C. Y. Chan, Z. Q. Wang, H. Jia, P. F. Ng, L. Chow, B. Fei, *J. Mater. Chem. A* **2021**, *9*, 2043.
[161] F. Mo, Q. Li, G. Liang, Y. Zhao, D. Wang, Y. Huang, J. Wei, C. Zhi, *Adv. Sci.* **2021**, *8*, 2100072.
[162] a) W. Hu, W. Huang, S. Yang, X. Wang, Z. Jiang, X. Zhu, H. Zhou, H. Liu, Q. Zhang, X. Zhuang, *Adv. Mater.* **2017**, *29*, 1703256; b) D. De Fazio, I. Goykhman, D. Yoon, M. Bruna, A. Eiden, S. Milana, U. Sassi, M. Barbone, D. Dumcenco, K. Marinov, A. Kis, A. C. Ferrari, *ACS Nano* **2016**, *10*, 8252.
[163] a) Q. Xu, Z. Yang, D. Peng, J. Xi, P. Lin, Y. Cheng, K. Liu, C. Pan, *Nano Energy* **2019**, *65*, 104001; b) W. Deng, L. Huang, X. Xu, X. Zhang, X. Jin, S.-T. Lee, J. Jie, *Nano Lett.* **2017**, *17*, 2482.
[164] A. Daus, C. Roldán-Carmona, K. Domanski, S. Knobelspies, G. Cantarella, C. Vogt, M. Grätzel, M. K. Nazeeruddin, G. Tröster, *Adv. Mater.* **2018**, *30*, 1707412.
[165] a) M. Y. Lee, J. Hong, E. K. Lee, H. Yu, H. Kim, J. U. Lee, W. Lee, J. Oh, *Adv. Funct. Mater.* **2016**, *26*, 1445; b) S. Huang, C. F. Guo, X. Zhang, W. Pan, X. Luo, C. Zhao, J. Gong, X. Li, Z. F. Ren, H. Wu, *Small* **2015**, *11*, 5712.
[166] Y. Zhang, P. Huang, J. Guo, R. Shi, W. Huang, Z. Shi, L. Wu, F. Zhang, L. Gao, C. Li, X. Zhang, J. Xu, H. Zhang, *Adv. Mater.* **2020**, *32*, 2001082.
[167] J. Song, J. Yuan, F. Xia, J. Liu, Y. Zhang, Y. L. Zhong, J. Zheng, Y. Liu, S. Li, M. Zhao, *Adv. Electron. Mater.* **2016**, *2*, 1600077.
[168] W. Lee, Y. Liu, Y. Lee, B. K. Sharma, S. M. Shinde, S. D. Kim, K. Nan, Z. Yan, M. Han, Y. Huang, Y. Zhang, J.-H. Ahn, J. A. Rogers, *Nat. Commun.* **2018**, *9*, 1417.
[169] Y. Do, D. Y. Jeong, S. Lee, S. Kang, S. Jang, J. Jang, *Adv. Eng. Mater.* **2020**, *22*, 1901430.
[170] J. Park, H. Yoon, G. Kim, B. Lee, S. Lee, S. Jeong, T. Kim, J. Seo, S. Chung, Y. Hong, *Adv. Funct. Mater.* **2019**, *29*, 1902412.
[171] a) Y. H. Lee, M. Jang, M. Y. Lee, O. Y. Kweon, J. H. Oh, *Chem* **2017**, *3*, 724; b) I. Lee, W. T. Kang, Y. S. Shin, Y. R. Kim, U. Y. Won, K. Kim, D. L. Duong, K. Lee, J. Heo, Y. Lee, *ACS Nano* **2019**, *13*, 8392; c) D. W. Kim, S.-Y. Min, Y. Lee, U. Jeong, *ACS Nano* **2020**.
[172] a) S. Lee, D. Jeong, M. Mativenga, J. Jang, *Adv. Funct. Mater.* **2017**, *27*, 1700437; b) P. Heremans, A. K. Tripathi, A. de Jamblinne de Meux, E. C. Smits, B. Hou, G. Pourtois, G. Gelinck, *Adv. Mater.* **2016**, *28*, 4266.
[173] a) Z. Zhang, L. Li, J. Horng, N. Z. Wang, F. Yang, Y. Yu, Y. Zhang, G. Chen, K. Watanabe, T. Taniguchi, X. H. Chen, F. Wang, Y. Zhang, *Nano Lett.* **2017**, *17*, 6097; b) W. G. Song, H. J. Kwon, J. Park, J. Yeo, M. Kim, S. Park, S. Yun, K. U. Kyung, C. P. Grigoropoulos, S. Kim, *Adv. Funct. Mater.* **2016**, *26*, 2426; c) K. Kim, K. Nam, X. Li, D. Y. Lee, S. Kim, *ACS Appl. Mater. Interfaces* **2019**, *11*, 42403.
[174] a) B. Xu, M. Zhu, W. Zhang, X. Zhen, Z. Pei, Q. Xue, C. Zhi, P. Shi, *Adv. Mater.* **2016**, *28*, 3333; b) X. Wu, S. Mao, J. Chen, J. Huang, *Adv. Mater.* **2018**, *30*, 1705642; c) S.-H. Shin, S. Ji, S. Choi, K.-H. Pyo, B. W. An, J. Park, J. Kim, J.-Y. Kim, K.-S. Lee, S.-Y. Kwon, J. Heo, B.-G. Park, J.-U. Park, *Nat. Commun.* **2017**, *8*, 14950.
[175] D. H. Park, H. W. Park, J. W. Chung, K. Nam, S. Choi, Y. S. Chung, H. Hwang, B. Kim, D. Kim, *Adv. Funct. Mater.* **2019**, *29*, 1808909.
[176] S. B. Singh, T. I. Singh, N. H. Kim, J. H. Lee, *J. Mater. Chem. A* **2019**, *7*, 10672.
[177] a) R. Bao, C. Wang, Z. Peng, C. Ma, L. Dong, C. Pan, *ACS Photonics* **2017**, *4*, 1344; b) Y. Tchoe, K. Chung, K. Lee, J. Jo, K. Chung, J. K. Hyun, M. Kim, G.-C. Yi, *NPG Asia Mater.* **2019**, *11*, 1; c) Z. Wu, Y. Lu, W. Xu, Y. Zhang, J. Li, S. Lin, *Nano Energy* **2016**, *30*, 362.
[178] a) M. Vosgueritchian, J. B.-H. Tok, Z. Bao, *Nat. Photonics* **2013**, *7*, 769; b) J. Liang, L. Li, X. Niu, Z. Yu, Q. Pei, *Nat. Photonics* **2013**, *7*, 817; c) R.-H. Kim, D.-H. Kim, J. Xiao, B. H. Kim, S.-I. Park, B. Panilaitis, R. Ghaffari, J. Yao, M. Li, Z. Liu, *Nat. Mater.* **2010**, *9*, 929.
[179] S. G. R. Bade, X. Shan, P. T. Hoang, J. Li, T. Geske, L. Cai, Q. Pei, C. Wang, Z. Yu, *Adv. Mater.* **2017**, *29*, 1607053.
[180] J. Liu, C. Yang, H. Wu, Z. Lin, Z. Zhang, R. Wang, B. Li, F. Kang, L. Shi, C. P. Wong, *Energy Environ. Sci.* **2014**, *7*, 3674.
[181] F. Brunetti, A. Operamolla, S. Castro-Hermosa, G. Lucarelli, V. Manca, G. M. Farinola, T. M. Brown, *Adv. Funct. Mater.* **2019**, *29*, 1806798.
[182] N. Nakanishi, *Prog. Mater. Sci.* **1980**, *24*, 143.
[183] T. P. Brody, *IEEE Trans. Electron Devices* **1984**, *31*, 1614.
[184] S. Emamian, B. B. Narakathu, A. A. Chlaihawi, B. J. Bazuin, M. Z. Atashbar, *Sens. Actuators, A* **2017**, *263*, 639.
[185] R. Bollström, D. Tobjörk, P. Dolietis, P. Salminen, J. Preston, R. Österbacka, M. Toivakka, *Chem. Eng. Process.* **2013**, *68*, 13.
[186] D. Tobjörk, H. Aarnio, P. Pulkkinen, R. Bollström, A. Määttänen, P. Ihalainen, T. Mäkelä, J. Peltonen, M. Toivakka, H. Tenhu, *Thin Solid Films* **2012**, *520*, 2949.
[187] Y. Wang, C. Yan, S. Y. Cheng, Z. Q. Xu, X. Sun, Y. H. Xu, J. J. Chen, Z. Jiang, K. Liang, Z. S. Feng, *Adv. Funct. Mater.* **2019**, *29*, 1902579.
[188] E. Hrehorova, A. Pekarovicova, V. Bliznyuk, P. D. Fleming, presented at *NIP & Digital Fabrication Conference* **2007**.
[189] L. Wang, J. Liu, *RSC Adv.* **2015**, *5*, 57686.
[190] Q. Tang, H. Guo, P. Yan, C. Hu, *EcoMat* **2020**, *2*, e12060.
[191] W. J. Hyun, E. B. Secor, G. A. Rojas, M. C. Hersam, L. F. Francis, C. D. Frisbie, *Adv. Mater.* **2015**, *27*, 7058.
[192] a) B. Y. Ahn, E. B. Duoss, M. J. Motala, X. Guo, S.-I. Park, Y. Xiong, J. Yoon, R. G. Nuzzo, J. A. Rogers, J. A. Lewis, *Mater. Lett.* **2009**, *323*, 1590; b) M. Grouchko, A. Kamyshny, S. Magdassi, *J. Mater. Chem.* **2009**, *19*, 3057; c) M. Shariq, S. Chattopadhyaya, R. Rudolf, A. R. Dixit, *Science* **2020**, 127332.
[193] L. Wu, Z. Dong, F. Li, H. Zhou, Y. Song, *Adv. Opt. Mater.* **2016**, *4*, 1915.
[194] L. Liu, Z. Niu, J. Chen, *Chem. Soc. Rev.* **2016**, *45*, 4340.
[195] P. Falcaro, R. Ricco, C. M. Doherty, K. Liang, A. J. Hill, M. Styles, *Chem. Soc. Rev.* **2014**, *43*, 5513.
[196] B. Yoon, D. Y. Ham, O. Yarimaga, H. An, C. W. Lee, J. Kim, *Adv. Mater.* **2011**, *23*, 5492.
[197] a) E. Quain, T. S. Mathis, N. Kurra, K. Maleski, K. L. Van Aken, M. Alhabeb, H. N. Alshareef, Y. Gogotsi, *Adv. Mater. Technol.* **2019**, *4*, 1800256; b) J. M. Nassar, M. D. Cordero, A. T. Kutbee, M. A. Karimi, G. A. T. Sevilla, A. M. Hussain, A. Shamim, M. M. Hussain, *Adv. Mater. Technol.* **2016**, *1*, 1600004; c) L. Polavarapu, A. L. Porta, S. M. Novikov, M. Coronado-Puchau, L. M. Liz-Marzán, *Small* **2014**, *10*, 3065; d) A. Russo, B. Y. Ahn, J. J. Adams, E. B. Duoss, J. T. Bernhard, J. A. Lewis, *Adv. Mater.* **2011**, *23*, 3426; e) C.-W. Lin, Z. Zhao, J. Kim, J. Huang, *Sci. Rep.* **2014**, *4*, 3812.
[198] X. Liao, Q. Liao, X. Yan, Q. Liang, H. Si, M. Li, H. Wu, S. Cao, Y. Zhang, *Adv. Funct. Mater.* **2015**, *25*, 2395.
[199] G. Zheng, L. Hu, H. Wu, X. Xie, Y. Cui, *Energy Environ. Sci.* **2011**, *4*, 3368.
[200] N. N. Jason, W. Shen, W. Cheng, *ACS Appl. Mater. Interfaces* **2015**, *7*, 16760.
[201] C.-V. Ngo, D.-M. Chun, *Sci. Rep.* **2016**, *6*, 36735.
[202] S. Große, P. Wilke, H. G. Börner, *Angew. Chem., Int. Ed.* **2016**, *55*, 11266.
[203] M. Amjadi, M. Sitti, *ACS Nano* **2016**, *10*, 10202.
[204] X. Zang, C. Shen, Y. Chu, B. Li, M. Wei, J. Zhong, M. Sanghadasa, L. Lin, *Adv. Mater.* **2018**, *30*, 1800062.
[205] I. Kim, H. Jeon, D. Kim, J. You, D. Kim, *Nano Energy* **2018**, *53*, 975.
[206] L. Bai, Y. He, J. Zhou, Y. Lim, V. C. Mai, Y. Chen, S. Hou, Y. Zhao, J. Zhang, H. Duan, *Adv. Opt. Mater.* **2019**, *7*, 1900522.
[207] a) V. T. N. Linh, J. Moon, C. Mun, V. Devaraj, J.-W. Oh, S.-G. Park, D.-H. Kim, J. Choo, Y.-I. Lee, H. Jung, *Sens. Actuators, B* **2019**, *291*,

369; b) T. G. Yun, D. Kim, S.-M. Kim, I.-D. Kim, S. Hyun, S. M. Han, *Adv. Energy Mater.* **2018**, *8*, 1800064; c) C. Wu, T. W. Kima, S. Sung, J. H. Park, F. Li, *Nano Energy* **2018**, *44*, 279; d) L. Dong, C. Xu, Y. Li, Z. Pan, G. Liang, E. Zhou, F. Kang, Q. Yang, *Adv. Mater.* **2016**, *28*, 9313; e) F. Xiao, S. Yang, Z. Zhang, H. Liu, J. Xiao, L. Wan, J. Luo, S. Wang, Y. Liu, *Sci. Rep.* **2015**, *5*, 9359; f) S. Kumar, M. Willander, J. G. Sharma, B. Malhotra, *J. Mater. Chem. B* **2015**, *3*, 9305.

[208] a) S. Thiemann, S. J. Sachnov, F. Pettersson, R. Bollström, R. Österbacka, P. Wasserscheid, J. Zaumseil, *Adv. Funct. Mater.* **2014**, *24*, 625; b) A. Pal, H. E. Cuellar, R. Kuang, H. F. Caurin, D. Goswami, R. V. Martinez, *Adv. Mater. Technol.* **2017**, *2*, 1700130; c) P. Chansri, B. Wanno, S. Keawwangchai, T. Tuntulani, B. Pulpoka, C. Kaewtong, *J. Appl. Polym. Sci.* **2020**, *137*, 48273.

[209] A. Asadpoordarvish, A. Sandström, C. Larsen, R. Bollström, M. Toivakka, R. Österbacka, L. Edman, *Adv. Funct. Mater.* **2015**, *25*, 3238.

[210] B. Yao, J. Zhang, T. Kou, Y. Song, T. Liu, Y. Li, *Adv. Sci.* **2017**, *4*, 1700107.

[211] a) J. Wang, M. Liang, Y. Fang, T. Qiu, J. Zhang, L. Zhi, *Adv. Mater.* **2012**, *24*, 2874; b) L. Hu, Y. Cui, *Energy Environ. Sci.* **2012**, *5*, 6423.

[212] L. Hu, J. W. Choi, Y. Yang, S. Jeong, F. La Mantia, L.-F. Cui, Y. Cui, *Proc. Natl. Acad. Sci. U. S. A.* **2009**, *106*, 21490.

[213] Y. Liu, B. Weng, J. M. Razal, Q. Xu, C. Zhao, Y. Hou, S. Seyedin, R. Jalili, G. G. Wallace, J. Chen, *Sci. Rep.* **2015**, *5*, 17045.

[214] N. M. Abbasi, Y. Xiao, L. Peng, Y. Duo, L. Wang, L. Zhang, B. Wang, H. Zhang, *Adv. Mater. Technol.* **2021**, *6*, 2001197.

[215] Z. Liu, S. Nie, J. Luo, Y. Gao, X. Wang, Q. Wan, *Adv. Electron. Mater.* **2019**, *5*, 1900235.

[216] W. Li, L. Li, S. Ge, X. Song, L. Ge, M. Yan, J. Yu, *Chem. Commun.* **2013**, *49*, 7687.

[217] L. Ge, S. Wang, J. Yu, N. Li, S. Ge, M. Yan, *Adv. Funct. Mater.* **2013**, *23*, 3115.

[218] L. Li, Y. Zhang, F. Liu, M. Su, L. Liang, S. Ge, J. Yu, *Chem. Commun.* **2015**, *51*, 14030.

[219] F. Liu, S. Ge, J. Yu, M. Yan, X. Song, *Chem. Commun.* **2014**, *50*, 10315.

[220] Y. Zhang, L. Ge, M. Li, M. Yan, S. Ge, J. Yu, X. Song, B. Cao, *Chem. Commun.* **2014**, *50*, 1417.

[221] N. Song, Y. Wu, W. Wang, D. Xiao, H. Tan, Y. Zhao, *Anal. Chim. Acta* **2019**, *111*, 267.

[222] N. Song, Y. Wu, W. Wang, D. Xiao, H. Tan, Y. Zhao, *Mater. Res. Bull.* **2019**, *111*, 267.

[223] a) G. Zhou, D.-W. Wang, P.-X. Hou, W. Li, N. Li, C. Liu, F. Li, H.-M. Cheng, *J. Mater. Chem.* **2012**, *22*, 17942; b) Z. Niu, W. Zhou, J. Chen, G. Feng, H. Li, W. Ma, J. Li, H. Dong, Y. Ren, D. Zhao, *Energy Environ. Sci.* **2011**, *4*, 1440.

[224] Y. Hu, C. Guan, G. Feng, Q. Ke, X. Huang, J. Wang, *Adv. Funct. Mater.* **2015**, *25*, 7291.

[225] Y. Cheng, L. Huang, X. Xiao, B. Yao, L. Yuan, T. Li, Z. Hu, B. Wang, J. Wan, J. Zhou, *Nano Energy* **2015**, *15*, 66.

[226] L. Yuan, B. Yao, B. Hu, K. Huo, W. Chen, J. Zhou, *Energy Environ. Sci.* **2013**, *6*, 470.

[227] S. Magdassi, M. Grouchko, O. Berezin, A. Kamyshny, *ACS Nano* **2010**, *4*, 1943.

[228] Z. Liu, H. Ji, S. Wang, W. Zhao, Y. Huang, H. Feng, J. Wei, M. Li, *Phys. Status Solidi* **2018**, *215*, 1800007.

[229] K. Kordás, T. Mustonen, G. Tóth, H. Jantunen, M. Lajunen, C. Soldano, S. Talapatra, S. Kar, R. Vajtai, P. Ajayan, *Small* **2006**, *2*, 1021.

[230] Y. Zhang, L. Zhang, K. Cui, S. Ge, X. Cheng, M. Yan, J. Yu, H. Liu, *Adv. Mater.* **2018**, *30*, 1801588.

[231] J. Ahn, J.-W. Seo, T.-I. Lee, D. Kwon, I. Park, T.-S. Kim, J.-Y. Lee, *ACS Appl. Mater. Interfaces* **2016**, *8*, 19031.

[232] S. Chen, J. Jiang, F. Xu, S. Gong, *Nano Energy* **2019**, *61*, 69.

[233] S. Chen, Y. Song, D. Ding, Z. Ling, F. Xu, *Adv. Funct. Mater.* **2018**, *28*, 1802547.

[234] N. Kurra, B. Ahmed, Y. Gogotsi, H. N. Alshareef, *Adv. Energy Mater.* **2016**, *6*, 1601372.

[235] A. Eshkeiti, M. Rezaei, B. B. Narakathu, A. S. G. Reddy, S. Emamian, M. Z. Atashbar, presented at *SENSORS*, 2013 IEEE **2013**.

[236] H. Zhu, B. B. Narakathu, Z. Fang, A. T. Aijazi, M. Joyce, M. Atashbar, L. Hu, *Nanoscale* **2014**, *6*, 9110.

[237] N. Raut, K. Al-Shamery, *J. Mater. Chem. C* **2018**, *6*, 1618.

[238] Z. Li, F. Li, Y. Xing, Z. Liu, M. You, Y. Li, T. Wen, Z. Qu, X. L. Li, F. Xu, *Biosens. Bioelectron.* **2017**, *98*, 478.

[239] R. Guo, J. Chen, B. Yang, L. Liu, L. Su, B. Shen, X. Yan, *Adv. Funct. Mater.* **2017**, *27*, 1702394.

[240] A. Hübler, B. Trnovec, T. Zillger, M. Ali, N. Wetzold, M. Mingebach, A. Wagenpfahl, C. Deibel, V. Dyakonov, *Adv. Energy Mater.* **2011**, *1*, 1018.

[241] V. R. Voggu, J. Sham, S. Pfeffer, J. Pate, L. Fillip, T. B. Harvey, R. M. BrownJr., B. A. Korgel, *ACS Energy Lett.* **2017**, *2*, 574.

[242] L. Hu, G. Zheng, J. Yao, N. Liu, B. Weil, M. Eskilsson, E. Karabulut, Z. Ruan, S. Fan, J. T. Bloking, M. D. McGehee, L. Wågberg, Y. Cui, *Energy Environ. Sci.* **2013**, *6*, 513.

[243] H. Song, J. Zhang, D. Chen, K. Wang, S. Niu, Z. Han, L. Ren, *Nanoscale* **2017**, *9*, 1166.

[244] H. Liu, H. Jiang, F. Du, D. Zhang, Z. Li, H. Zhou, *ACS Sustainable Chem. Eng.* **2017**, *5*, 10538.

[245] X. Liao, Z. Zhang, Q. Liang, Q. Liao, Y. Zhang, *ACS Appl. Mater. Interfaces* **2017**, *9*, 4151.

[246] B. Saha, S. Baek, J. Lee, *ACS Appl. Mater. Interfaces* **2017**, *9*, 4658.

[247] P. J. Bracher, M. Gupta, G. M. Whitesides, *Adv. Mater.* **2009**, *21*, 445.

[248] B. Gao, X. Wang, T. Li, Z. Feng, C. Wang, Z. Gu, *Adv. Mater. Technol.* **2019**, *4*, 1800392.

[249] C. Zheng, L. Xiang, W. Jin, H. Shen, W. Zhao, F. Zhang, C. a. Di, D. Zhu, *Adv. Mater. Technol.* **2019**, *4*, 1900247.

[250] E. W. Nery, L. T. Kubota, *Anal. Bioanal. Chem.* **2013**, *405*, 7573.

[251] D.-Y. Yoon, T.-Y. Kim, D.-G. Moon, *Curr. Appl. Phys.* **2010**, *10*, e135.

[252] a) K. A. Mirica, J. G. Weis, J. M. Schnorr, B. Esser, T. M. Swager, *Angew. Chem.* **2012**, *124*, 10898; b) L. L. Tay, S. Poirier, A. Ghaemi, J. Hulse, S. Wang, *J. Raman Spectrosc.* **2021**, *52*, 563; c) G. Qin, L. Yang, Z. Fan, H. Dong, S. Yu, *Microwave Opt. Technol. Lett.* **2021**.

[253] S. Li, D. Huang, B. Zhang, X. Xu, M. Wang, G. Yang, Y. Shen, *Adv. Energy Mater.* **2014**, *4*, 1301655.

[254] L. David, R. Bhandavat, U. Barrera, G. Singh, *Nat. Commun.* **2016**, *7*, 10998.

[255] Z. Liu, F. Mo, H. Li, M. Zhu, Z. Wang, G. Liang, C. Zhi, *Small Methods* **2018**, *2*, 1800124.

[256] H. Li, X. Li, J. Liang, Y. Chen, *Adv. Energy Mater.* **2019**, *9*, 1803987.

[257] X. Jia, Z. Chen, A. Suwarnasarn, L. Rice, X. Wang, H. Sohn, Q. Zhang, B. M. Wu, F. Wei, Y. Lu, *Energy Environ. Sci.* **2012**, *5*, 6845.

[258] S. Ko, J. I. Lee, H. S. Yang, S. Park, U. Jeong, *Adv. Mater.* **2012**, *24*, 4451.

[259] P. Meduri, C. Pendyala, V. Kumar, G. U. Sumanasekera, M. K. Sunkara, *Nano Lett.* **2009**, *9*, 612.

[260] Y. Sun, X. Hu, W. Luo, Y. Huang, *ACS Nano* **2011**, *5*, 7100.

[261] Z.-S. Wu, W. Ren, L. Wen, L. Gao, J. Zhao, Z. Chen, G. Zhou, F. Li, H.-M. Cheng, *ACS Nano* **2010**, *4*, 3187.

[262] X. Zhu, Y. Zhu, S. Murali, M. D. Stoller, R. S. Ruoff, *ACS Nano* **2011**, *5*, 3333.

[263] H. Tian, F. Xin, X. Wang, W. He, W. Han, *J. Materiomics* **2015**, *1*, 153.

[264] H. Wu, G. Chan, J. W. Choi, I. Ryu, Y. Yao, M. T. McDowell, S. W. Lee, A. Jackson, Y. Yang, L. Hu, *Nat. Nanotechnol.* **2012**, *7*, 310.

[265] C. Wei, H. Fei, Y. Tian, Y. An, G. Zeng, J. Feng, Y. Qian, *Small* **2019**, *15*, 1903214.

[266] a) K. Xia, Z. Zhu, H. Zhang, C. Du, Z. Xu, R. Wang, *Nano Energy* **2018**, *50*, 571; b) S. A. Shankaregowda, R. F. S. M. Ahmed, C. B. Nanjegowda, J. Wang, S. Guan, M. Puttaswamy, A. Amini, Y. Zhang, D. Kong, K. Sannathammegowda, *Nano Energy* **2019**, *66*, 104141.
[267] Y. H. Jung, T.-H. Chang, H. Zhang, C. Yao, Q. Zheng, V. W. Yang, H. Mi, M. Kim, S. J. Cho, D.-W. Park, H. Jiang, J. Lee, Y. Qiu, W. Zhou, Z. Cai, S. Gong, Z. Ma, *Nat. Commun.* **2015**, *6*, 7170.
[268] G.-W. Huang, Q.-P. Feng, H.-M. Xiao, N. Li, S.-Y. Fu, *ACS Nano* **2016**, *10*, 8895.
[269] K. Nagashima, H. Koga, U. Celano, F. Zhuge, M. Kanai, S. Rahong, G. Meng, Y. He, J. De Boeck, M. Jurczak, W. Vandervorst, T. Kitaoka, M. Nogi, T. Yanagida, *Sci. Rep.* **2014**, *4*, 5532.
[270] R. F. Martins, A. Ahnood, N. Correia, L. M. Pereira, R. Barros, P. M. Barquinha, R. Costa, I. M. Ferreira, A. Nathan, E. E. Fortunato, *Adv. Funct. Mater.* **2013**, *23*, 2153.
[271] a) P. T. Gomathi, P. Sahatiya, S. Badhulika, *Adv. Funct. Mater.* **2017**, *27*, 1701611; b) C.-H. Lin, D.-S. Tsai, T.-C. Wei, D.-H. Lien, J.-J. Ke, C.-H. Su, J.-Y. Sun, Y.-C. Liao, J.-H. He, *ACS Nano* **2017**, *11*, 10230; c) W. Zou, A. González, D. Jampaiah, R. Ramanathan, M. Taha, S. Walia, S. Sriram, M. Bhaskaran, J. M. Dominguez-Vera, V. Bansal, *Nat. Commun.* **2018**, *9*, 3743.
[272] J. Jin, D. Lee, H. G. Im, Y. C. Han, E. G. Jeong, M. Rolandi, K. C. Choi, B. S. Bae, *Adv. Mater.* **2016**, *28*, 5169.
[273] Y. Yao, J. Tao, J. Zou, B. Zhang, T. Li, J. Dai, M. Zhu, S. Wang, K. K. Fu, D. Henderson, *Energy Environ. Sci.* **2016**, *9*, 2278.
[274] Y. Yang, W. Liu, Q. Huang, X. Li, H. Ling, J. Ren, R. Sun, J. Zou, X. Wang, *ACS Sustainable Chem. Eng.* **2020**, *8*, 3392.
[275] M. Stoppa, A. Chiolerio, *Sensors* **2014**, *14*, 11957.
[276] B. Wang, A. Facchetti, *Adv. Mater.* **2019**, *31*, 1901408.
[277] T. Agcayazi, K. Chatterjee, A. Bozkurt, T. K. Ghosh, *Adv. Mater. Technol.* **2018**, *3*, 1700277.
[278] J. Hayward, *IDTechEx report* **2015**.
[279] R. Cao, X. Pu, X. Du, W. Yang, J. Wang, H. Guo, S. Zhao, Z. Yuan, C. Zhang, C. Li, Z. L. Wang, *ACS Nano* **2018**, *12*, 5190.
[280] H. Jin, N. Matsuhisa, S. Lee, M. Abbas, T. Yokota, T. Someya, *Adv. Mater.* **2017**, *29*, 1605848.
[281] B. M. Li, I. Kim, Y. Zhou, A. C. Mills, T. J. Flewwellin, J. S. Jur, *Adv. Mater. Technol.* **2019**, *4*, 1900511.
[282] I. Kim, B. Ju, Y. Zhou, B. M. Li, J. S. Jur, *ACS Appl. Mater. Interfaces* **2021**.
[283] a) J. Zhu, M. Cho, Y. Li, T. He, J. Ahn, J. Park, T.-L. Ren, C. Lee, I. Park, *Nano Energy* **2021**, *86*, 106035; b) S. Uzun, M. Schelling, K. Hantanasirisakul, T. S. Mathis, R. Askeland, G. Dion, Y. Gogotsi, *Small* **2021**, *17*, 2006376.
[284] H. Shahariar, I. Kim, H. Soewardiman, J. S. Jur, *ACS Appl. Mater. Interfaces* **2019**, *11*, 6208.
[285] T. Gao, Z. Yang, C. Chen, Y. Li, K. Fu, J. Dai, E. M. Hitz, H. Xie, B. Liu, J. Song, *ACS Nano* **2017**, *11*, 11513.
[286] J. Zhao, Y. Zhang, Y. Huang, J. Xie, X. Zhao, C. Li, J. Qu, Q. Zhang, J. Sun, B. He, *Adv. Sci.* **2018**, *5*, 1801114.
[287] M. Zhang, M. Zhao, M. Jian, C. Wang, A. Yu, Z. Yin, X. Liang, H. Wang, K. Xia, X. Liang, J. Zhai, Y. Zhang, *Matter* **2019**, *1*, 168.
[288] L. X. Liu, W. Chen, H. B. Zhang, Q. W. Wang, F. Guan, Z. Z. Yu, *Adv. Funct. Mater.* **2019**, *29*, 1905197.
[289] Q. W. Wang, H. B. Zhang, J. Liu, S. Zhao, X. Xie, L. Liu, R. Yang, N. Koratkar, Z. Z. Yu, *Adv. Funct. Mater.* **2019**, *29*, 1806819.
[290] Q. Huang, D. Wang, Z. Zheng, *Adv. Energy Mater.* **2016**, *6*, 1600783.
[291] W. Lu, P. Yu, M. Jian, H. Wang, H. Wang, X. Liang, Y. Zhang, *ACS Appl. Mater. Interfaces* **2020**, *12*, 11825.
[292] J. Hu, M. Zhang, Y. He, M. Zhang, R. Shen, Y. Zhang, M. Wang, G. Wu, *Polymers* **2020**, *12*, 2333.
[293] Y. Han, Y. Lu, S. Shen, Y. Zhong, S. Liu, X. Xia, Y. Tong, X. Lu, *Adv. Funct. Mater.* **2019**, *29*, 1806329.
[294] S. Dong, L. Shen, H. Li, G. Pang, H. Dou, X. Zhang, *Adv. Funct. Mater.* **2016**, *26*, 3703.
[295] D. Kong, Y. Wang, Y. Von Lim, S. Huang, J. Zhang, B. Liu, T. Chen, H. Y. Yang, *Nano Energy* **2018**, *49*, 460.
[296] L. Zhang, M. Fairbanks, T. L. Andrew, *Adv. Funct. Mater.* **2017**, *27*, 1700415.
[297] M. Liu, Z. Cong, X. Pu, W. Guo, T. Liu, M. Li, Y. Zhang, W. Hu, Z. L. Wang, *Adv. Funct. Mater.* **2019**, *29*, 1806298.
[298] B. Dudem, A. R. Mule, H. R. Patnam, J. S. Yu, *Nano Energy* **2019**, *55*, 305.
[299] Z. Liu, F. Mo, H. Li, M. Zhu, Z. Wang, G. Liang, C. Zhi, **2018**, *2*, 1800124.
[300] a) K. Wang, Q. Meng, Y. Zhang, Z. Wei, M. Miao, *Adv. Mater.* **2013**, *25*, 1494; b) H. Sun, S. Xie, Y. Li, Y. Jiang, X. Sun, B. Wang, H. Peng, *Adv. Mater.* **2016**, *28*, 8431; c) B. C. Kim, J. Y. Hong, G. G. Wallace, H. S. Park, *Adv. Energy Mater.* **2015**, *5*, 1500959.
[301] A. R. Mule, B. Dudem, H. Patnam, S. A. Graham, J. S. Yu, *ACS Sustainable Chem. Eng.* **2019**, *7*, 16450.
[302] B. Fang, D. Chang, Z. Xu, C. Gao, *Adv. Mater.* **2019**, *32*, 1902664.
[303] J. Zhang, S. Seyedin, S. Qin, P. A. Lynch, Z. Wang, W. Yang, X. Wang, J. M. Razal, *J. Mater. Chem. A* **2019**, *7*, 6401.
[304] a) Z. Xu, Y. Liu, X. Zhao, L. Peng, H. Sun, Y. Xu, X. Ren, C. Jin, P. Xu, M. Wang, *Adv. Mater.* **2016**, *28*, 6449; b) S. J. Choi, H. Yu, J. S. Jang, M. H. Kim, S. J. Kim, H. S. Jeong, I. D. Kim, *Small* **2018**, *14*, 1703934.
[305] S. Seyedin, E. R. S. Yanza, J. M. Razal, *J. Mater. Chem. A* **2017**, *5*, 24076.
[306] J. Di, X. Zhang, Z. Yong, Y. Zhang, D. Li, R. Li, Q. Li, *Adv. Mater.* **2016**, *28*, 10529.
[307] Y. Lu, J. Jiang, S. Yoon, K.-S. Kim, J.-H. Kim, S. Park, S.-H. Kim, L. Piao, *ACS Appl. Mater. Interfaces* **2018**, *10*, 2093.
[308] Z. Li, Z. Xu, Y. Liu, R. Wang, C. Gao, *Nat. Commun.* **2016**, *7*, 13684.
[309] S. Ling, Z. Qin, C. Li, W. Huang, D. L. Kaplan, M. J. Buehler, *Nat. Commun.* **2017**, *8*, 1387.
[310] Y. Zhao, D. Dong, S. Gong, L. Brassart, Y. Wang, T. An, W. Cheng, *Adv. Electron. Mater.* **2019**, *5*, 1800462.
[311] X. Dou, Q. Wang, Z. Li, J. Ju, S. Wang, L. Hao, K. Sui, Y. Xia, Y. Tan, *Adv. Funct. Mater.* **2019**, *29*, 1905610.
[312] a) Y. Ding, W. Xu, W. Wang, H. Fong, Z. Zhu, *ACS Appl. Mater. Interfaces* **2017**, *9*, 30014; b) Z. Yin, M. Jian, C. Wang, K. Xia, Z. Liu, Q. Wang, M. Zhang, H. Wang, X. Liang, X. Liang, *Nano Lett.* **2018**, *18*, 7085.
[313] S. Ling, Q. Wang, D. Zhang, Y. Zhang, X. Mu, D. L. Kaplan, M. Buehler, *Adv. Funct. Mater.* **2018**, *28*, 1705291.
[314] M.-F. Lin, J. Xiong, J. Wang, K. Parida, P. S. Lee, *Nano Energy* **2018**, *44*, 248.
[315] Y. Zhu, M. Yang, Q. Huang, D. Wang, R. Yu, J. Wang, Z. Zheng, D. Wang, *Adv. Mater.* **2020**, *32*, 1906205.
[316] Y. Li, S. Arumugam, C. Krishnan, M. D. Charlton, S. Beeby, *ChemistrySelect* **2019**, *4*, 407.
[317] X. Pu, M. Liu, L. Li, S. Han, X. Li, C. Jiang, C. Du, J. Luo, W. Hu, Z. L. Wang, *Adv. Energy Mater.* **2016**, *6*, 1601254.
[318] B. Krykpayev, M. F. Farooqui, R. M. Bilal, M. Vaseem, A. Shamim, *Microelectron. J.* **2017**, *65*, 40.
[319] E. Bihar, T. Roberts, E. Ismailova, M. Saadaoui, M. Isik, A. Sanchez-Sanchez, D. Mecerreyes, T. Hervé, J. B. De Graaf, G. G. Malliaras, *Adv. Mater. Technol.* **2017**, *2*, 1600251.
[320] T. Lee, W. Lee, S. W. Kim, J. J. Kim, B. S. Kim, *Adv. Funct. Mater.* **2016**, *26*, 6206.
[321] Y. Hao, M. Tian, H. Zhao, L. Qu, S. Zhu, X. Zhang, S. Chen, K. Wang, J. Ran, *Ind. Eng. Chem. Res.* **2018**, *57*, 13437.
[322] L.-C. Jia, G. Zhang, L. Xu, W.-J. Sun, G.-J. Zhong, J. Lei, D.-X. Yan, Z.-M. Li, *ACS Appl. Mater. Interfaces* **2018**, *11*, 1680.
[323] Z. Gao, C. Bumgardner, N. Song, Y. Zhang, J. Li, X. Li, *Nat. Commun.* **2016**, *7*, 11586.

[324] S. Xu, Y. Yao, Y. Guo, X. Zeng, S. D. Lacey, H. Song, C. Chen, Y. Li, J. Dai, Y. Wang, *Adv. Mater.* **2018**, *30*, 1704907.
[325] J. Xiong, P. Cui, X. Chen, J. Wang, K. Parida, M.-F. Lin, P. S. Lee, *Nat. Commun.* **2018**, *9*, 4280.
[326] W.-R. Huang, C.-X. Yu, Y.-R. Lu, H. Muhammad, J.-L. Wang, J.-W. Liu, S.-H. Yu, *Nano Res.* **2019**, *12*, 1483.
[327] T. He, Q. Shi, H. Wang, F. Wen, T. Chen, J. Ouyang, C. Lee, *Nano Energy* **2019**, *57*, 338.
[328] L. Cai, A. Y. Song, P. Wu, P.-C. Hsu, Y. Peng, J. Chen, C. Liu, P. B. Catrysse, Y. Liu, A. Yang, C. Zhou, C. Zhou, S. Fan, Y. Cui, *Nat. Commun.* **2017**, *8*, 496.
[329] X. Yu, X. Su, K. Yan, H. Hu, M. Peng, X. Cai, D. Zou, *Adv. Mater. Technol.* **2016**, *1*, 1600009.
[330] A. Hu, J. Long, C. Shu, C. Xu, T. Yang, R. Liang, J. Li, *ChemElectroChem* **2019**, *6*, 349.
[331] T. Zhao, G. Zhang, F. Zhou, S. Zhang, C. Deng, *Small* **2018**, *14*, 1802320.
[332] D. Wickramasinghe, J.-M. Oh, S. McGraw, K. Senecal, K.-F. Chow, *ACS Appl. Energy Mater.* **2018**, *2*, 372.
[333] W.-Y. Ko, Y.-F. Chen, K.-M. Lu, K.-J. Lin, *Sci. Rep.* **2016**, *6*, 18887.
[334] H. Bae, B. C. Jang, H. Park, S.-H. Jung, H. M. Lee, J.-Y. Park, S.-B. Jeon, G. Son, I.-W. Tcho, K. Yu, *Nano Lett.* **2017**, *17*, 6443.
[335] Y. Yan, B. Y. Xia, X. Ge, Z. Liu, A. Fisher, X. Wang, *Chem. - Eur. J.* **2015**, *21*, 18062.
[336] R. Wu, L. Ma, C. Hou, Z. Meng, W. Guo, W. Yu, R. Yu, F. Hu, X. Y. Liu, *Small* **2019**, *15*, 1901558.
[337] P. Li, L. Zhao, Z. Jiang, M. Yu, Z. Li, X. Zhou, Y. J. S. r. Zhao, *Sci. Rep.* **2019**, *9*, 14457.
[338] T. He, H. Wang, J. Wang, X. Tian, F. Wen, Q. Shi, J. S. Ho, C. Lee, *Adv. Sci.* **2019**, *6*, 1901437.
[339] a) M. A. Booth, S. A. Gowers, M. Hersey, I. C. Samper, S. Park, P. Anikeeva, P. Hashemi, M. M. Stevens, M. G. Boutelle, *Anal. Chem.* **2021**, *93*, 6646; b) Y. Guo, C. F. Werner, A. Canales, L. Yu, X. Jia, P. Anikeeva, T. Yoshinobu, *PLoS One* **2020**, *15*, e0228076; c) A. Frutiger, J. T. Muth, D. M. Vogt, Y. Mengüç, A. Campo, A. D. Valentine, C. J. Walsh, J. Lewis, *Adv. Mater.* **2015**, *27*, 2440.
[340] C. Lu, S. Park, T. J. Richner, A. Derry, I. Brown, C. Hou, S. Rao, J. Kang, C. T. Mortiz, Y. Fink, P. Anikeeva, *Sci. Adv.* **2017**, *3*, e1600955.
[341] Z. Yang, Y. Pang, X.-l. Han, Y. Yang, J. Ling, M. Jian, Y. Zhang, Y. Yang, T.-L. Ren, *ACS Nano* **2018**, *12*, 9134.
[342] B. Nie, R. Huang, T. Yao, Y. Zhang, Y. Miao, C. Liu, J. Liu, X. Chen, *Adv. Funct. Mater.* **2019**, *29*, 1808786.
[343] T. Sun, B. Zhou, Q. Zheng, L. Wang, W. Jiang, G. Snyder, *Nat. Commun.* **2020**, *11*, 572.
[344] L. Yu, S. Parker, H. Xuan, Y. Zhang, S. Jiang, M. Tousi, M. Manteghi, A. Wang, X. Jia, *Adv. Funct. Mater.* **2020**, *30*, 1908915.
[345] J. Lee, S. Chun, J. H. Song, E. S. Yoo, J. K. Kim, C. Pang, *Adv. Mater. Technol.* **2020**.
[346] W. He, C. Wang, H. Wang, M. Jian, W. Lu, X. Liang, X. Zhang, F. Yang, Y. Zhang, *Science* **2019**, *5*, eaax0649.
[347] a) X. Su, H. Li, X. Lai, Z. Chen, X. Zeng, *ACS Appl. Mater. Interfaces* **2018**, *10*, 10587; b) L. Li, Y. Bai, L. Li, S. Wang, T. Zhang, *Adv. Mater.* **2017**, *29*, 1702517.
[348] P. Wang, B. Sun, Y. Liang, H. Han, X. Fan, W. Wang, Z. Yang, *J. Mater. Chem. A* **2018**, *6*, 10404.
[349] H. Liu, Q. Li, Y. Bu, N. Zhang, C. Wang, C. Pan, L. Mi, Z. Guo, C. Liu, C. Shen, *Nano Energy* **2019**, 66.
[350] J. H. Yoon, S.-M. Kim, Y. Eom, J. M. Koo, H.-W. Cho, T. J. Lee, K. G. Lee, H. J. Park, Y. K. Kim, H.-J. Yoo, *ACS Appl. Mater. Interfaces* **2019**, *11*, 46165.
[351] K. Jost, G. Dion, Y. Gogotsi, *J. Mater. Chem. A* **2014**, *2*, 10776.
[352] Y. Cho, S. Pak, Y. G. Lee, J. S. Hwang, P. Giraud, G. H. An, S. Cha, *Adv. Funct. Mater.* **2020**, *30*, 1908479.
[353] J. Ren, L. Li, C. Chen, X. Chen, Z. Cai, L. Qiu, Y. Wang, X. Zhu, H. Peng, *Adv. Mater.* **2013**, *25*, 1155.
[354] F. Mo, G. Liang, Z. Huang, H. Li, D. Wang, C. Zhi, *Adv. Mater.* **2020**, *32*, 1902151.
[355] W. G. Chong, J. Q. Huang, Z. L. Xu, X. Qin, X. Wang, J. K. Kim, *Adv. Funct. Mater.* **2017**, *27*, 1604815.
[356] X. Fan, Z. Chu, F. Wang, C. Zhang, L. Chen, Y. Tang, D. Zou, *Adv. Mater.* **2008**, *20*, 592.
[357] Y. Fu, X. Cai, H. Wu, Z. Lv, S. Hou, M. Peng, X. Yu, D. Zou, *Adv. Mater.* **2012**, *24*, 5713.
[358] H. Sun, Y. Zhang, J. Zhang, X. Sun, H. Peng, *Nat. Rev. Mater.* **2017**, *2*, 17023.
[359] a) X. Pu, L. Li, M. Liu, C. Jiang, C. Du, Z. Zhao, W. Hu, Z. L. Wang, *Adv. Mater.* **2016**, *28*, 98; b) S. Pan, Z. Yang, P. Chen, J. Deng, H. Li, H. Peng, *Angew. Chem.* **2014**, *126*, 6224.
[360] Z. Chai, N. Zhang, P. Sun, Y. Huang, C. Zhao, H. J. Fan, X. Fan, W. Mai, *ACS Nano* **2016**, *10*, 9201.
[361] Z. Bai, Z. Zhang, J. Li, J. Guo, *Nano Energy* **2019**, *65*, 104012.
[362] Y. Yang, Q. Huang, L. Niu, D. Wang, C. Yan, Y. She, Z. Zheng, *Adv. Mater.* **2017**, *29*, 1606679.
[363] D. Wang, J. Sun, Q. Xue, Q. Li, Y. Guo, Y. Zhao, Z. Chen, Z. Huang, Q. Yang, G. Liang, B. Dong, C. Zhi, *Energy Storage Mater.* **2021**, *36*, 272.
[364] M. Kang, S.-A. Lee, S. Jang, S. Hwang, S.-K. Lee, S. Bae, J.-M. Hong, S. H. Lee, K.-U. Jeong, J. Lim, *ACS Appl. Mater. Interfaces* **2019**, *11*, 22575.
[365] A. Yang, Y. Li, C. Yang, Y. Fu, N. Wang, L. Li, F. Yan, *Adv. Mater.* **2018**, *30*, 1800051.
[366] Y. J. Song, J.-W. Kim, H.-E. Cho, Y. H. Son, M. H. Lee, J. Lee, K. C. Choi, S.-M. Lee, *ACS Nano* **2020**.
[367] Z. Zhu, Y. Gu, S. Wang, Y. Zou, H. Zeng, *Adv. Electron. Mater.* **2017**, *3*, 1700281.
[368] S. Kwon, Y. H. Hwang, M. Nam, H. Chae, H. S. Lee, Y. Jeon, S. Lee, C. Y. Kim, S. Choi, E. G. Jeong, *Adv. Mater.* **2020**, *32*, 1903488.
[369] D. Yin, Z. Y. Chen, N. R. Jiang, Y. F. Liu, Y. G. Bi, X. L. Zhang, W. Han, J. Feng, H. B. Sun, *Adv. Mater. Technol.* **2020**, *5*, 1900942.
[370] a) S. Cai, X. Xu, W. Yang, J. Chen, X. Fang, *Adv. Mater.* **2019**, *31*, 1808138; b) Q. Wang, D. Zhang, Y. Wu, T. Li, A. Zhang, M. Miao, *Energy Technol.* **2017**, *5*, 1449; c) W. Yan, A. Page, T. Nguyen-Dang, Y. Qu, F. Sordo, L. Wei, F. Sorin, *Adv. Mater.* **2019**, *31*, 1802348.
[371] X. Xu, J. Chen, S. Cai, Z. Long, Y. Zhang, L. Su, S. He, C. Tang, P. Liu, H. Peng, *Adv. Mater.* **2018**, *30*, 1803165.

Muhammad Hassan received his Ph.D. degree under the supervision of Academician Prof. Shu-Hong Yu in the Department of Chemistry, University of Science and Technology of China (USTC) in 2019. Currently, he is a Postdoctoral Fellow in the College of Physics and Optoelectronics, Shenzhen University, China (SZU). He is interested in the synthesis, self-assembly of nanomaterials for flexible and stretchable nanodevice fabrication and applications.

Xiuru Xu received her Ph.D. in Chemistry and Physics of Polymers from Jilin University in 2014. During 2012–2014, she joined Alan G. MacDiarmid Nanotech Institute at the University of Texas at Dallas. Then she finished her postdoctoral work in the College of Engineering at Peking University. Currently, she is an Assistant Professor at Shenzhen University. Her research interests are in smart materials, artificial muscles, and tactile and visual perception in soft robots.

Zhengchun Peng received his Ph.D. in MEMS from the Georgia Institute of Technology, Atlanta, GA, in 2010. He then joined Intel Corp. as a senior R&D engineer. He is currently a distinguished Professor at Shenzhen University. His main research interests are in the fields of flexible and stretchable electronics, nanosensors, MEMS, microfluidics, and tactile intelligence.